GENETIC AND BIOCHEMICAL DISSECTION OF PHOSPHOLIPID TRANSPORT TO THE MITOCHONDRIA

A Dissertation

By

DONNA M. IADAROLA

Submitted to the Office of Graduate and Professional Studies of
Texas A&M University
in partial fulfillment of the requirements for the degree of

DOCTOR OF PHILOSOPHY

Thesis Advisor,	Vishal M. Gohil
Chair of Committee,	Junjie Zhang
Committee Members,	Robert S. Chapkin
	Pingwei Li
Head of Department,	Joshua A. Wand

May 2021

Major Subject: Biochemistry

ABSTRACT

How phospholipids are transported to different organelles within the cell is a major unsolved question in cell biology. To address this gap in knowledge, I utilized *Saccharomyces cerevisiae* as a model organism to study phospholipid trafficking to the mitochondria. I mainly focused on identifying genes required for phosphatidylserine (PS) and phosphatidylethanolamine (PE) transport to the mitochondria since they are essential for the mitochondrial respiratory chain (MRC).

Through genetic and biochemical analysis of inter-organelle membrane tethering complexes, I discovered that Vps39, a protein involved in vacuole to mitochondria contact site formation as well as vesicular fusion, is essential for PE transport from the endoplasmic reticulum (ER) to the mitochondria. I showed that the loss of Vps39 specifically abrogates the transport of PE to the mitochondria without compromising its biosynthesis in the ER or its transport to other subcellular organelles. The recruitment of Vps39 to the ER and mitochondria is dependent on the PE levels of these organelles, directly implicating Vps39 in PE transport. Furthermore, I identified the essential domains of the Vps39 protein required for its PE transport functions and provided evidence that the role of Vps39 in intracellular PE trafficking is independent of its known roles in contact site formation and vesicular trafficking.

In addition to PE transport from the ER to the mitochondria, I discovered that Vps39 is also essential for PE transport from the endosomes to the mitochondria. The endosomal PE transport to PE-deficient mitochondria is triggered in response to phosphatidylcholine (PC) biosynthesis from choline, which obviated the need of PC

biosynthesis from endosomal PE. In this manner, choline supplementation is able to rescue mitochondrial respiration in PE deficient cells.

Mitochondria can also biosynthesize PE *in situ* from phosphatidylserine (PS), which has to be imported from the ER. However, PS import to the mitochondria is not fully understood. I designed and performed a genome-wide screen using yeast deletion mutants to identify genes required for PS transport to the mitochondria. This experiment has yielded a number of novel candidates of mitochondrial PS import. Together, the research in this dissertation identifies novel genes in phospholipid trafficking to the mitochondria.

ACKNOWLEDGEMENTS

I would like to thank my advisor, Dr. Gohil, for teaching me what it means to accomplish a Doctorate in Philosophy. I will use these tools in my future research and my personal life. I would also like to thank my committee members, Dr. Kaplan, Dr. Chapkin, Dr. Zhang, and Dr. Li, for their suggestions and guidance in my project. I would like to thank all my lab members because each of their unique traits taught me something about both science and life. A special thank you to Sagnika Ghosh and Natalie Garza for edits on this dissertation and extra support in lab. Finally, I would like to thank my family, Lois Iadarola, Robert Iadarola, Sabrina Iadarola, Vincent Iadarola, and Chase Pectol, for your unwavering support and love. Each of you was instrumental in helping me through this journey.

CONTRIBUTORS AND FUNDING SOURCES

This work was supported by a dissertation committee consisting of my advisor Dr. Vishal M. Gohil of the Department of Biochemistry and Biophysics and the Interdisciplinary Program in Genetics, Dr. Craig D. Kaplan of the Department of Biochemistry and Biophysics, Dr. Robert S. Chapkin of the Departments of Nutrition and Food Science, Biochemistry and Biophysics, Veterinary Medicine and Biomedical Sciences, and Microbial and Molecular Pathogenesis at Texas A&M Health Science Center, Dr. Junjie Zhang of the Department of Biochemistry and Biophysics, and Dr. Pingwei Li of the Department of Biochemistry and Biophysics. The head of the Biochemistry and Biophysics department, Dr. Joshua A. Wand, also supported this work.

Chapter II is a reprint of a publication for which I am the first author. I performed all the experimental work described in this chapter except for the phospholipid measurement (Figure 2.7D) and western blot (Figure 2.6A), which was performed by Dr. Writoban Basu Ball of the Department of Biochemistry and Biophysics at Texas A&M University. Dr. Guo Fu of the Department of Biology in the lab of Dr. Beiyan Nan also helped in fluorescent imaging of cells (Figure 2.10) We thank Dr. Christian Ungermann (University of Osnabruck) for yeast strains as well as Dr. Jan Brix (University of Freiberg), and Dr. Paul Lindahl (Texas A&M University) for their generous gift of antibodies. I am also thankful to Dr. Craig Kaplan, Dr. Will Prinz and the members of the Gohil lab for valuable discussions and comments. The research reported in this chapter was supported by the Welch Foundation grant [A-1810] and the National Institutes of Health award [R01GM111672] to Vishal M. Gohil and the National Institutes of Health award

[R01GM129000] to Beiyan Nan. The content is solely the responsibility of the authors and does not necessarily represent the official views of the National Institute of Health.

Chapter III is a reprint of a manuscript for which I am the first author. I performed all the experimental work described in this chapter except for technical replicates of phospholipid measurements performed by Alaumy Joshi of the Department of Biochemistry and Biophysics at Texas A&M University (Figure 3.5A) and of spotting performed by Cameron B. Caldwell of the Department of Biochemistry and Biophysics at Texas A&M University (Figure 3.2B&C). I thank Dr. Akinori Ohta and Dr. Ryouichi Fukuda for generously providing us with yeast strains. I also thank the current and former members of the Gohil lab for their valuable comments in the preparation of this manuscript. This work was supported by the Welch Foundation Grant [A-1810] and the National Institutes of Health award [R01GM111672] to Vishal M. Gohil. The content is solely the responsibility of the authors and does not necessarily represent the official views of the National Institutes of Health.

The work in Chapters IV has not been previously published. I performed all the experimental work described in this chapter except for performing the screen side-by-side with Dr. Writoban Basu Ball of the Department of Biochemistry and Biophysics at Texas A&M University. I thank Aaron Griffin of the Department of Biochemistry and Biophysics at Texas A&M University and Dr. Chenxi Qui of the Department of Biochemistry and Biophysics at Texas A&M University for their help in troubleshooting the analysis of the sequencing data.

The work in Appendix A has not been previously published. I performed all the experimental work described in this appendix except for two trials of the growth curve in Figure A.4 which was performed by Dr. Writoban Basu Ball of the Department of Biochemistry and Biophysics at Texas A&M University. The work in Appendix B has also not been previously published. I performed all the experimental work in this section except for one trial of spotting in Figure B.1A performed by Cameron Caldwell of the Department of Biochemistry and Biophysics at Texas A&M University. I also thank Cameron Caldwell for his help in constructing the plasmids seen in Figure B.1B.

NOMENCLATURE

MRC	Mitochondrial respiratory chain
PE	Phosphatidylethanolamine
Etn	Ethanolamine
PC	Phosphatidylcholine
Cho	Choline
PS	Phosphatidylserine
CL	Cardiolipin
PI	Phosphatidylinositol
PA	Phosphatidic acid
ER	Endoplasmic reticulum
vCLAMP	Vacuole and mitochondrial patch
ERMES	ER and mitochondria encounter structure

TABLE OF CONTENTS

Page

LIST OF FIGURES

Page

LIST OF TABLES

Page

CHAPTER I

INTRODUCTION

Phospholipids are a class of lipids that form cellular membranes. Phospholipids are amphiphilic molecules with a hydrophilic "head" group containing a phosphate moiety connected to a hydrophobic "tail" group containing two fatty acids attached to a glycerol backbone. The fatty acids in the "tail" group are referred to as acyl chains and they vary in the number of carbons and saturation state. The head group defines the identity of each phospholipid; for example, an ethanolamine (Etn) head group is characteristic of the phospholipid phosphatidylethanolamine (PE) and a serine head group is characteristic of phosphatidylserine (PS) (Figure 1.1A&B). Based on the head groups, there are six major classes of phospholipids in eukaryotic cells: PE, PS, phosphatidylcholine (PC), phosphatidylinositol (PI), phosphatidic acid (PA), and cardiolipin (CL). These phospholipids can further be classified as bilayer or non-bilayer phospholipids depending on the overall shape they acquire in aqueous solution. Bilayer-forming phospholipids- PC, PI, and PS- are cylindrical phospholipids that aggregate to form a bilayer structure typically shown in biological membranes (Basu Ball et al., 2018b; Holthuis and Menon, 2014; van Meer et al., 2008) (Figure 1.1C). Non-bilayer-forming phospholipids- PE, CL, and PA- are cone-shaped phospholipids that self-assemble into inverted hexagonal phase structures due to their small head groups (Basu Ball et al., 2018b; Holthuis and Menon, 2014; van Meer et al., 2008) (Figure 1.1D). These non-bilayer phospholipids introduce

curvature in the membrane and contribute to the physical properties of the membrane (Holthuis and Menon, 2014).

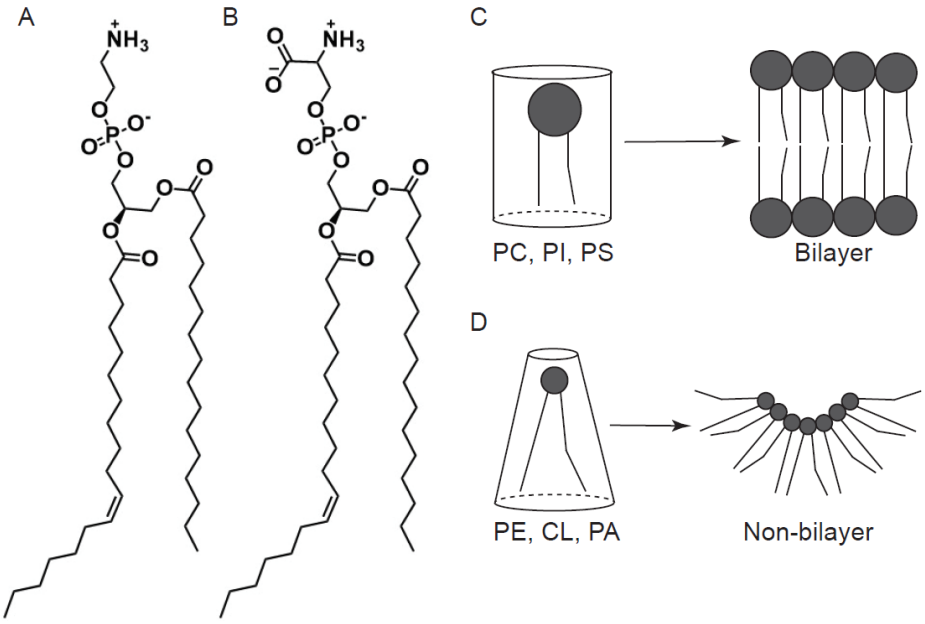

Figure 1.1 The structure of phosphatidylethanolamine (PE) and phosphatidylserine (PS).
(A) The ethanolamine "head" group, connected to a phosphate moiety, defines this phospholipid as PE. The two acyl chains connected to the glycerol backbone can vary, depicted here is 1-palmitoyl-2-oleoyl phosphatidylethanolamine. (B) A serine "head" group defines this phospholipid as PS, depicted here is 1-palmitoyl-2-oleoyl phosphatidylserine. PE and PS are the two phospholipids mainly focused on in this dissertation. (C) Cylinder-shaped phospholipids such as PC, PI, and PS form bilayer structures. (D) Cone-shaped phospholipids such as PE, CL, and PA form non-bilayer structures. PC, phosphatidylcholine; PI, phosphatidylinositol; CL, cardiolipin; PA, phosphatidic acid.

Phospholipid Function

The main function of phospholipids is to form biological membranes that enclose cells and organelles, acting as a physical barrier from the surrounding environment to provide defined compartments that allow essential biochemical reactions and physiological processes to occur. The three unique characteristics of each phospholipid-

the type of head group, the length of the acyl chain and the saturation of the acyl chains-influence the bulk physiochemical features of the membranes including viscosity, curvature, thickness, and electrostatic charge of the bilayer (Casares et al., 2019; de Kroon et al., 2013). Combinations of these three characteristics gives rise to thousands of unique phospholipids that are present in different stoichiometries in each organellar membrane (Yang et al., 2018). A unique phospholipid composition defines each organelle and influences the function of its membrane proteins (Yang et al., 2018; Zinser et al., 1991). Phospholipids interact with both integral membrane proteins that are embedded in the membrane as well as proteins that are peripherally associated with the membrane through hydrophobic or electrostatic forces (Casares et al., 2019). Through their bulk membrane properties, phospholipids contribute to membrane budding, tubulation, fission/fusion, and cell division (de Kroon et al., 2013). In addition to affecting bulk membrane properties, phospholipids can also directly affect protein activity through specific interactions with membrane proteins (Basu Ball et al., 2018b). Importantly, phospholipids can also act as signaling molecules as first and second messengers (de Kroon et al., 2013). The signaling role of phosphatidylinositol and its derivatives have been studied in great detail (reviewed in Balla, 2013). Therefore, phospholipids are not only diverse in terms of their structure but also in terms of their function.

Yeast *Saccharomyces cerevisiae* as a model organism for phospholipid research

Historically, yeast *Saccharomyces cerevisiae* has served as an excellent model organism to study phospholipid biosynthesis, regulation and function (Henry et al., 2012). There are a number of reasons for this. First, the phospholipid biosynthetic enzymes and

their localization are highly conserved from yeast to humans (Henry et al., 2012; de Kroon et al., 2013). As a result, the phospholipid composition of different organelles from yeast to humans is also highly conserved (Henry et al., 2012; Daum, 1985). Second, unlike in mammals, where many of the phospholipid biosynthetic pathways are essential (Vance 2014), most yeast mutants of phospholipid biosynthetic enzymes are viable or at least conditionally viable making *in vivo* studies of phospholipid function feasible. Third, yeast are a genetically tractable model organism with a fully sequenced genome, well-annotated genes, and the availability of molecular tools to precisely and easily edit genes (de Kroon et al., 2013).

Importantly, yeast can be cultured in defined media conditions. This is particularly important when studying phospholipids because the phospholipid composition depends on the nutritional and culture conditions (Storey et al., 2001; Gohil et al., 2005; Santos and Riezman, 2012). Phospholipid precursors such as ethanolamine, choline, and inositol, are abundantly found in undefined "complex" yeast media. These phospholipid precursors present in the media are imported by the cells and contribute to phospholipid biosynthesis, which makes it very difficult to control the levels of the phospholipids in the cell. Defined synthetic yeast media can be made without these phospholipid precursors. Thus, we have utilized yeast growth in defined synthetic media to control phospholipid levels to further our understanding of their precise roles in various cellular processes.

Phospholipid biosynthetic pathways in the yeast *Saccharomyces cerevisiae*

Saccharomyces cerevisiae as a model organism for the study of phospholipids has extensively contributed to the characterization of all the major phospholipid biosynthetic

enzymes (Figure 1.2) (Henry et al., 2012). PA biosynthesized from a glycolytic intermediate - dihydroxyacetone phosphate (DHAP) is the simplest phospholipid that serves as a precursor for many other phospholipids (Figure 1.2) (Carmen and Han, 2011; Henry et al., 2012). DHAP is reduced to form glycerol-3-phosphate (Gro-3-P), which provides the glycerol backbone of a PA and PA-derived phospholipids.

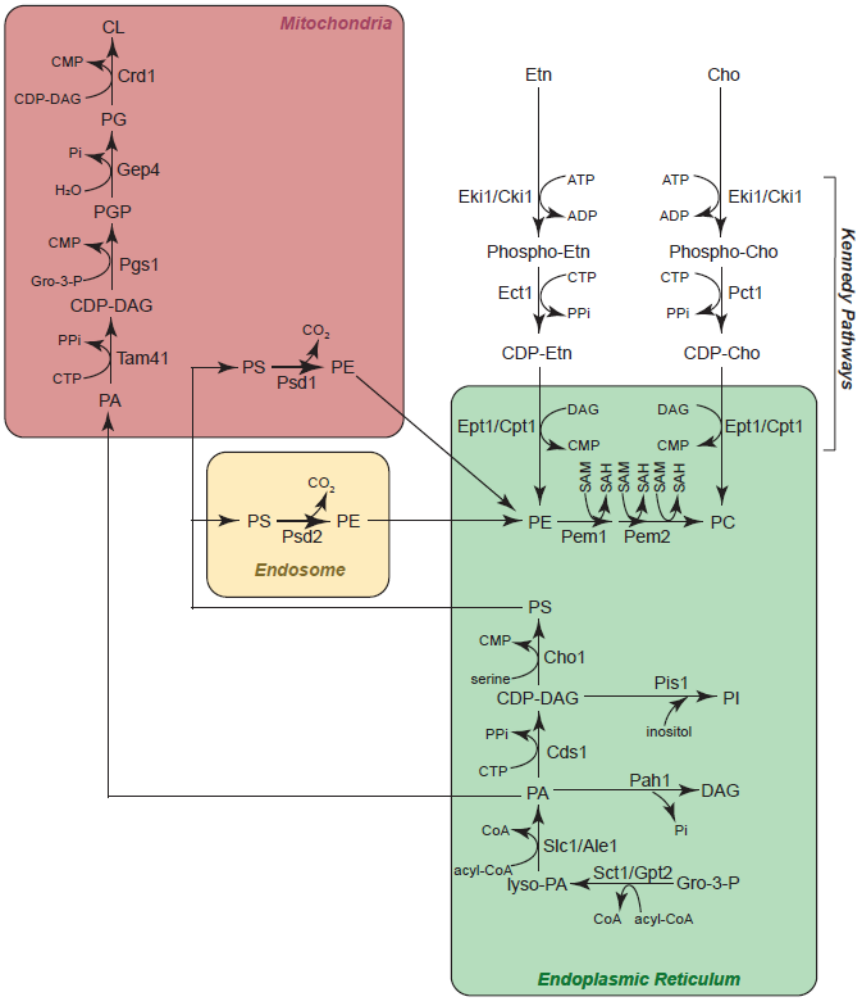

Figure 1.2 Phospholipid biosynthetic pathways in yeast *Saccharomyces cerevisiae*.
The pathways for biosynthesis of phospholipids PE, PC, CL, PI, PS, and PA are depicted schematically. Gro-3-P, Glycerol-3-Phosphate; Pi, Phosphate; PPi, Pyrophosphate; CTP, cytidine triphosphate; CDP, cytidine diphosphate; CMP, cytidine monophosphate; DAG, diacylglycerol; ATP, adenosine triphosphate; ADP, adenosine diphosphate; SAM, S-adenosyl methionine; SAH, S-adenosyl homocysteine.

Gro-3-P is acylated to form lyso-PA by Gro-3-P acyltransferases, Sct1 and Gpt2. Finally, lyso-PA receives its second acyl chain from lysophospholipid acyltransferases, Slc1 and Ale1, to form PA. All five other major phospholipids are biosynthesized through two different pathways: 1) the cytidine diphosphate-diacylglycerol (CDP-DAG) pathway, which utilizes CDP-DAG and 2) the Kennedy pathways, which utilize DAG. PA is converted to CDP-DAG in the ER by Cds1, a phosphatidate cytidylyltransferase. The CDP-DAG pathway is the *de novo* pathway for the biosynthesis of all other phospholipids. For example, phosphatidylinositol synthase (Pis1) utilizes CDP-DAG and inositol to biosynthesize PI in the ER (Paulus and Kennedy, 1960; Fischl and Carmen, 1983). CL is biosynthesized in the mitochondria from two molecules of CDP-DAG through the sequential action of mitochondrial enzymes Tam41, phosphatidylglycerophosphate (PGP) synthase (Pgs1), PGP phosphatase (Gep4), and cardiolipin synthase (Crd1) (Basu Ball et al., 2018b; Henry et al., 2012). Interestingly, it was recently discovered that mitochondria contain their own CDP-DAG synthesizing enzyme, Tam41, to provide CDP-DAG for CL biosynthesis (Tamura et al., 2013). Finally, CDP-DAG is also utilized in the biosynthesis of PS, which serves as a substrate for PE and PC biosynthesis. Serine and CDP-DAG are converted to PS by ER-localized enzyme PS synthase, which is encoded by Cho1 (Letts et al., 1983; Bae-Lee and Carmen, 1984). PS is decarboxylated by either mitochondrially-localized PS decarboxylase Psd1 or endosome-localized Psd2 to biosynthesize PE. Psd1-synthesized PE is a major contributor of both mitochondrial and cellular PE (Trotter et al., 1993; Clancey et al., 1993; Bürgermeister et al., 2004). On the other hand, Psd2-synthesized PE is mainly utilized in the methylation reactions of PE methyltransferases

(Pem1/Pem2) in the ER to synthesize PC (Gulshan et al., 2010; Trotter and Voelker, 1995; Bürgermeister et al., 2004; Gaynor and Carmen, 1990; Kodaki and Yamashita, 1987).

The Kennedy pathways represent alternate pathways for PE and PC biosynthesis (Figure 1.2). In this pathway, soluble precursors - ethanolamine (Etn) and choline (Cho) - are utilized to biosynthesize PE and PC respectively. Both Etn and Cho undergo three sequential reactions for biosynthesis of their respective phospholipids, 1) phosphorylation, 2) cytidylylation, and 3) phospho-Etn/Cho transfer onto DAG. The enzymes required for these reactions are 1) Eki1/Cki1, 2) Ect1/Pct1, and 3) Ept1/Cpt1 (Henry et al., 2012; Kim et al., 1999; Henneberry et al., 2001; McGee et al., 1994; Min-Seok et al., 1996; Tsukagoshi et al., 1987). Interestingly, only the cytidylylation step performed by Ect1 and Pct1 is unique for PE and PC biosynthesis respectively. The reactions carried out by Eki1/Cki1 and Ept1/Cpt1 are redundant for Etn and Cho utilization (Kim et al., 1999; Henneberry et al., 2001; McGee et al., 1994; Menon and Stevens, 1992). Therefore, all major phospholipids are synthesized in yeast with redundant pathways present for PE and PC biosynthesis.

Intracellular Phospholipid Transport Mechanisms

Most phospholipid biosynthesis occurs in the ER; however, how these phospholipids are transported throughout the cell to different membrane-enclosed organelles is not fully understood. Phospholipids are likely not transported through the cell by diffusion because they are hydrophobic molecules and are not readily soluble in water (Vance 2015). Traditionally, it was thought that phospholipids are transported

through an inter-organelle endomembrane system originating at the ER that utilizes vesicles to transport proteins to other organelles (Figure 1.3).

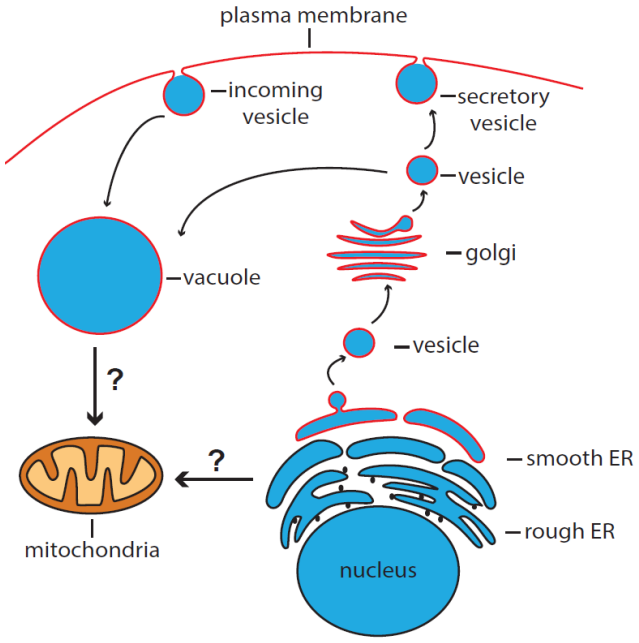

Figure 1.3 Vesicular transport of phospholipids.
A model depicting the biosynthesis of phospholipids in the smooth ER and their transport throughout the endomembrane system via vesicles. The mitochondria are not part of the endomembrane system, begging the question of how the mitochondria receives its phospholipids.

Indeed, vesicular transport was thought to be the major mechanism by which phospholipids were transported throughout the cell (Novick and Schekman, 1979). But a number of follow-up studies have raised questions about the overall contribution of vesicle mediated intracellular trafficking of phospholipids. First, each organelle could not have a unique phospholipid composition by this mechanism of phospholipid transport due to a lack of lipid specificity (Hanada 2018; Balla et al., 2019). Second, the rate by which newly synthesized phospholipids can be transported to the plasma membrane is faster than that of newly synthesized protein (Kaplan and Simoni et al., 1985), implying different modes

of transport. Third, mitochondria, which are not a part of the endomembrane system but contains phospholipids derived from the ER, begs the question of how they receive phospholipids (Figure 1.3). Furthermore, an elegant study by the Vance group showed that inhibition of vesicular trafficking with inhibitors and decreased temperature did not reduce phospholipid trafficking throughout the cell (Vance et al., 1991). This data suggests that there must be alternate machinery responsible for transporting phospholipids that is independent of vesicular transport. For phospholipid transport to occur, phospholipids must be: 1) taken from the donor membrane, 2) shielded from the aqueous environment, and 3) dropped off at the recipient membrane. Protein-mediated transport of phospholipids has been proposed to accomplish all the above criteria. In fact, several phospholipid transport proteins, referred to as lipid transfer proteins (LTPs), have been identified to date (Hanada 2018; Balla et al., 2019).

LTPs are characteristically one or more proteins in a complex that have a hydrophobic cavity to extract and exchange lipid molecules between membranes (Hanada 2018; Tamura et al., 2020; Nishimura and Stefan, 2020). These proteins are often cytoplasmic and can act through one of the two mechanisms (Figure 1.4). The first mechanism is the "soluble-carrier" LTP which involves a soluble protein(s) that undergo seven distinct steps to transfer the phospholipid from the donor membrane to the acceptor membrane: 1) Recognition and docking of the LTP to the donor membrane, 2) Extraction of a specific phospholipid by the LTP, 3) Detachment of the LTP from the membrane and the closing of the hydrophobic cavity to shield the phospholipid from the aqueous environment, 4) Recruitment of LTP to the acceptor membrane, 5) Docking of the LTP to

the acceptor membrane, 6) Opening of the hydrophobic cavity to release the phospholipid into the acceptor membrane, and finally 7) the detachment of LTP from the membrane (Nishimura and Stefan, 2020). These soluble carrier LTPs are often localized to membrane contact sites (MCSs), where the shorter distance to diffuse between the two membranes may allow for ease of recruitment (Nishimura and Stefan, 2020; Hanada 2018).

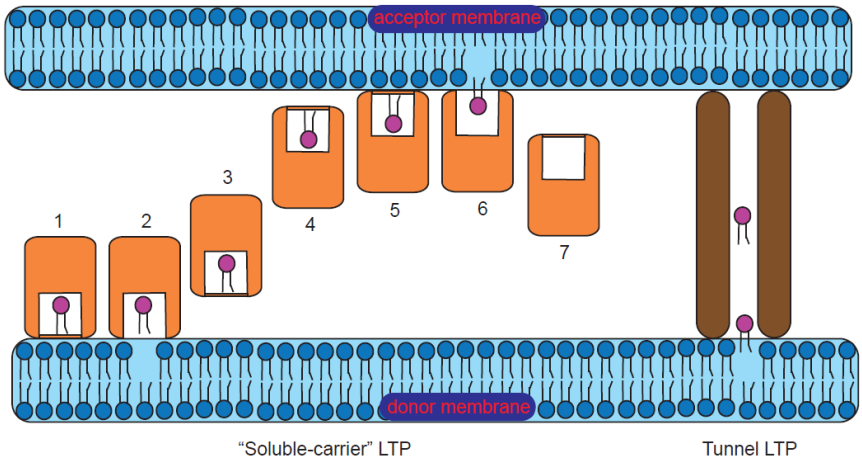

Figure 1.4 Mechanisms of Lipid Transport Protein (LTP)-mediated phospholipid transport.
A model depicting the mechanism of 1) "soluble-carrier" LTPs in orange which undergoes seven distinct steps to transfer a phospholipid from the donor membrane to the acceptor membrane, and 2) tunnel LTPs in brown that create a hydrophobic tube to transport phospholipids. The above figure is modified from Nishimura and Stefan, 2020.

The second mechanism is the "tunnel" LTP, which bridges two membranes with a hydrophobic cavity in the middle that forms a conduit for lipid transfer (Tamura et al., 2020). The regulation of tunnel LTPs is not well understood. LTPs of both mechanisms transfer phospholipids down their lipid concentration gradient in an ATP-independent manner (Lev 2012). In order to maintain the unique phospholipid composition of each organelle, LTPs generate unidirectional flux of phospholipids by coupling metabolic

reactions specific to the recipient organelle to produce a thermodynamically favored direction of transport (Hanada 2018).

Mitochondrial Phospholipid Transport

Mitochondria contain all six major phospholipids; however, how most of these phospholipids are imported into the mitochondria is not known (Figure 1.5). In mammalian cells, soluble carrier LTP, VAT1, has been shown to facilitate PS transport from the ER to the mitochondria (Junker and Rapoport, 2015; Wanatabe et al., 2020). There is no yeast homolog of VAT1, instead import of PS into the mitochondria is thought to be facilitated by the ER and Mitochondria Encounter Structure (ERMES). ERMES is the MCS that tethers the ER to the mitochondria in yeast and is composed of four core subunits (Kornmann et al., 2009). This complex is hypothesized to transfer PS from the ER to the mitochondria via the tunnel mechanism (Kawano et al., 2018; Tamura et al., 2020; AhYoung et al., 2015; Jeong et al., 2016; Jeong et al., 2017). Controversy surrounds whether ERMES is required for PS transport to the mitochondria because loss of ERMES subunits do not affect the steady state levels of PS or PE in the mitochondria (Nguyen et al., 2012; Baker et al., 2016). However, it is possible that redundant phospholipid transport pathways mask the role of ERMES in the transport of PS *in vivo* (Elbaz-Alon et al., 2014; Hönscher et al, 2014). Interestingly, dominant mutations in the Vps13-vacuole and mitochondrial patch (Vps13-vCLAMP), the vacuole and mitochondria MCS, can bypass defects associated with ERMES deletion (Lang et al., 2015; Gonzalez Montoro et al., 2018). Additionally, the human homolog of Vps13 has been shown to transfer both PS and PE *in vitro* (Kumar et al., 2018). The divide in the field can only be remedied with

careful *in vivo* experiments to establish if both ERMES and Vps13 transport PS from the ER to the mitochondria.

Much more is known about intra-mitochondrial phospholipid transport. For example, the transporters from the OMM to the IMM have been identified for PA (Ups1/Mdm35), PS (Ups2/Mdm35 and MICOS), and PC (mammalian STARD7) (Connerth et al., 2012; Wantanabe et al., 2015; Miyata et al., 2016; Aaltonen et al., 2016; Saita et al., 2018). Ups1/Mdm35, Ups2/Mdm35, and STARD7 use the soluble-carrier LTP mechanism of phospholipid transport, much like the VAT1. The MCS that tethers the OMM to the IMM is called the mitochondrial contact site and cristae organizing system (MICOS). It is a unique complex containing six subunits that facilitate phospholipid transport without physically binding phospholipids. MICOS is thought to facilitate PS transport from the OMM to the IMM by closing the distance between these two membranes such that Psd1, the mitochondrial phosphatidylserine decarboxylase, can act *in trans* converting PS presenting in the OMM to PE, usurping the need for physical phospholipid transport. From this MICOS-facilitated mechanism of phospholipid "transport," MICOS could also be involved in PE export from the IMM to the OMM. Much like ERMES, the *in vivo* data for the role of MICOS in PS transport is lacking and needs to be further investigated. Identifying the protein machinery required for mitochondrial phospholipid transport is important because it is an essential activity for mitochondrial biogenesis, function, and formation as described in the next section.

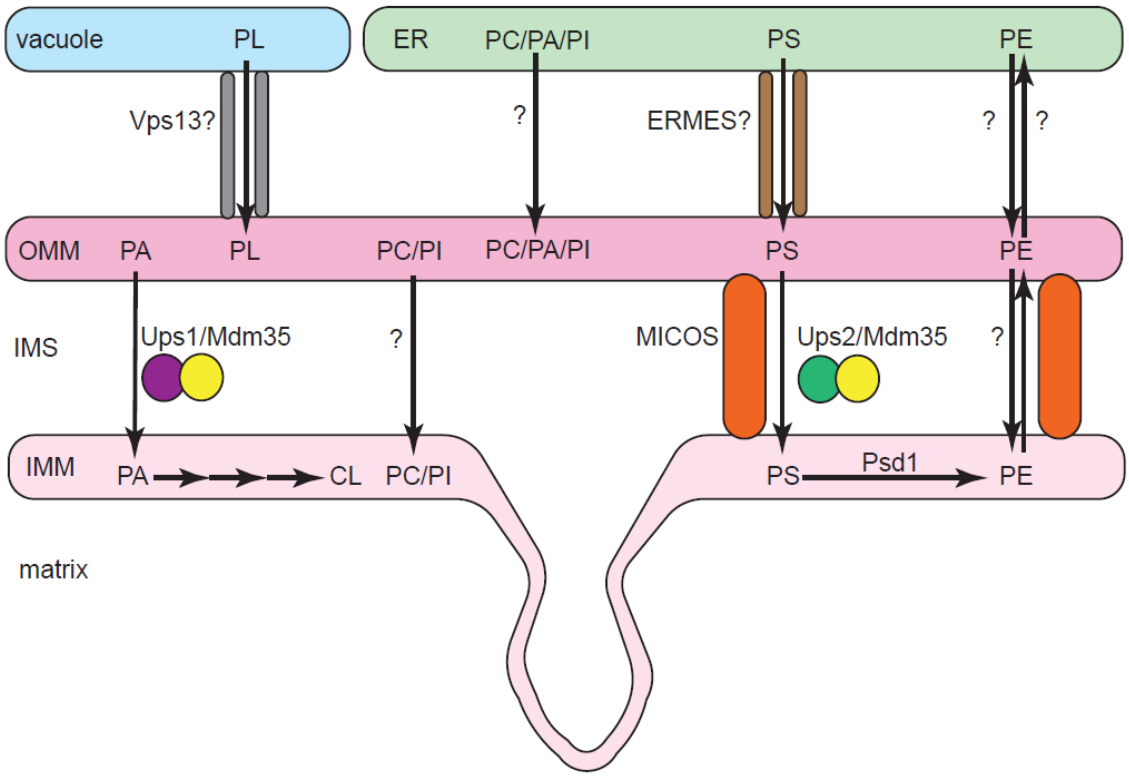

Figure 1.5 Proteins involved in phospholipid transport to the mitochondria.
The model depicts yeast proteins involved in phospholipid transport from the ER and vacuole to the mitochondria. Ups1, Ups2, and Mdm35 are depicted as "soluble-carrier" LTPs. Vps13 and ERMES are depicted as tunnel LTPs. Finally, MICOS has been implicated in PS import and PE export. OMM, outer mitochondrial membrane; IMM, inner mitochondrial membrane; IMS, intermembrane space.

The Impact of Phospholipid Composition on Mitochondrial Function

Mitochondria are unique double membrane-bound organelles, known for their role in energy production. The outer mitochondrial membrane (OMM) contains pores that make this membrane highly permeable. The inner mitochondrial membrane (IMM) is characterized by its ion impermeability and the distinctive curves in the membrane, known as the cristae. The IMM is the site of the energy production machinery: the mitochondrial respiratory chain (MRC), which generates an electrochemical gradient to drive ATP

production. The MRC consists of four multimeric complexes that transport electrons from cellular reducing agents to molecular oxygen, a process coupled to the pumping of protons from the mitochondrial matrix to the inter-membrane space (IMS) of the mitochondria leading to the generation an electrochemical gradient (Lasserre et al, 2015). In yeast *Saccharomyces cerevisiae*, complex I (CI) is limited to three separate enzymes that are each nicotinamide adenine dinucleotide (NADH) dehydrogenases instead of a multiprotein complex as found in mammals (Joseph-Horne et al., 2001). Yeast and human complex II (CII) consist of four subunits and acts as succinate dehydrogenase. CI and CII transfer electrons from NADH and succinate, respectively, to ubiquinone, a lipid soluble mobile electron carrier. Ubiquinone, also known as Coenzyme Q, transfers two electrons to complex III (CIII), which is also referred to as cytochrome *c* reductase. The transfer of electrons from CIII to the single electron carrier cytochrome *c*, is coupled to pumping of protons from the matrix to the IMS to generate the electrochemical gradient. Complex IV, or cytochrome *c* oxidase, receives electrons from cytochrome *c*, which are ultimately accepted by molecular oxygen, reducing it to water. During this electron transfer, protons are again pumped from the matrix to the IMS. The electrochemical gradient, thus formed by the proton pumping activity of CIII and CIV, drives the synthesis of ATP via ATP synthase, which is localized in the IMM. The presence of the MRC complexes and ATP synthase within the IMM predicts that their function is influenced by the surrounding phospholipids.

Mitochondria contain all six major phospholipids, although only PE and CL are biosynthesized *in situ* (Horvath and Daum, 2013; Basu Ball et al., 2018b). In fact, the

signature phospholipid of the mitochondria, CL, is solely biosynthesized in the mitochondria. Importantly, mitochondria contain the highest non-bilayer to bilayer phospholipid ratio of all the organelle membranes, and this phospholipid composition is highly conserved from yeast to humans (Horvath and Daum, 2013; Basu Ball et al., 2018b). The phospholipid composition of the OMM and IMM are distinct with the IMM enriched in PE and CL. The enrichment of these non-bilayer phospholipids suggests their specialized role in mitochondrial function (Gohil and Greenberg, 2009). Indeed, a large body of literature describes the specific roles of PE and CL in different aspects of mitochondrial function (reviewed in Basu Ball et al., 2018b). PE is specifically required for CIII and CIV activity of the MRC, thus loss of mitochondrial PE biosynthesis in *psd1Δ* cells results in reduced oxygen consumption, ATP synthesis, and respiratory growth (Baker et al., 2016; Böttinger et al., 2012). CL is required for the formation of supercomplexes, which are supra-molecular structures consisting of MRC CIII and CIV (Pfeiffer et al., 2003; Zhang et al., 2002). Supercomplexes have been suggested to play an important role in electron channeling, which would increase the efficiency of the MRC (Schägger and Pfeiffer, 2000; Acín-Pérez et al., 2008). In addition to mitochondrial bioenergetics, PE and CL also have roles in mitochondrial dynamics and protein import (DeVay et al., 2009; Bustillo-Zabalbeitia et al., 2014; Osman et al., 2009; Joshi et al., 2012; Becker et al., 2013; Jiang et al., 2000). Surprisingly, the most abundant bilayer-forming mitochondrial phospholipid, PC, is largely dispensable for mitochondrial function (Baker et al., 2016) highlighting the specific requirement of non-bilayer phospholipids in mitochondrial function and formation.

CHAPTER 2

VPS39 IS REQUIRED FOR ETHANOLAMINE-STIMULATED ELEVATION IN MITOCHONDRIAL PHOSPHATIDYLETHANOLAMINE*

---

* This research was originally published in Biochimica et Biophysica Acta Molecular and Cell Biology of Lipids. Iadarola DM, Basu Ball W, Trivedi PP, Fu G, Nan B, Gohil VM. Vps39 is required for ethanolamine-stimulated elevation in mitochondrial phosphatidylethanolamine. *Biochim Biophys Acta Mol Cell Biol Lipids*. 2020; 1865(6):158655.

Summary:

Mitochondrial membrane biogenesis requires the import of phospholipids; however, the molecular mechanisms underlying this process remain elusive. Recent work has implicated membrane contact sites between the mitochondria, endoplasmic reticulum (ER), and vacuole in phospholipid transport. Utilizing a genetic approach focused on these membrane contact site proteins, we have discovered a 'moonlighting' role of the membrane contact site and vesicular fusion protein, Vps39, in phosphatidylethanolamine (PE) transport to the mitochondria. We show that the deletion of Vps39 prevents ethanolamine-stimulated elevation of mitochondrial PE levels without affecting PE biosynthesis in the ER or its transport to other sub-cellular organelles. The loss of Vps39 did not alter the levels of other mitochondrial phospholipids that are biosynthesized ex situ, implying a PE-specific role of Vps39. The abundance of Vps39 and its recruitment to the mitochondria and the ER is dependent on PE levels in each of these organelles, directly implicating Vps39 in the PE transport process. Deletion of essential subunits of Vps39-containing complexes, vCLAMP and HOPS, did not abrogate ethanolamine-stimulated PE elevation in the mitochondria, suggesting an independent role of Vps39 in intracellular PE trafficking. Our work thus identifies Vps39 as a novel player in ethanolamine-stimulated PE transport to the mitochondria.

Introduction:

Mitochondrial membrane biogenesis requires coordinated import and synthesis of proteins as well as phospholipids, the major lipid constituents of mitochondrial membranes (Zinser et al., 1991). The molecular machineries required for mitochondrial

protein import have been studied in great detail (Schmidt et al., 2010); however, the molecular mechanism(s) by which phospholipids are transported to the mitochondria have remained elusive (Tamura et al., 2014; Tatsuta et al., 2014; Voelker 2009). While phospholipid movement between the organelles of the endomembrane system can occur via vesicles, mitochondria are not part of the vesicular transport system. This raises an intriguing question – how do mitochondria acquire phospholipids? A number of non-vesicular lipid trafficking mechanisms such as inter-organelle phospholipid transfer proteins have been proposed (Voelker 2009; Prinz 2014; Wong et al., 2018), but the contribution of these mechanisms to phospholipid transport to the mitochondria is not fully understood (Vance 2015).

Mitochondria contain all the major classes of phospholipids, a majority of which are synthesized in the ER (Flis and Daum 2013). One of the key phospholipids required for mitochondrial respiratory function is phosphatidylethanolamine (PE) (Baker et al., 2016; Böttinger et al., 2012; Tasseva et al., 2013), which in the yeast Saccharomyces cerevisiae is synthesized via three main pathways that are localized to different sub-cellular compartments (Figure 2.1A). Decarboxylation of phosphatidylserine (PS) either by Psd1 in the mitochondria or by Psd2 in the endosomal compartment generates PE (Trotter et al.,1993; Clancey et al., 1993; Trotter and Voelker 1995; Gulshan et al., 2010). PE can also be synthesized de novo from ethanolamine (Etn) through the cytidine diphosphate (CDP)-Etn Kennedy pathway via the sequential action of the enzymes Eki1, Ect1, and Ept1 (Figure 2.1A) (Henry et al., 2012). In wild type (WT) yeast cells, Psd1-derived PE is the major source of mitochondrial and cellular PE (Bürgermeister et al.,

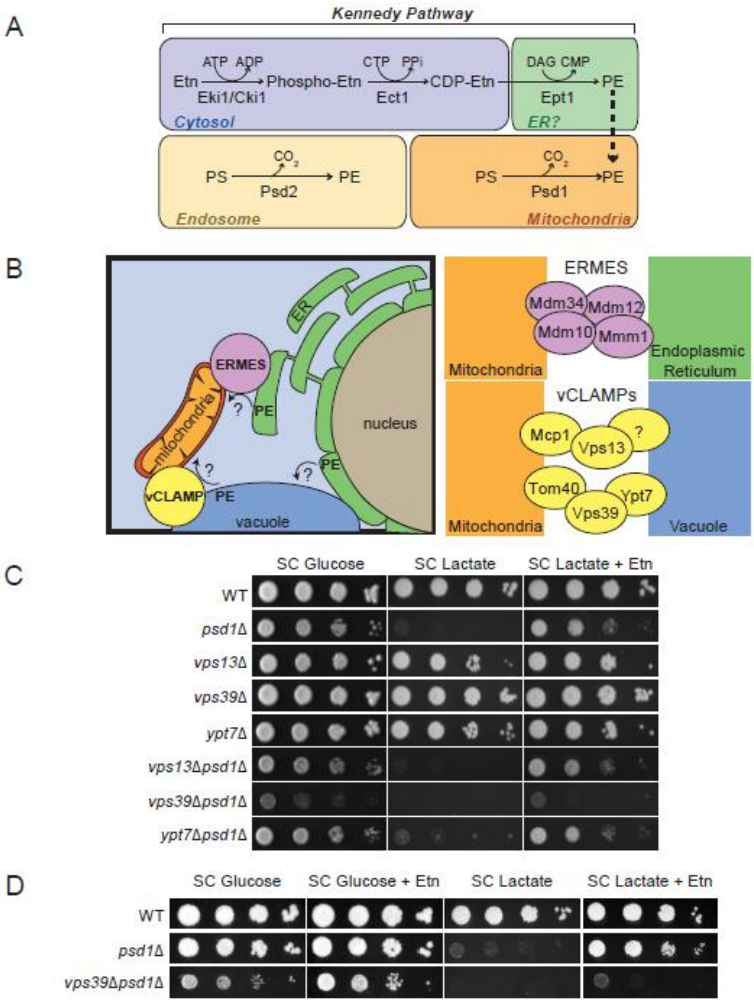

Figure 2.1 Utilizing Etn-supplementing strategy to identify proteins required for PE transport to the mitochondria.

(A) Major phosphatidylethanolamine biosynthetic pathways in the yeast *Saccharomyces cerevisiae*. (B) Schematic representation of two membrane contact sites, ERMES and vCLAMP, connecting mitochondria with ER and vacuole, respectively. ERMES consists of Mdm34, Mdm12, Mdm10, and Mmm1. vCLAMPs consist of two independent complexes, one consisting of Vps39, Ypt7, Tom40 and the second consisting of Vps13, Mcp1, and an unknown vacuole anchor protein. (C) Ten-fold serial dilution of the indicated yeast mutants were seeded onto synthetic complete (SC) Glucose and SC Lactate ± Etn plates. Images were captured after 2d (SC Glucose media) and 5d (SC Lactate media) of growth at 30°C. (D) WT, *psd1Δ*, and *vps39Δpsd1Δ* were seeded onto SC Glucose ± Etn and SC Lactate ± Etn plates and imaged after 2d and 5d of growth at 30°C, respectively. The figures are representative image of three independent biological replicates. PE, phosphatidylethanolamine; PS, phosphatidylserine; Etn, ethanolamine; ATP, adenosine triphosphate, ADP, adenosine diphosphate; CTP, cytidine triphosphate; CDP, cytidine diphosphate; CMP, cytidine monophosphate; DAG, diacylglycerol; PPi, pyrophosphate; ERMES, endoplasmic reticulum-mitochondria encounter structure; vCLAMP, vacuole and mitochondria patch. Reprinted from Iadarola et al., 2020.

2004); however, PE synthesized via the Kennedy pathway can also be imported into the mitochondria, where it can functionally compensate for the loss of mitochondrial PE biosynthesis (Baker et al., 2016; Birner et al., 2001). This finding implies that mitochondrial PE transport machinery must exist; however, its identity has remained unknown.

New evidence (Kawano et al., 2018; Kumar et al., 2018; AhYoung et al., 2015; Jeong et al., 2016; Jeong et al., 2017) suggests that membrane contact sites (MCSs), regions of close apposition of organelle membranes, play an important role in the transport of phospholipids between organelles (Gatta and Levine 2017; Lahiri et al., 2015). Two mitochondrial MCSs directly implicated in phospholipid transport are Endoplasmic Reticulum Mitochondria Encounter Structure (ERMES), a protein complex that tethers the ER and mitochondria, and Vacuole and Mitochondria Patch (vCLAMP), which connects the vacuole to mitochondria (Figure 2.1B) (Kornmann et al., 2009; Elbaz-Alon et al., 2014; Hönscher et al., 2014). Recent structural studies documenting the presence of phospholipid-binding hydrophobic pockets in the subunits of ERMES and vCLAMP further supports a direct role of these MCS's in inter-organelle phospholipid transport (Kawano et al., 2018; Kumar et al., 2018; AhYoung et al., 2015; Jeong et al., 2016; Jeong et al., 2017). Previously, we had explored the role of ERMES in the transport of the CDP-Etn Kennedy pathway PE to the mitochondria and found that although ERMES facilitated the efficient Etn-mediated rescue of respiratory growth of mitochondrial PE-deficient *psd1*Δ cells, ERMES was not essential for PE transport (Baker et al., 2016). Consistently, the phospholipid transport tunnel formed by the ERMES components, Mdm12-Mmm1

does not bind PE in vitro (Jeong et al., 2016). Recently, it has been shown that vCLAMP can serve as an alternate route for phospholipid transport from the ER to the mitochondria via vacuole (Elbaz-Alon et al., 2014). Therefore, in this report, we explored the role of vCLAMP in the transport of PE to the mitochondria and demonstrate that Vps39, a vCLAMP subunit, has a critical role in Etn-stimulated trafficking of PE from the ER to the mitochondria.

Materials and Methods

Yeast strains, growth medium composition, and culture conditions

Yeast *Saccharomyces cerevisiae* strains used in the study are listed in Table 2.1. Yeast cells were routinely maintained and pre-cultured in YPGE medium (1% yeast extract, 2% peptone, 3% glycerol, and 1% ethanol) to prevent the loss of mitochondrial DNA from *psd1*Δ cells. In the cases where cells cannot grow in YPGE medium or wherever indicated, the pre-cultures were prepared in the YPD medium (1% yeast extract, 2% peptone, and 2% glucose). To allow for efficient incorporation of Etn in PE, yeasts were grown in synthetic complete (SC) medium, which contained 0.17% yeast nitrogen base without amino acids, 0.5% ammonium sulfate, 0.2% dropout mix containing amino acids, and either 2% glucose or 2% lactate (pH 5.5) (Amberg et al., 2005). Final cultures were started at an optical density (OD600) of 0.1 and were grown to late logarithmic phase at 30°C. Solid media were prepared by the addition of 2% agar. For measuring growth on solid media, 3 μL of 10-fold serial dilutions of pre-cultures were seeded onto SC Glucose or SC Lactate plates and incubated at 30°C for the indicated times. For Etn supplementation experiments, 2mM Etn was added to SC growth medium. Petite

formation was determined by spreading 100µl of SC Glucose-grown cells (~200 cells) onto YPD and YPGE plates. The percent of petite colonies was determined by counting the number of colonies in each of these growth media. Single and double knockout yeast strains were constructed by one-step gene disruption using geneticin, hygromycin, and nourseothricin cassettes (Janke et al., 2004).

Table 2.1 *Saccharomyces cerevisiae* strains used in this study.
Reprinted from Iadarola et al., 2020.

Yeast Strains	**Genotype**	**Source**
BY4741 WT	*MATa, his3Δ1, leu2Δ0, met15Δ0, ura3Δ0*	Miriam L. Greenberg
BY4741 *psd1*Δ	*MATa, his3Δ1, leu2Δ0, met15Δ0, ura3Δ0, psd1::hphNT1*	This Study
BY4741 *vps39*Δ	*MATa, his3Δ1, leu2Δ0, met15Δ0, ura3Δ0, vps39::KanMX4*	Open Biosystems
BY4741 *vps13*Δ	*MATa, his3Δ1, leu2Δ0, met15Δ0, ura3Δ0, vps13::KanMX4*	Open Biosystems
BY4741 *ypt7*Δ	*MATa, his3Δ1, leu2Δ0, met15Δ0, ura3Δ0, ypt7::KanMX4*	Open Biosystems
BY4741 *vps41*Δ	*MATa, his3Δ1, leu2Δ0, met15Δ0, ura3Δ0, vps41::KanMX4*	Open Biosystems
BY4741 *vps11*Δ	*MATa, his3Δ1, leu2Δ0, met15Δ0, ura3Δ0, vps11::KanMX4*	This study
BY4741 *vps33*Δ	*MATa, his3Δ1, leu2Δ0, met15Δ0, ura3Δ0, vps33::KanMX4*	This study
BY4741 *vps39*Δ*psd1*Δ	*MATa, his3Δ1, leu2Δ0, met15Δ0, ura3Δ0, vps39::KanMX4, psd1:: hphNT1*	This study
BY4741 *vps13*Δ*psd1*Δ	*MATa, his3Δ1, leu2Δ0, met15Δ0, ura3Δ0, vps13::KanMX4, psd1:: hphNT1*	This study
BY4741 *ypt7*Δ*psd1*Δ	*MATa, his3Δ1, leu2Δ0, met15Δ0, ura3Δ0, ypt7::KanMX4, psd1:: hphNT1*	This study
BY4741 *vps41*Δ*psd1*Δ	*MATa, his3Δ1, leu2Δ0, met15Δ0, ura3Δ0, vps41::KanMX4, psd1:: hphNT1*	This study
BY4741 *vps11*Δ*psd1*Δ	*MATa, his3Δ1, leu2Δ0, met15Δ0, ura3Δ0, vps11::KanMX4, psd1:: hphNT1*	This study
BY4741 *vps33*Δ*psd1*Δ	*MATa, his3Δ1, leu2Δ0, met15Δ0, ura3Δ0, vps33::KanMX4, psd1:: hphNT1*	This study

Table 2.2 Continued *Saccharomyces cerevisiae* strains used in this study.

Yeast Strains	Genotype	Source
CUY8994 GFP-Vps39	*MATalpha, leu2-3, leu2-112, ura3-52, his3-Δ200, trp1-Δ101, lys2-801, suc2-Δ9, GAL, VPS39 ClonNAT-TEFpr-GFP, SHM1 3xmCherry-HIS3*	Christian Ungermann
CUY8992 GFP-Vps41	*MATalpha, leu2-3, leu2-112, ura3-52, his3-Δ200, trp1-Δ101, lys2-801, suc2-Δ9, GAL, VPS41 ClonNAT-TEFpr-GFP, SHM1 3xmCherry-HIS3*	Christian Ungermann
CUY8994 GFP-Vps39 *psd1*Δ	*MATalpha, leu2-3, leu2-112, ura3-52, his3-Δ200, trp1-Δ101, lys2-801, suc2-Δ9, GAL, VPS39 ClonNAT-TEFpr-GFP, SHM1 3xmCherry-HIS3, psd1::HphMX4*	This study
CUY8992 GFP-Vps41 *psd1*Δ	*MATalpha, leu2-3, leu2-112, ura3-52, his3-Δ200, trp1-Δ101, lys2-801, suc2-Δ9, GAL, VPS41 ClonNAT-TEFpr-GFP, SHM1 3xmCherry-HIS3, psd1::HphMX4*	This study

Table 2.3 Plasmids used in this study.
Reprinted from Iadarola et al., 2020.

Plasmid	Source
pRS416	Craig D. Kaplan
pRS426	Craig D. Kaplan
pRS426 Ept1-V5 (contains endogenous Ept1 promoter)	This study
pRS416 6xHis2xHA-Vps39 (contains endogenous Vps39 promoter)	This study
pRS416 6xHis2xHA-Vps39 431-1049 aa (contains endogenous Vps39 promoter)	This study
pRS416 6xHis2xHA-Vps39 531-1049 aa (contains endogenous Vps39 promoter)	This study
pRS416 6xHis2xHA-Vps39 1-860 aa (contains endogenous Vps39 promoter)	This study
pRS416 6xHis2xHA-Vps39 1-980 aa (contains endogenous Vps39 promoter)	This study

Table 2.4 Oligonucleotides used in this study.
Reprinted from Iadarola et al., 2020.

Oligonucleotide Number	Sequence (5' to 3')
1	CCCTCCGAGCTCAACCTTAGTTGGCGCCATGTGTGTA
2	CCCCATTCTAGACATTTAATTTTTGGTATAAATTGATATT
3	CCGCGGTGGCGGCCGCTCTAGAACT
4	CCCATGACGCGTAGCGTAGTCTGGGAC
5	CCCTAAACGCGTTTAAGAGCTCAAAAGCTACACT
6	CCCATCGGATCCTTACTTATTATTTAGCTCATTTATA
7	CCCGTTGAGCTCAGTGACTTGTAAGTAAACGG
8	CCCTTACTCGAGTGTCAGCTTGGAGCGCTTGAT
9	CCCTAAACGCGTGAAGAATCCTTGGATATATGTGCTATG
10	CCCTAAACGCGTGAAACTTATGACATCCCGCCACACTTA
11	CCCATCGGATCCATCTATCTCATCAAGTAATATATGCACAGC
12	CCCATCGGATCCTGATAAGACTCCATACGATGACATGCGTTC

Plasmids and Molecular Biology

All plasmids and oligonucleotides used in this study are listed in the Table 2.2 and Table 2.3, respectively. VPS39 constructs were engineered as follows: the full-length VPS39 insert was generated by PCR amplification of yeast genomic DNA with primer pair 5/6. Vps39 431-1049, 531-1049, 1-860, 1-980 truncations were generated with primer pairs 9/6, 10/6, 11/5, and 12/5 respectively. The VPS39 promoter region and 6xHis2xHA tag were amplified by PCR using primer pairs 1/2 and 3/4, respectively. Full length VPS39 and each of the VPS39 truncation PCR products were digested with the restriction enzymes MluI/BamHI. The DNA fragments encoding 6xHis2xHA and VPS39 promoter were digested with XbaI/MluI and SacI/XbaI, respectively. Each plasmid containing a full-length or a truncated version of VPS39 was constructed by ligation of SacI/BamHI digested pRS416 and the above-mentioned digested DNA fragments. The Ept1 insert was

generated by PCR amplification of genomic DNA with primer pair 7/8. The Ept1 insert and pRS426 containing V5-epitope encoding sequence were digested with SacI/XhoI and ligated. All constructs were sequence verified.

Organelle Isolation

Mitochondria

Isolation of crude and pure mitochondria was performed as previously described (Meisinger et al., 2006). Yeast cells grown to late logarithmic phase were pelleted (1-5 grams wet weight depending upon the intended use) and resuspended in DTT buffer (0.1 M Tris-HCl, pH 9.4, 10 mM DTT) for 20 min at 30°C. The cells in DTT buffer were pelleted by centrifugation at 3000xg for 5 min and were resuspended in spheroplasting buffer (1.2 M sorbitol, 20 mM potassium phosphate, pH 7.4) and treated with 3 mg zymolyase (US Biological Life Sciences) per gram of cell pellet for 45 min at 30°C. Spheroplasts were pelleted by centrifugation at 3000g for 5 min and were homogenized in homogenization buffer (0.6 M sorbitol, 10 mM Tris-HCl, pH 7.4, 1 mM EDTA, 1 mM PMSF [Phenylmethanesulfonyl fluoride], 0.2% [w/v] BSA [essentially fatty acid-free, Sigma-Aldrich]) with 15 strokes using a glass teflon homogenizer. After two subsequent centrifugation steps for 5 min at 1,500xg and 4,000xg, the final supernatant was centrifuged at 12,000xg for 15 min to pellet mitochondria. Crude mitochondrial fractions were resuspended in SEM buffer (250 mM sucrose, 1 mM EDTA, 10 mM MOPS-KOH, pH 7.2) and diluted to a protein concentration of 5 mg/ml. The diluted mitochondria are loaded on top of a step sucrose gradient, which consists of 15%, 23%, 32%, and 60% (w/v) sucrose in EM buffer (1 mM EDTA, 10 mM MOPS-KOH, pH 7.2) from top to bottom.

The gradient is centrifuged for 1 hr at 134,000xg at 4°C. Pure mitochondria were collected at the 32% to 60% sucrose interface, diluted with SEM buffer, and centrifuged at 12,000xg for 15 min. Pellets were resuspended in small volume of (~50 to 200 µL) SEM buffer and protein concentration was determined by BCA assay (PierceTM BCA Protein Assay, Catalog number: 23225).

ER

Isolation of pure ER was performed as described previously (Wuestehube et al., 1992). As described in the above section, 1-5 grams of yeast cells were spheroplasted with zymolyase and lysed with a homogenizer. After two subsequent centrifugation steps for 5 min at 1,500xg and 4,000xg, the final supernatant was centrifuged at 27,000xg for 15 min to pellet the crude ER fraction. The pellet was resuspended in 500 µL HEPES buffer (20 mM HEPES/KOH pH 6.8, 50 mM potassium acetate, 100 mM sorbitol, 2 mM EDTA, 1 mM DTT, and 1 mM PMSF). The crude ER fraction is loaded on top of a step-sucrose gradient consisting of two steps: 1.2 M sucrose above 1.5 M sucrose in HEPES buffer. The gradient was centrifuged at 100,000xg for 1 h at 4°C. Pure ER fraction was collected in the interface of 1.2 M/1.5 M sucrose gradient, diluted 10-fold in HEPES buffer and centrifuged at 27,000xg for 10 min. The purified ER fraction was resuspended in HEPES buffer and protein concentration was determined by BCA assay.

Vacuole

Isolation of pure vacuole was performed as previously described (Haas et al., 1995). Yeast spheroplasts were pelleted at 3,000xg at 4°C for 5 min. Dextran-mediated spheroplast lysis of 2.5-5 grams of yeast cells was performed by gently resuspending pellet

in 2.5 mL of 15% (w/v) Ficoll400 in Ficoll Buffer (10 mM PIPES/KOH pH 6.8, 200 mM sorbitol, protease inhibitor cocktail, and 1 mM PMSF) on ice. 200 µL of 0.4 mg/mL dextran in Ficoll buffer was added to the spheroplasts and was incubated for 2 min on ice. Spheroplasts were lysed by heating at 30°C for 75 sec and returned to ice. A step-ficoll gradient was constructed on top of the lysate with 3 mL each of 8%, 4%, and 0% (w/v) Ficoll400 in Ficoll Buffer. The step-gradient was centrifuged at 110,000xg for 90 min at 4°C. Vacuoles were removed from the 0%/4% Ficoll interface and protein concentration was determined by the BCA assay.

Phospholipid Extraction

Phospholipids were extracted by modified Folch method (Folch et al., 1957). For cellular phospholipid extraction, 1 g (wet weight) of yeast cells were digested with zymolyase and the spheroplasts, thus obtained, were diluted with 20x volume of Folch solution (2:1 chloroform:methanol) in a glass tube and shaken vigorously for an hour. Water equivalent to 1/5 the volume of Folch solution was added and shaken vigorously for 1 min followed by centrifugation at 1000xg for 2 min to yield a top aqueous phase and a bottom organic phase containing lipids. The bottom phase was transferred to a fresh glass tube to which 1:1 methanol:water equivalent of 1/5 the volume of lipid solution was added and shaken vigorously for 1 min. The tube was centrifuged at 1000xg for 2 min. The bottom phase was again transferred to a fresh tube and dried with N2. The lipids dried in the glass tube were resuspended in chloroform (~ 100 µL). Bartlett quantification was used to measure total phospholipid phosphorus. Mitochondrial phospholipid extraction was performed using the same procedure.

Phospholipid separation and quantification

1-D Thin Layer Chromatography

The thin layer chromatography (TLC) plate (HPTLC Silica gel 60 F254 AMD extra thin, Merck, HX381899) was prepared by soaking in 1.8% boric acid in ethanol and dried at 110°C. Extracted phospholipids corresponding to 50 nmol phosphate (as determined by Bartlett method) was loaded to the plate in evenly spaced lanes using a 50 μL Hamilton syringe. The tank was equilibrated with a 51.5 mL of solvent consisting of 25:25:1.5 chloroform:methanol:ammonium hydroxide. To equilibrate the TLC tank with the solvent system, a filter paper was placed vertically into the tank, followed by the phospholipid-loaded TLC plate. The TLC plate was removed from the tank when the solvent front reached the top of the plate (~45 min) and was air-dried for 30 min. To visualize the lipids, the plate was soaked in copper staining solution (7.5% CuSO4 and 8.5% ortho-phosphoric acid) and charred at 180°C. The plate was scanned and densitometric analysis was performed using ImageJ software. Statistical significance was calculated using Student's t-test.

2-D Thin Layer Chromatography

This method was performed as previously described (Baker et al., 2016). The extracted phospholipids (15-50 μL) were spotted in a drop-by-drop fashion on the bottom left corner, 1-inch from each side, on a TLC plate (Merck TLC Silica gel 60 HX69032853). To separate phospholipids in the first dimension, a solvent system consisting of 32.5:17.5:2.5 chloroform:methanol:ammonium hydroxide was used. After ~45 min of TLC run time, the plate was taken out from the tank and air dried for 30 min.

To separate the phospholipids in the second dimension (perpendicular to the first dimension), the plate was placed in a separate TLC tank containing 37.5:12.5:2.5:1.1 chloroform:acetic acid:methanol:water. The solvent front was run to the top and air dried for another 30 min. Phospholipids were visualized by placing the dried plate in a TLC tank containing iodine. The phospholipids spots were marked with pencil and scraped using a razor blade, and silica from each spot is collected into glass tube for phosphorus quantification by the Bartlett method.

Bartlett Assay

To quantify phospholipid phosphorus, the phospholipid samples were digested in 400 µL of 72% perchloric acid on a 160°C heat block. After overnight digestion, 4 mL of water was added to each tube followed by the addition of 200 µL of 5% (w/v) ammonium molybdate. The tubes were vortexed and 200 µL of 1% (w/v) amidol in 20% (w/v) sodium bisulfite was added and mixed by vortexing. The glass tubes were then placed in a boiling water bath for 10 minutes. The light blue color indicating phosphorus is quantified by taking optical density measurement at 830 nm. In order to quantify the absolute amount of phosphorus in each of the samples, a standard curve was obtained by using KH_2PO_4 standard solution in the 0.5-10 µg of phosphorus range.

Sub-mitochondrial localization

Proteinase K Protection Assay

The assay was performed as previously described (Gabriel et al., 2007). 20 µL of 5 µg/µL mitochondria was added to 180 µL of SEM. The diluted mitochondria were split into two tubes. One tube was treated with 5.26 µL of 1 mg/mL proteinase K in SEM and

the other with an equivalent volume of SEM. The tubes were incubated on ice for 15 min and the reaction was stopped by adding 1.063 µL 200 mM PMSF. Proteins were precipitated by adding 1/5 the sample volume of 72% trichloroacetic acid (TCA). The samples were incubated on ice for 30 min and then centrifuged at 18,000xg for 30 min at 4°C. The TCA was gently aspirated, and the pellet was washed with 500 µL of acetone. The pellet was resuspended in 50 µL acetone and air-dried. The dried pellet was resuspended in SDS-PAGE loading buffer and analyzed by western blotting.

High Salt Extraction

The assay was performed as previously described (Boldogh et al., 1998). 125 µL of 30 µg/µL mitochondria was centrifuged at 12,000xg for 15 min at 4°C. The supernatant was discarded and an equivalent volume of SM1 buffer (0.6 M sorbitol, 20 mM HEPES KOH pH 7.4, 2 mM MgCl2, 1 mM PMSF, 1 M NaCl) containing protease inhibitor cocktail (Roche Diagnostics 11836170001) was added to the mitochondria. The mitochondria were incubated on ice for 15 min and pelleted by centrifugation at 12000xg. The supernatant was collected in a fresh tube and the pellet was resuspended with SEM. The protein concentration was determined in both the pellet and supernatant fractions and no more than 150 µg of each fraction was aliquoted into fresh tubes. Both fractions were brought to an equal volume (~300 µL) by adding SEM, followed by TCA precipitation and acetone wash as described in the previous section. The pellets were resuspended in SDS-PAGE loading buffer and analyzed by SDS-PAGE/western blot.

Image Acquisition and Analysis

For quantitative fluorescent microscopy, imaging was performed on an inverted Nikon Eclipse-Ti microscope with a 100×1.49 NA TIRF objective, and the images were collected using a Hamamatsu ImagEM X2™ EMCCD camera C9100-23B (effective pixel size, 160 nm). GFP-Vps39 *psd1*Δ cells cultured with and without Etn supplementation were imaged using a 488-nm laser (0.2 kW/cm2) and a 561-nm laser (0.2 kW/cm2) to visualize GFP-Vps39 and mCherry-labelled mitochondria, respectively. To determine the overlap in signal from the GFP and the mCherry, we calculated fractional overlap using a custom algorithm written in MATLAB (The MathWorks, Inc., Natick, MA), which is available upon request. In the fluorescence images, we used 80% of maximum fluorescence intensity in each channel as the threshold to identify regions containing GFP-Vps39 or mCherry-labelled mitochondria. Based on the method described previously (Dunn et al., 2011), we calculated the fractional overlap of GFP-Vps39 with the mitochondria by the ratio of the GFP-Vps39 co-localized with the mitochondria to the total GFP-Vps39 fluorescence signal. For higher resolution confocal microscopic images, samples were mounted on agarose pads and imaged using Olympus® FV1000 confocal microscope equipped with an UPLSAPO 100x/1.4 oil immersion objective with confocal pinhole size corresponding to 1 Airy unit. All images were taken using wavelengths as follows: GFP (Ex. 488 nm, Em. 500-530nm), mCherry (Ex. 543 nm, Em. 565-615 nm) and processed to display a z-projection, pseudo-color, and the scale bar in ImageJ.

Statistical Analysis

Graphpad prism software was used to determine the mean ± S.D. values from at least three biological replicates (which is defined as independent experiments performed

on three different days each starting from a different clone). Statistical analyses were performed by unpaired Student's t-test. The statistical significance is indicated by the p value in each figure.

Results:

Vps39 is required for ethanolamine-mediated respiratory growth rescue of psd1Δ cells

Mitochondrial MCSs formed by the vCLAMP protein complexes has been implicated in inter-organellar phospholipid exchange (Elbaz-Alon et al., 2014). Therefore, we decided to test the requirement of vCLAMP subunits in PE transport to the mitochondria. To this end, we utilized Etn auxotrophy of *psd1*Δ yeast cells. The assay is based on the observation that respiratory growth of *psd1*Δ cells, which lack mitochondrial PE biosynthesis, relies on the import of PE biosynthesized from exogenously supplemented Etn through the CDP-Etn Kennedy pathway. We utilized this growth-based readout of mitochondrial PE import by constructing yeast deletion strains lacking vCLAMP subunits in a *psd1*Δ background. The inability of Etn to rescue respiratory growth of yeast cells lacking Psd1 and vCLAMP subunit(s) would suggest a role of these subunits in PE transport to the mitochondria. Using this experimental design, we tested the requirement of two recently identified vCLAMP complexes in PE transport to the mitochondria (Gonzalez Montoro et al., 2018) (Figure 2.1B, right panel). Deletion of Vps13, a key component of one vCLAMP complex, or deletion of Ypt7, an essential component of the second vCLAMP complex, did not abrogate Etn-mediated rescue, suggesting that intact vCLAMP complexes are not required for PE transport to the mitochondria (Figure 2.1C). Interestingly, we found that the deletion of Vps39, a subunit

of one of the vCLAMP complexes, led to a disruption in Etn-mediated rescue of *psd1*Δ cells (Figure 2.1C). We also observed a growth defect of the *vps39*Δ*psd1*Δ mutant in fermentative (SC glucose) conditions (Figure 2.1C), indicative of a negative genetic interaction between these two genes in cellular processes that are independent of mitochondrial function (Figure 2.1C). However, unlike the growth defect in respiratory medium (SC lactate), the growth in glucose could be rescued by Etn supplementation, ruling out a role of Vps39 in Etn-mediated PE biosynthesis (Figure 2.1D). Episomal expression of Vps39 in the *vps39*Δ*psd1*Δ double mutant could restore the Etn-mediated respiratory growth, demonstrating a Vps39-specific effect (Figure 2.2). Collectively, these data show that Vps39 is specifically required for the Etn-mediated rescue of respiratory growth of *psd1*Δ cells.

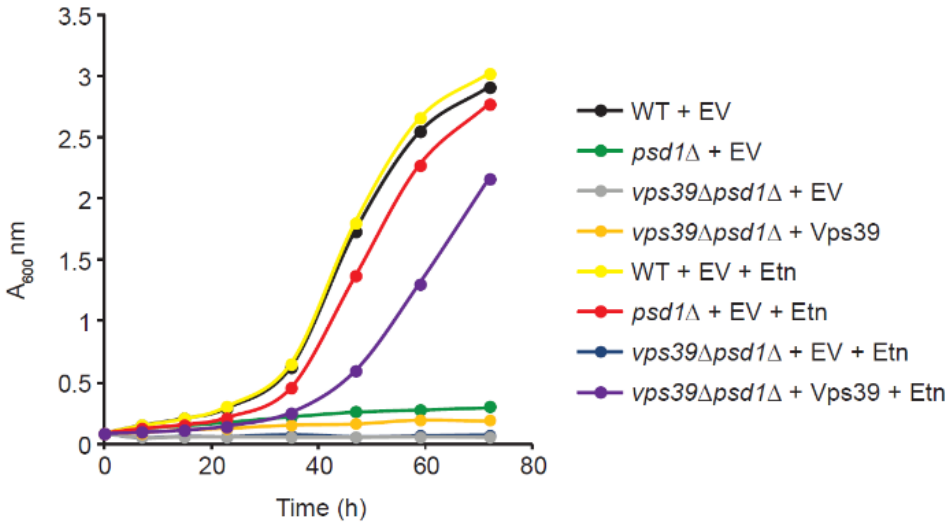

Figure 2.2 Episomal expression of Vps39 restores Etn-mediated rescue of *vps39Δpsd1Δ*.
The growth of the indicated yeast strains cultured in SC Lactate ± Etn at 30°C were monitored by measuring absorbance at 600 nm. The growth curve is a representative image of three independent biological replicates (n=3). EV, empty vector. Reprinted from Iadarola et al., 2020.

Vps39 is required for ethanolamine-stimulated increase in mitochondrial PE levels

In order to test whether growth-based phenotypes correlate to PE levels, we measured the steady state levels of PE in yeast mutants grown in the presence or absence of Etn. Whole cell PE levels were increased upon Etn supplementation in *vps39*Δ cells, indicating that the CDP-Etn Kennedy Pathway is functional in a *vps39*Δ background (Figure 2.3A and B). Next, we analyzed the mitochondrial phospholipid composition and observed no increase in mitochondrial PE levels upon Etn supplementation in cells lacking Vps39, suggesting that Vps39 is required for PE transport to the mitochondria (Figure 2.3C and D). Notably, Etn supplementation did not fully restore mitochondrial PE levels of *psd1*Δ cells to that of Etn-supplemented WT cells (Figure 2.3C and D). This could be due to the limiting amounts of Vps39 in cells. Therefore, we overexpressed Vps39 in *psd1*Δ cells supplied with Etn and found that mitochondrial PE levels were not increased upon Vps39 overexpression (Figure 2.4), suggesting Vps39 abundance is not limiting in PE transport to the mitochondria. WT and *vps39*Δ mitochondria contained comparable steady state levels of other mitochondrial phospholipids that are imported from the ER, including phosphatidylcholine (PC) and phosphatidylinositol (PI) (Figure 2.3E), suggesting a PE-specific role of Vps39 in phospholipid transport.

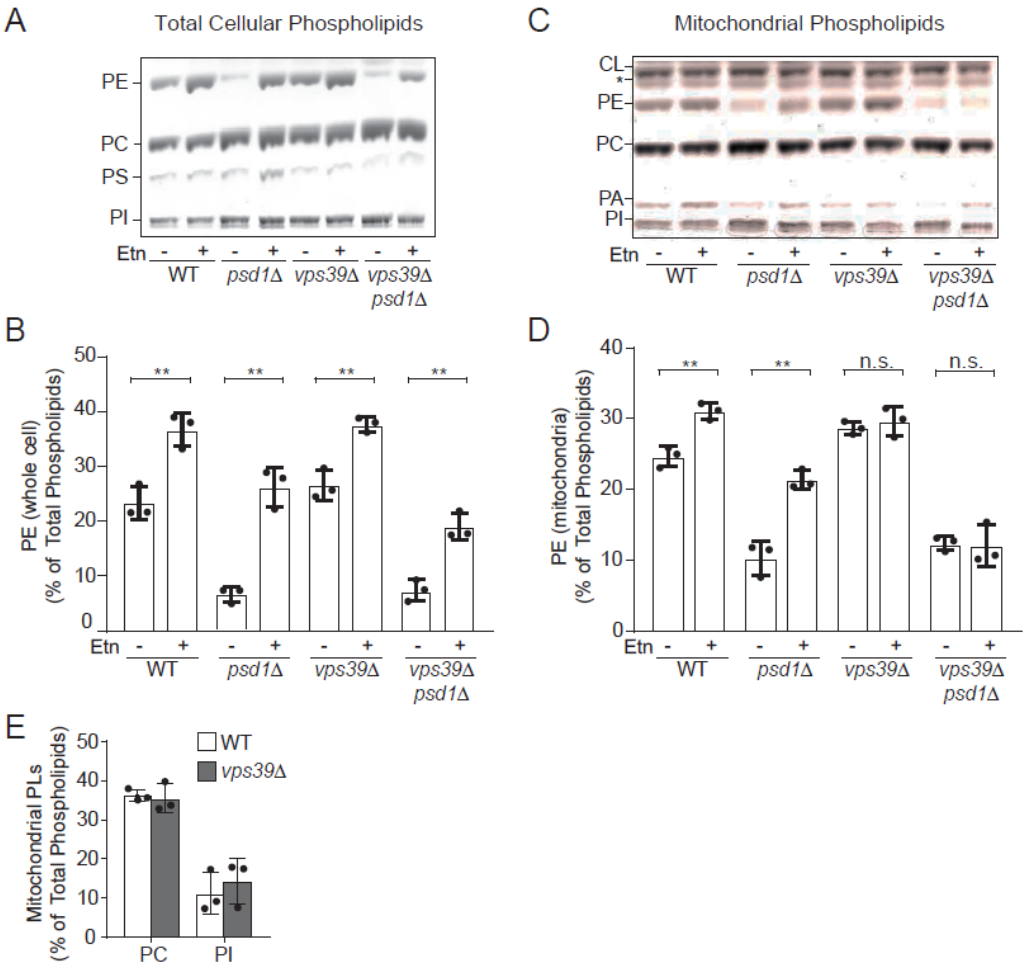

Figure 2.3 Vps39 is required for Etn-stimulated PE elevation in the mitochondria. (A) One dimensional-thin layer chromatography (1D-TLC)-based separation of phospholipids extracted from whole cells of the indicated yeast mutants cultured in SC Lactate ± Etn and (B) the quantification of relative PE levels from A by densitometry. (C) 1D-TLC of phospholipids extracted from density-gradient purified mitochondria from the indicated yeast mutants cultured in SC Lactate ± Etn and (D) the quantification of relative PE levels from C by densitometry. (E) Mitochondrial PC and PI levels of WT and *vps39Δ* cells grown in SC Lactate ± Etn from C. Phospholipid levels are expressed as the percent of total phospholipids. Data are expressed as mean ± SD; **p<0.01, *p<0.05, n.s. not significant, (n=3). Each data point represents a biological replicate. PE, phosphatidylethanolamine; PS, phosphatidylserine; PC, phosphatidylcholine; PI, phosphatidylinositol; PA, phosphatidic acid; CL, cardiolipin, PL, phospholipids. Reprinted from Iadarola et al., 2020.

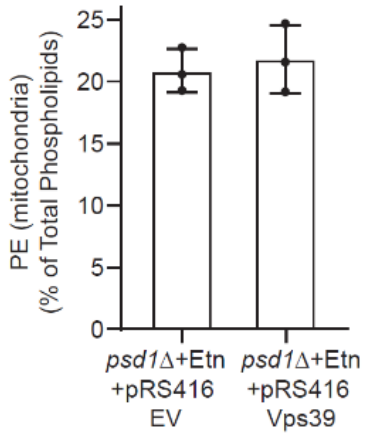

Figure 2.4 Vps39 overexpression does not increase Etn-stimulated mitochondrial PE levels.
PE levels in purified mitochondria of *psd1*Δ cells with and without episomal overexpression of Vps39. PE levels are expressed as the percent of total phospholipid phosphorous. Data are expressed as mean ± SD, (n=3). Each data point represents a biological replicate. EV, empty vector. Reprinted from Iadarola et al., 2020.

Vps39 is not required for ethanolamine-stimulated PE elevation in the ER and vacuole

Next, we asked whether the role of Vps39 in PE transport is specific to the mitochondria or is it required for PE transport to the other subcellular organelles. To test this idea, we purified ER and vacuole from WT and *vps39*Δ cells grown in the presence and absence of Etn and found that unlike in the mitochondria, Etn-supplementation led to an equivalent and significant increase in PE levels in the ER and vacuole in WT and *vps39*Δ cells (Figure 2.5A and B). This result indicates that loss of Vps39 does not impair Etn-mediated elevation in the PE levels of the ER and vacuole.

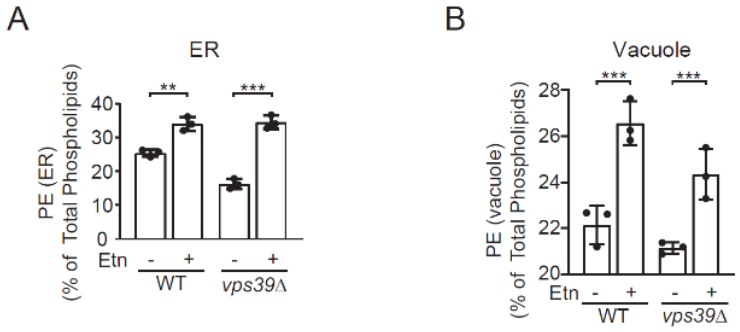

Figure 2.5 Vps39 is not required for Etn-stimulated PE elevation in the ER and vacuole.
PE levels of WT and *vps39*Δ cells grown in SC Lactate ± Etn in density-gradient purified (A) endoplasmic reticulum and (B) vacuole. PE levels are expressed as the percent of total phospholipid phosphorous. Data are expressed as mean ± SD; ***p<0.001, **p<0.01, (n=3). Each data point represents a biological replicate. Reprinted from Iadarola et al., 2020.

Vps39 is required for the rescue of PE-dependent mitochondrial functions

Mitochondrial PE is required for the maintenance of the mitochondrial DNA (mtDNA), which is evident by the loss of mtDNA-encoded proteins and increased formation of petite colonies in *psd1*Δ cells that are cultured in fermentable medium (Baker et al., 2016; Trotter et al., 1993; Birner et al., 2001). Consistent with a previous study (Baker et al., 2016), Etn supplementation rescued both of these phenotypes in *psd1*Δ cells (Figure 2.6A and B); however, deletion of Vps39 in *psd1*Δ cells abrogated Etn-mediated rescue of mtDNA-encoded Cox2 and Cox3 protein levels and petite formation (Figure 2.6A and B). This data provides a functional read-out of PE levels in the inner mitochondrial membrane and further confirms the Vps39 requirement of CDP-Etn Kennedy pathway PE transport to the mitochondria.

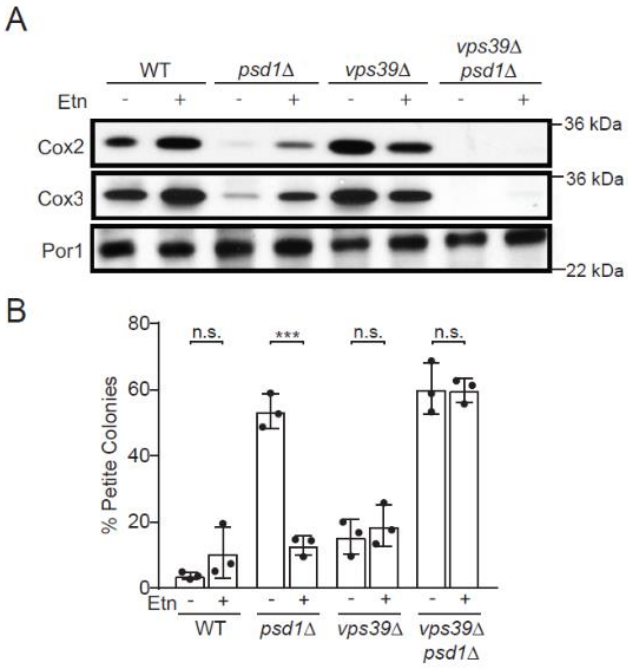

Figure 2.6 Vps39 is required for the expression and maintenance of mtDNA in Etn-supplemented *psd1Δ* cells.
(A) SDS-PAGE/western blot analysis of mtDNA-encoded proteins, Cox2 and Cox3, from mitochondria isolated from the indicated yeast mutants that were cultured in SC Glucose ± Etn media. Por1 is used as a loading control. (B) The percentage of respiratory deficient petite colonies of the indicated mutants cultured in SC Glucose ± Etn media. Percent petite colonies is calculated by counting the number of colonies grown in non-fermentable and fermentable media. Data are expressed as mean ± SD; ***p<0.001, n.s. not significant, (n=3). Each image is a representative of three independent experiments and each data point on bar charts represent a biological replicate. Reprinted from Iadarola et al., 2020.

Vps39-dependent PE transport is independent of intact vCLAMP and HOPS complexes

Vps39 is part of two different protein complexes of separable function within the cell, vCLAMP and the homotypic fusion and protein sorting (HOPS) complex (Gonzalez Montoro et al., 2018). Therefore, Vps39 may facilitate PE transport to the mitochondria via its membrane tethering function as a component of vCLAMP or via a vesicular route as a component of the HOPS complex. To dissect the role of vCLAMP and HOPS in PE transport to the mitochondria, we investigated the requirement of other essential subunits

of these complexes in the rescue of mitochondrial PE levels in Etn supplemented *psd1*Δ cells. We measured the mitochondrial PE levels in *ypt7*Δ*psd1*Δ and *vps13*Δ*psd1*Δ yeast strains that lack essential vCLAMP subunits (Figure 2.7A), and found that Etn supplementation significantly increased mitochondrial PE levels in both of these mutants (Figure 2.7B). These data suggest that intact vCLAMP complex is not required for PE transport to the mitochondria.

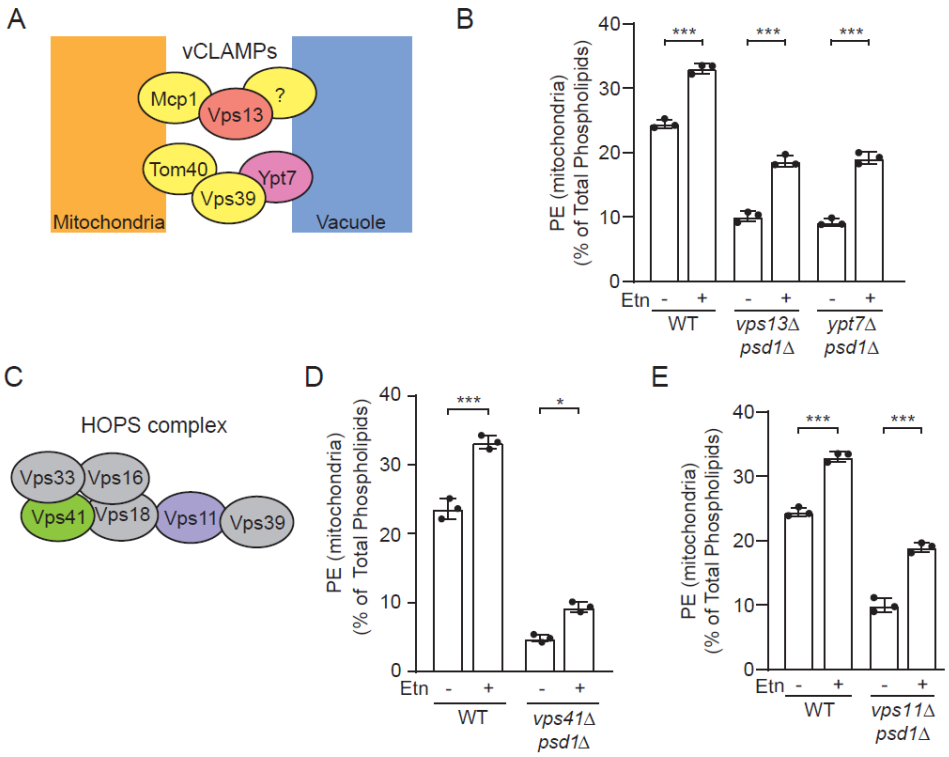

Figure 2.7 PE transport to the mitochondria is independent of essential subunits of vCLAMP and HOPS complexes.
(A) A schematic of two vCLAMPs which consist of Vps39, Ypt7, Tom40 and Vps13, Mcp1, and an unknown vacuole anchor protein. (B) Density-gradient purified mitochondrial PE levels of WT, *vps13Δpsd1Δ*, and *ypt7Δpsd1Δ* cells grown in SC Glucose ± Etn. (C) A schematic of the HOPS complex which consists of six proteins, with Vps39 and Vps41 being the unique members. Density-gradient purified mitochondrial PE levels from (D) WT and *vps41Δpsd1Δ* cultured in SC Lactate ± Etn and (E) WT and *vps11Δpsd1Δ* cultured in SC Glucose ± Etn. PE levels are expressed as the percent of total phospholipids. Data are expressed as mean ± SD; ***p<0.001, *p<0.05, (n=3). Each data point represents a biological replicate. Reprinted from Iadarola et al., 2020.

Vps39 is also a member of the HOPS complex, which is a tethering complex that facilitates fusion of vesicles from the Golgi/late endosome to the vacuole (Balderhaar and Ungermann 2013). The HOPS complex is a heterohexamer of six different subunits (Figure 2.7C). To determine whether Vps39 mediates PE transport through the HOPS complex, we constructed the yeast strain lacking Vps41, a unique and essential component of the HOPS complex. Unlike *vps39*Δ mutants, Etn supplementation led to a modest but significant increase in mitochondrial PE levels (Figure 2.7D). Furthermore, in contrast to Vps39, we found that Vps41 is not localized to the mitochondria in either PE-enriched WT or PE-depleted *psd1*Δ cells (Figure 2.8), suggesting that Vps39 functions independent of the HOPS complex in mitochondrial PE trafficking. In order to further interrogate the role of the HOPS complex in the transport of CDP-Etn Kennedy pathway PE to the mitochondria, we examined Vps11, another essential and a core component of the HOPS complex (Balderhaar and Ungermann 2013). We found that Etn-supplementation leads to increased mitochondrial PE in cells lacking Vps11 (Figure 2.7E), further precluding a HOPS complex requirement in PE trafficking to the mitochondria. Taken together, these data suggest that Vps39-mediated transport of PE to the mitochondria is independent of intact vCLAMP and HOPS complexes.

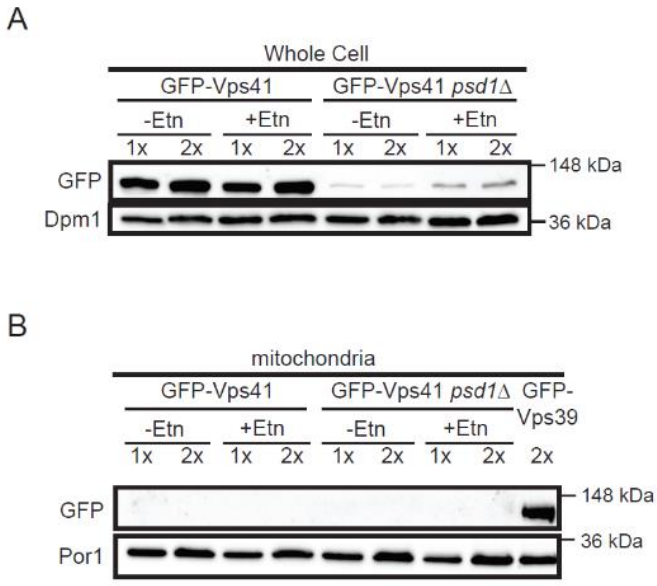

Figure 2.8 Vps39 but not Vps41 localizes to the mitochondria.
Western blots of GFP-tagged Vps41 from (A) whole cells and (B) Vps41 and Vps39 from density-gradient purified mitochondria from WT and *psd1*Δ cells cultured in SC Lactate ± Etn media. Por1 and Dpm1 are marker proteins and loading controls for the mitochondria and ER, respectively. 1x and 2x refer to the amount of protein loaded into each lane. The figure is a representative image of three independent biological replicates (n=3). Reprinted from Iadarola et al., 2020.

Vps39 is recruited to the ER and mitochondria in a PE-dependent manner

For Vps39 to directly transport the CDP-Etn Kennedy pathway PE from its site of synthesis to the mitochondria, it should localize to both the donor and recipient organelles. Although the localization of Ept1, the terminal enzyme of the CDP-Etn Kennedy pathway that catalyzes PE synthesis, has been suggested to be the ER, it has not yet been conclusively determined in yeast (Henry et al., 2012). Therefore, we decided to first determine the sub-cellular localization of Ept1. Sub-cellular fractionation followed by western-blot analysis of density-gradient purified ER, mitochondria, and vacuole showed that Ept1 co-localizes with ER marker protein (Figure 2.9A), demonstrating that it indeed

resides in the ER. Thus, Ept1 localization is consistent with our model that the final step in PE biosynthesis via the CDP-Etn Kennedy pathway occurs in the ER.

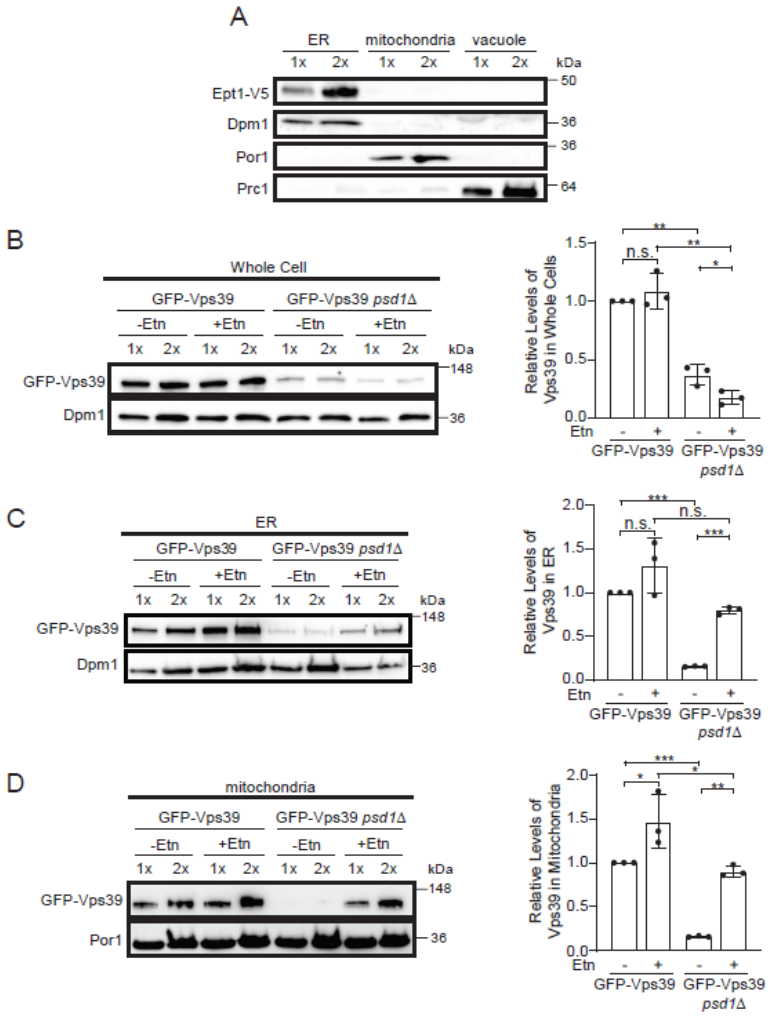

Figure 2.9 Subcellular localization of Ept1 and Vps39.
(A) Western blot detection of V5-tagged Ept1 from density gradient purified ER, mitochondria, and vacuole. Dpm1, Por1, and Prc1 antibodies were used to probe for the purity of the ER, mitochondria, and vacuole, respectively. Ept1-V5 expressing cells were cultured in SC Glucose - Ura medium to mid-logarithmic phase before performing subcellular fractionation. 1x and 2x refer to the amount of protein loaded into each lane. (B-D) Western blot detection (*left*) and quantification (*right*) of GFP-tagged Vps39 in WT and *psd1Δ* cells from whole cell (B), ER (C) and mitochondria (D). GFP-Vps39 expressing cells were cultured in SC lactate medium to late-logarithmic phase before performing subcellular fractionation as shown in (A). Por1 and Dpm1 are used as loading controls. Data are expressed as mean ± SD; ***p<0.001, **p<0.01, *p<0.05, n.s. not significant, (n=3). Each image is a representative of three independent experiments and each data point on bar charts represent a biological replicate. Reprinted from Iadarola et al., 2020.

Vps39 has been previously shown to localize to different subcellular sites in accordance with its multiple roles in cellular functions (Elbaz-Alon et al., 2014). Based on our newly discovered role of Vps39 in PE trafficking, we hypothesized that Vps39 is recruited to the ER and mitochondria in conditions requiring PE transport. We chose four conditions of varying PE concentrations – WT and *psd1*Δ cells with and without Etn supplementation – to determine the subcellular localization of Vps39. Similarly to the reduced levels of Vps41 (Figure 2.8A), we found that the total cellular levels of Vps39 are significantly reduced in *psd1*Δ cells (Figure 2.9B). These unexpected observations suggest interdependence between Vps39/HOPS abundance and PE metabolism. Consistent with our hypothesis, sub-cellular fractionation showed co-localization of Vps39 with both ER and mitochondrial fractions (Figure 2.9C and D), which were purified by density gradient centrifugation as shown for Ept1 in Figure 2.9A. Furthermore, quantification of Western blots of the ER fraction showed that Etn supplementation significantly increases Vps39 localization to the ER in *psd1*Δ cells and there is also a trend towards increased ER localization in the Etn-supplemented WT cells (Figure 2.9C). Similar to the ER data, we found that Vps39 localization to the mitochondria also significantly increased upon Etn supplementation (Figure 2.9D). The pattern of Vps39 localization to the mitochondria correlated with mitochondrial PE levels, such that Vps39 abundance was highest in Etn supplemented WT mitochondria and lowest in *psd1*Δ mitochondria (Figure 2.9D). Quantitative fluorescent microscopy also showed increased co-localization of Vps39 signal with the mitochondria of Etn supplemented *psd1*Δ cells (Figure 2.10A). We also captured confocal microscopic images of GFP-tagged Vps39 in WT and Etn supplemented

psd1Δ cells, which shows redistribution of Vps39 in these two conditions (Figure 2.10B). Taken together, our data indicate that Etn supplementation promotes redistribution of Vps39 to the ER and mitochondria, suggesting a direct role of Vps39 in PE transport from the ER to the mitochondria.

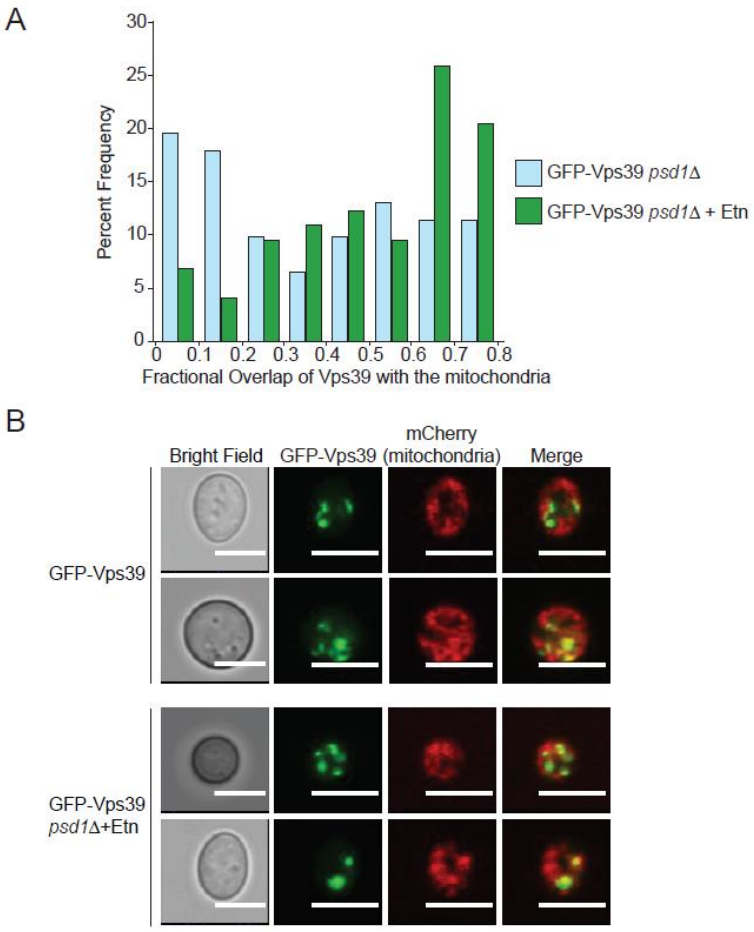

Figure 2.10 Vps39 localization to the mitochondria increases upon Etn supplementation.
(A) Histogram depicting fractional overlap of GFP-Vps39 with the mitochondrial signal from mCherry. The fractional overlap is the comparison of the GFP-Vps39 signal that colocalizes with the mitochondrial mCherry signal compared to the total GFP-Vps39 signal. Percent frequency is defined as the percent of all cells with a fractional overlap between the indicated interval. Number of cell (n) = 61 for -Etn and n=73 for +Etn. Data was obtained from TIRF microscopy. (B) Representative images of GFP-Vps39 localization captured via confocal microscopy of GFP-Vps39, WT, and *psd1*Δ yeast cells cultured + Etn. Mitochondria are probed with mitochondria-targeted mCherry. The scale bar indicates 5 μm. Reprinted from Iadarola et al., 2020.

Vps39 domain analysis for Etn-mediated rescue of psd1Δ respiratory growth

To understand the mechanism by which Vps39 might act in the PE transport pathway to the mitochondria, it is necessary to determine its sub-mitochondrial localization. Recent work by González Montoro et al., has shown that Vps39, as a member of vCLAMP, localizes to the mitochondria via its interaction with Tom40, a well-characterized essential outer mitochondrial membrane (OMM) protein required for mitochondrial protein import. This finding led us to hypothesize that Vps39 is peripherally attached to the OMM. Consistent with our hypothesis, proteinase K treatment of the isolated mitochondria led to the degradation of Vps39 and the OMM protein Tom70, but not the mitochondrial intermembrane space protein Coa6 (Figure 2.11A). To determine if Vps39 is a peripheral or an integral OMM protein, isolated mitochondria were subjected to high salt extraction, which releases peripheral proteins into the supernatant. Through this treatment, we observed that, similar to Act1, which has been shown to localize peripherally on the OMM (Boldogh et al., 1998), but unlike integral membrane protein Cox2, Vps39 was released in the supernatant (Figure 2.11B). These observations suggested that Vps39 is peripherally associated to the OMM (Figure 2.11C).

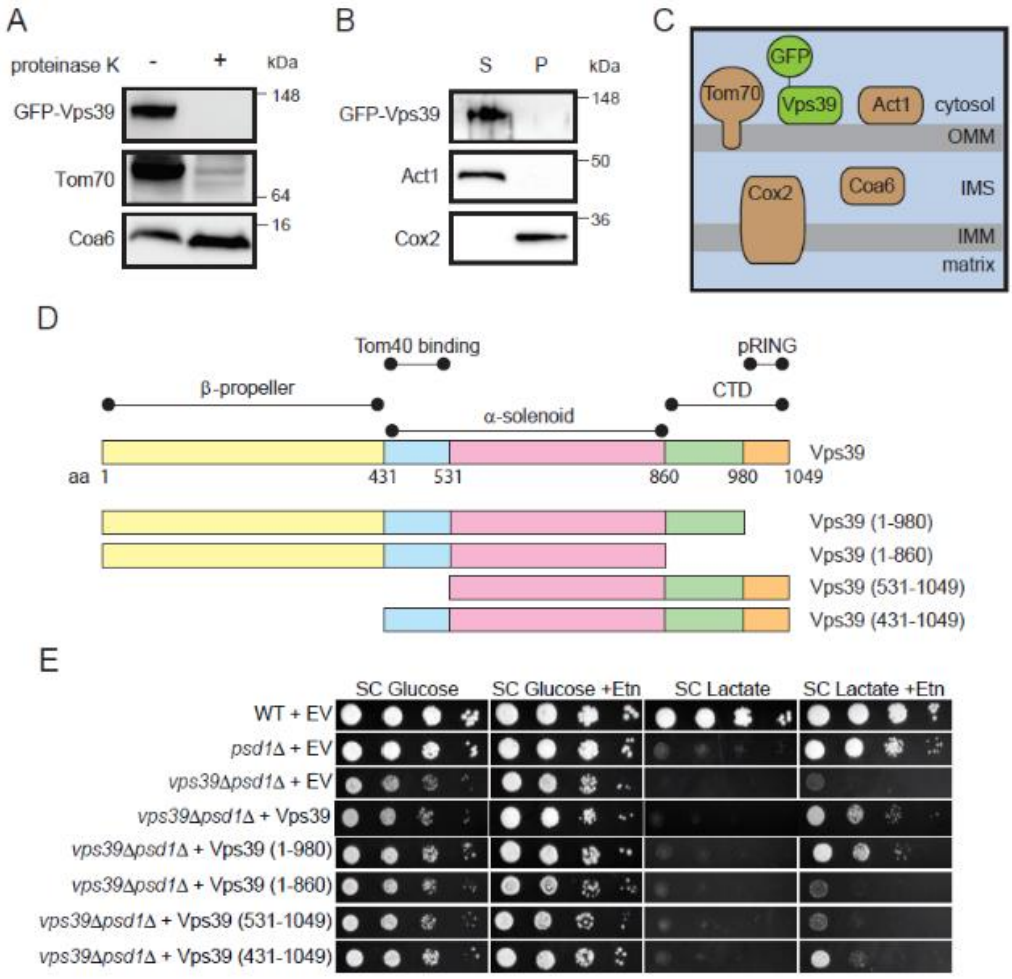

Figure 2.11 Vps39 localizes to the outer mitochondrial membrane and does not require the β-propeller or pRING domain for Etn-mediated rescue of *psd1Δ* cells.
Western blot detection of GFP-Vps39 in isolated mitochondria before and after proteinase K treatment (A) and in the supernatant (S) and pellet (P) fractions after high salt extraction (B). To identify sub-mitochondrial localization of GFP-Vps39, the following marker proteins were used: Tom70, OMM; Coa6, IMS; Act1, peripheral OMM; and Cox2, integral IMM. OMM, outer mitochondrial membrane; IMS, inter membrane space; IMM, inner mitochondrial membrane. (C) A schematic representation of sub-mitochondrial localization of GFP-Vps39. (D) A schematic representation of predicted structural elements of Vps39 and the truncation mutants used in this study. (E) Ten-fold serial dilution of the WT and indicated yeast mutants were seeded onto SC Glucose ± Etn and SC Lactate ± Etn plates. Images were captured after 2d (SC Glucose media) and 5d (SC Lactate media) of growth at 30°C. The cells were pre-cultured in YPD media for 10h prior to seeding. The figure is a representative image of three independent biological replicates (n=3). EV, empty vector. Reprinted from Iadarola et al., 2020.

Vps39 is a 123 kDa protein with many predicted structural elements including the N-terminal β-propeller, α-solenoid, and pRING domains (Plemel et al., 2011) (Figure 2.11D). The β-propeller and the C-terminal domains of Vps39 are required for its HOPS-related function (Plemel et al., 2011; Lürick et al., 2017); however, the roles of the α-solenoid and pRING domains of Vps39 have not been characterized. To determine which of these domains of Vps39 are essential for PE transport, we generated Vps39 truncation constructs for these domains, which were then transformed into *vps39*Δ*psd1*Δ cells and assayed for Etn-dependent growth rescue. The respiratory growth of *vps39*Δ*psd1*Δ cells expressing truncation constructs lacking the β-propeller or the pRING domain were partially rescued upon Etn supplementation suggesting that these domains of Vps39 are not essential for PE trafficking from the ER to the mitochondria (Figure 2.11E). However, Vps39 lacking the Tom40-binding domain, the α-solenoid, and the C-terminal domain failed to rescue the respiratory growth of *vps39*Δ*psd1*Δ cells (Figure 2.11E). Together, these data identify critical domains of Vps39 required for Etn-mediated rescue of *psd1*Δ respiratory growth.

Discussion:

Mitochondria can biosynthesize some phospholipids; however, a majority of phospholipids are imported from the ER (Flis and Daum 2013). The phospholipid biosynthetic enzymes and their localization are conserved in eukaryotes, which necessitates the presence of conserved phospholipid trafficking mechanism(s) that transport phospholipids from the ER to the mitochondria. Recent work has implicated MCS complexes, ERMES and vCLAMP, in phospholipid transport from the ER to the

mitochondria (Kawano et al., 2018; Kumar et al., 2018; AhYoung et al., 2015; Jeong et al., 2016; Jeong et al., 2017; Gatta and Levine 2017; Lahiri et al., 2015; Lang et al., 2015). In this study, we show that Etn-stimulated increase in mitochondrial PE is dependent on Vps39, an evolutionarily conserved subunit of vCLAMP. Furthermore, we demonstrate that Vps39 and Ept1, an enzyme that catalyzes the final step in PE biosynthesis from Etn, localizes to the ER. Vps39 abundance and recruitment to the ER and mitochondria is driven by an increase in the PE levels in these organelles. Remarkably, deletion of other subunits of Vps39-containing complexes, vCLAMP or HOPS, do not impair Etn-mediated increase in mitochondrial PE. These findings solely implicate Vps39 in PE trafficking from its site of synthesis in the ER to the mitochondria.

PE is required for the optimal activities of the mitochondrial respiratory chain enzymes and is thus essential for mitochondrial energy generation in both yeast and mammalian cells (Baker et al., 2016; Böttinger et al., 2012; Tasseva et al., 2013). Not surprisingly, the majority of mitochondrial PE is biosynthesized in situ by Psd1 (Bürgermeister et al., 2004). However, mitochondrial dysfunction caused by Psd1 deletion can be ameliorated by Etn-mediated stimulation of the CDP-Etn Kennedy pathway of PE biosynthesis, implying that PE can be transported from the ER to the mitochondria (Baker et al., 2016). Consistent with these findings in yeast cells, PE biosynthesized via the CDP-Etn Kennedy pathway has been shown to rapidly equilibrate with mitochondrial membranes in mammalian cells, suggesting that PE transport from the ER to the mitochondria is evolutionarily conserved (Bleijerveld et al., 2007). Indeed, a recent study has shown that phenotypes associated with mutations in the human homolog of Psd1 can

be rescued with Etn supplementation (Girisha et al., 2019). Despite the importance of PE transport from the ER to mitochondria, the molecular basis for this process remained unknown. Therefore, our identification of the role of Vps39 in PE transport provides new insights into phospholipid trafficking to the mitochondria. Although here we find that Vps39 is essential for the Etn-mediated elevation in the mitochondrial PE levels, cells lacking Psd1 and Vps39 still contained measurable levels of PE (Figure 2.3C and D), which could be attributed to the residual ER contamination in the mitochondrial preparation. Alternatively, this observation implies that there are other mechanisms of non-mitochondrial PE transport to the mitochondria. Indeed, Elbaz-Alon et al, 2014 have suggested redundant roles of Vps39-containing vCLAMP and ERMES in phospholipid trafficking (Jeong et al., 2016).

Intracellular phospholipid trafficking between different organelles involves both vesicular and non-vesicular routes (Voelker 2009; Vance 2015). Our identification of Vps39, a member of the HOPS vesicular transport pathway, raised an intriguing possibility of Etn-stimulated vesicular transport of PE to the mitochondria, an organelle that has not been previously linked to the vesicular pathway (Prinz 2010). Deletion of other essential members of the HOPS complex failed to abrogate Etn-stimulated elevation in mitochondrial PE levels (Figure 2.7D and E), arguing against HOPS-mediated vesicular transport of PE to the mitochondria. Consistent with these results, we found that the β-propeller region of Vps39, which is required for HOPS function (Lürick et al., 2017), is not essential for PE transport to the mitochondria (Figure 2.11E), further precluding HOPS-mediated vesicular transport as a probable mechanism.

In addition to being a critical component of the HOPS complex, Vps39 has been shown to be a member of a MCS complex, vCLAMP, which connects vacuoles to the mitochondria (Elbaz-Alon et al., 2014; Hönscher et al., 2014). We examined the possibility that PE formed in the ER is transported via the vacuole through vCLAMP in a non-vesicular route to the mitochondria by deleting the essential members of vCLAMPs, Vps13, which has been shown to bind phospholipids (Kumar et al., 2018) and Ypt7 (Gonzalez Montoro et al., 2018). The deletion of Vps13 or Ypt7 failed to inhibit Etn-stimulated elevation of mitochondrial PE (Figure 2.7B), suggesting that intact vCLAMP complexes are not required for Etn-stimulated PE transport to the mitochondria.

Since Vps39 mediated-PE transport to the mitochondria is independent of its previously defined functions within the cell, the question arises as to how is Vps39 involved in PE transport? Vps39 may act indirectly in this process by regulating localization or function of transport proteins or could play a more direct role in the transport process itself. A significant fraction of intracellular lipid transport is mediated by a large group of soluble 'lipid cargo proteins' called Lipid Transport Proteins (LTPs) that traffic lipid molecules between intracellular organelles in their hydrophobic cavities (Wong et al., 2018). Vps39 exhibits many of the criteria of an LTP - first, Vps39 localizes to both the donor (ER) and the recipient membranes (mitochondria) (Figure 2.9C and D). Second, it is specifically required for PE transport (Figure 2.3). Third, it contains an α-solenoid domain, which has been shown to bind phospholipids in other proteins. Further in vitro experiments demonstrating PE-binding and PE transfer activities are needed to determine if Vps39 is indeed a bona fide LTP. It is notable that recent studies have

uncovered new sub-cellular localizations and unanticipated roles of other vCLAMP subunits, including Vps13 and Mcp1, in intracellular lipid transport and homeostasis (Kumar et al., 2018; Lang et al., 2015; Park et al., 2016; Bean et al., 2018; Tan et al., 2013; John Peter et al., 2017).

Our study also raises many important questions in ER-mitochondrial PE exchange. For example, is Vps39 essential for PE trafficking from the ER to the mitochondria under basal conditions or only upon Etn supplementation? Does Vps39 also play a role in the export of mitochondrially synthesized PE? Are there dedicated adaptor proteins required for Vps39 localization to the ER for the PE transport processes? Critical analyses of our data provide answers to some of these questions. For example, we observed an increased steady state level of PE in the *vps39*Δ mitochondria (Figure 2.3C and D) and a decrease in PE levels in the ER of *vps39*Δ mutants (Figure 2.5A). This finding is consistent with a PE export defect because under basal conditions mitochondria are the major source of cellular PE; therefore, inhibiting PE export from the mitochondria is expected to result in elevation of mitochondrial PE levels and a decrease in the ER PE levels. Although the factors required for Vps39 localization to the ER are not yet identified, our Vps39 protein truncation data suggest that Tom40 binding could be crucial for PE trafficking to the mitochondria (Figure 2.11D and E). This idea is consistent with the recent report showing that Vps39 localizes to the mitochondria via its interaction with Tom40, an outer mitochondrial membrane protein (Gonzalez Montoro et al., 2018). In summary, our study uncovered a critical role of Vps39 in ER-mitochondria PE transport contributing to our understanding of inter-organellar phospholipid trafficking.

CHAPTER III

CHOLINE RESTORES RESPIRATION IN PSD1-DEFICIENT YEAST BY REPLENISHING MITOCHONDRIAL PHOSPHATIDYLETHANOLAMINE*

* This research was originally published in *Journal of Biological Chemistry*. Iadarola DM, Joshi A, Caldwell CB, Gohil VM. Choline restores respiration in Psd1-deficient yeast by replenishing mitochondrial phosphatidylethanolamine. *J Biol Chem.* 2021; 100539.

Summary:

Phosphatidylethanolamine (PE) is essential for mitochondrial respiration in yeast *Saccharomyces cerevisiae*, whereas the most abundant mitochondrial phospholipid, phosphatidylcholine (PC), is largely dispensable. Surprisingly, choline (Cho), which is a biosynthetic precursor of PC, has been shown to rescue the respiratory growth of mitochondrial PE deficient yeast; however, the mechanism underlying this rescue has remained unknown. Here, we uncover the mechanism by showing that Cho rescues mitochondrial respiration by partially replenishing mitochondrial PE levels in yeast cells lacking the mitochondrial PE-biosynthetic enzyme Psd1. This rescue is dependent on the conversion of Cho to PC via the Kennedy pathway as well as on Psd2, an enzyme catalyzing PE biosynthesis in the endosome. Metabolic labeling experiments reveal that in the absence of exogenously supplied Cho, PE biosynthesized via Psd2 is mostly directed to the methylation pathway for PC biosynthesis and is unavailable for replenishing mitochondrial PE in Psd1-deleted cells. In this setting, stimulating the Kennedy pathway for PC biosynthesis by Cho spares Psd2-synthesized PE from the methylation pathway and redirects it to the mitochondria. Cho-mediated elevation in mitochondrial PE is dependent on Vps39, which has been recently implicated in PE trafficking to the mitochondria. Accordingly, epistasis experiments placed Vps39 downstream of Psd2 in choline-based rescue. Our work, thus, provides a mechanism of choline-based rescue of mitochondrial PE deficiency and uncovers an intricate inter-organelle phospholipid regulatory network that maintains mitochondrial PE homeostasis.

Introduction:

Mitochondrial membranes have a highly conserved and unique phospholipid composition, characterized by high abundance of non-bilayer phospholipids such as phosphatidylethanolamine (PE) and cardiolipin (CL) (Basu Ball et al., 2018b; Horvath and Daum, 2013). Perturbation of this phospholipid composition alters the bulk physical properties of the membrane and specific phospholipid:protein interactions, disrupting many processes including but not limited to mitochondrial bioenergetics, cristae architecture, and protein import (Basu Ball et al., 2018b; Mejia and Hatch, 2016; Calzada et al., 2019). A systematic analysis of the role of phospholipids in mitochondrial bioenergetics has uncovered specific requirements of PE and CL in the assembly and activity of mitochondrial respiratory chain (MRC) complexes (Baker et al., 2016). Our recent study has also uncovered a specific requirement of CL in the stability and function of mitochondrial calcium channel (Ghosh et al., 2020). These studies show that mitochondrial function primarily depends on the non-bilayer phospholipids, and within this class of phospholipids, individual non-bilayer phospholipids, PE and CL, perform specific roles.

Among all the major classes of phospholipids, PE is the second most abundant mitochondrial phospholipid and is essential for respiration in yeast and mammalian cells (Baker et al., 2016; Girisha et al., 2019; Böttinger et al., 2012; Tasseva et al., 2013). PE can be biosynthesized by multiple pathways in yeast *Saccharomyces cerevisiae* (Figure 3.1). Decarboxylation of phosphatidylserine (PS) by Psd1 in the mitochondria is the major source of *in situ* and cellular PE (Trotter et al., 1993; Clancey et al., 1993; Bürgermeister

et al., 2004). Cytidine diphosphate-ethanolamine (CDP-Etn) Kennedy pathway biosynthesis of PE involves conversion of the substrate, ethanolamine (Etn), to PE by the sequential action of the enzymes Eki1/Cki1, Ect1, and Ept1/Cpt1 in the endoplasmic reticulum (ER) (Kim et al., 1999; Henneberry et al., 2001; McGee et al., 1994). Additionally, decarboxylation of PS by Psd2 in the endosomal compartments generates PE (Trotter and Voelker, 1995; Gulshan et al., 2010). A majority of PE biosynthesized by Psd2 is methylated to become phosphatidylcholine (PC) by methyltransferases Pem1 and Pem2 in the ER (Bürgermeister et al., 2004; Gaynor and Carmen, 1990; Kodaki and Yamashita, 1987). PC can also be synthesized from choline (Cho) through the CDP-Cho Kennedy Pathway via the sequential action of Cki1/Eki1, Pct1, and Cpt1/Ept1 (Figure 3.1) (Kim et al., 1999; Henneberry et al., 2001; McGee et al., 1994).

Unlike PE, depletion of PC, the most abundant bilayer forming mitochondrial phospholipid, does not impair MRC function or formation in yeast (Baker et al., 2016; Schuler et al., 2016). The respiratory defect of *psd1Δ* cells is specifically due to a decrease in PE-dependent activities of MRC complexes III and IV (Baker et al., 2016; Böttinger et al., 2012). Notably, stimulating CDP-Etn Kennedy pathway of PE biosynthesis by Etn supplementation can restore respiratory growth and mitochondrial respiration of *psd1Δ* cells (Baker et al., 2016; Birner et al., 2001). The Etn-mediated rescue requires transport of PE from the ER to the mitochondria in a Vps39-dependent manner (Iadarola et al., 2020). This rescue of mitochondrial PE deficiency by Etn supplementation is consistent with the critical requirements of non-bilayer phospholipids for mitochondrial functions (Gohil et al., 2005; Joshi et al., 2012). However, rescue of respiratory growth of *psd1Δ*

cells by Cho (Birner et al., 2001) is surprising considering that Cho is a precursor for the bilayer forming PC (Figure 3.1).

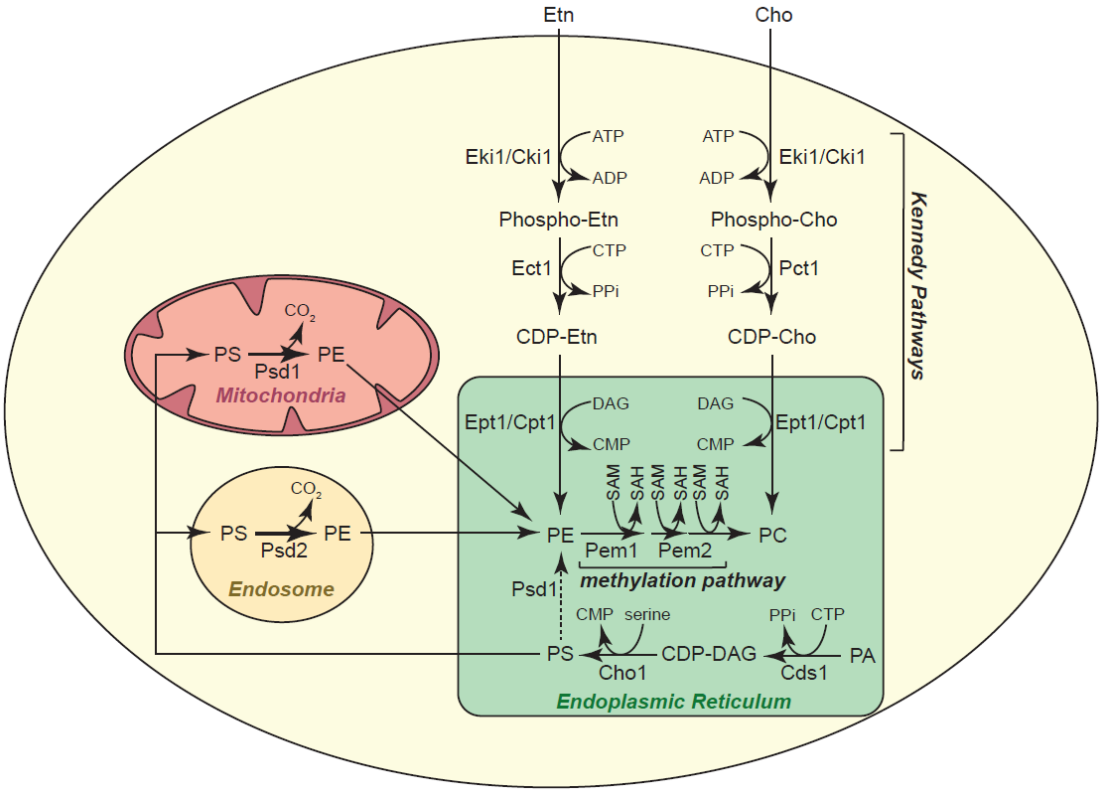

Figure 3.1 Aminoglycerophospholipid biosynthetic pathways in yeast *Saccharomyces cerevisiae*.
The three major pathways for PE biosynthesis are- 1) mitochondrial decarboxylation of PS by Psd1, 2) endosomal decarboxylation of PS by Psd2, and 3) synthesis by incorporation of Etn via the CDP-Etn Kennedy Pathway. The two major pathways for PC biosynthesis are- 1) methylation of PE by Pem1 and Pem2, and 2) synthesis by incorporation of Cho via the CDP-Cho Kennedy Pathway. Phosphatidylserine is biosynthesized from PA in a two-step reaction involving CDP-DAG synthesis followed by the addition of serine by Cho1. PE, phosphatidylethanolamine; PC, phosphatidylcholine; PS, phosphatidylserine; Etn, ethanolamine; Cho, choline; PA, phosphatidic acid; ATP, adenosine triphosphate, ADP, adenosine diphosphate; CTP, cytidine triphosphate; CDP, cytidine diphosphate; CMP, cytidine monophosphate; DAG, diacylglycerol; PPi, pyrophosphate; SAH, S-adenosyl homocysteine; SAM, S-adenosyl methionine. Reprinted from Iadarola et al., 2021.

Here, we uncover the mechanism of Cho-based rescue of mitochondrial respiration in *psd1Δ* cells. We show that Cho supplementation stimulates PC biosynthesis via the CDP-Cho Kennedy pathway, alleviating the need for PC biosynthesis from PE via the methylation pathway. The PE, biosynthesized via Psd2, is thus spared from entering the methylation pathway and becomes available for mitochondrial function. Apart from CDP-Cho Kennedy pathway enzymes and Psd2, the Cho-based rescue of mitochondrial PE deficiency also requires Vps39, implicating its role in the mitochondrial PE transport. These findings reinforce the idea that MRC function specifically requires non-bilayer phospholipids.

Experimental Procedures:

Yeast Strains, growth media composition, and culture conditions.

All *Saccharomyces cerevisiae* strains used in this study are listed in Table 3.1. Yeast cells were maintained and precultured in YPGE media (1% yeast extract, 2% peptone, 3% glycerol, and 1% ethanol) or YPD medium (1% yeast extract, 2% peptone, and 2% glucose) for strains that cannot grow in YPGE medium. For final culture, yeast were grown in synthetic complete (SC) medium (0.17% yeast nitrogen base without amino acids, 0.5% ammonium sulfate, 0.2% dropout mix containing amino acids) with either glucose (2%) or lactate (2% and pH 5.5) as a carbon source (Amberg et al., 2005). Etn, Cho, or serine (Ser) were added at 2 mM concentrations to SC media, wherever indicated. Cultures were started at an optical density (OD_{600}) of 0.1 and were grown to late logarithmic phase at 30^{o}C. Solid media was prepared with addition of 2% agar. Growth measurements on agar plates were performed by seeding 3 µL of 10-fold serial dilutions

of preculture onto the indicated plates. The pictures were taken after 2 days of growth in SC glucose medium and 5 days of growth in SC lactate medium. The petite formation assay was performed by spreading ~200 cells from SC glucose medium onto YPD and YPGE plates. Percent petite colonies were calculated by counting the number of colonies grown in YPGE and YPD. Knockout yeast strains were constructed by one-step gene disruption using geneticin, hygromycin, and nourseothricin cassettes (Janke et al., 2004).

Table 3.1 *Saccharomyces cerevisiae* strains used in this study.
Reprinted from Iadarola et al., 2021.

Yeast Strains	**Genotype**	**Source**
BY4741 WT	*MATa, his3Δ1, leu2Δ0, met15Δ0, ura3Δ0*	Miriam L. Greenberg
BY4741 *psd1*Δ	*MATa, his3Δ1, leu2Δ0, met15Δ0, ura3Δ0, psd1Δ::hphNT1*	This Study
BY4741 *pct1*Δ	*MATa, his3Δ1, leu2Δ0, met15Δ0, ura3Δ0, pct1Δ::kanMX4*	Open Biosystems
BY4741 *psd2*Δ	*MATa, his3Δ1, leu2Δ0, met15Δ0, ura3Δ0, psd2Δ::kanMX4*	Open Biosystems
BY4741 *psd1*Δ *psd2*Δ	*MATa, his3Δ1, leu2Δ0, met15Δ0, ura3Δ0, psd2Δ::kanMX4, psd1Δ::hphNT1*	This study
BY4741 *pct1*Δ *psd1*Δ	*MATa, his3Δ1, leu2Δ0, met15Δ0, ura3Δ0, pct1Δ::kanMX4, psd1Δ::hphNT1*	This study
W3031A WT	*MATa, ade2-1, ura3-1, his3-11,15, trp1-1, leu2-3,112, can1-100*	Akinori Ohta
SKY010 *pem1*Δ *pem2*Δ	*MATa, ade2-1, ura3-1, his3-11,15, trp1-1, leu2-3,112, can1-100, pem1Δ::HIS3, pem2Δ::hph*	Akinori Ohta
SKY011 *pem1*Δ*pem2*Δ *psd1*Δ	*MATa, ade2-1, ura3-1, his3-11,15, trp1-1, leu2-3,112, can1-100, pem1Δ::HIS3, pem2Δ::hph, psd1Δ::ADE2*	Akinori Ohta
W3031A *psd1*Δ	*MATa, ade2-1, ura3-1, his3-11,15, trp1-1, leu2-3,112, can1-100, psd1Δ::hphNT1*	This study
BY4741 *vps39*Δ	*MATa, his3Δ1, leu2Δ0, met15Δ0, ura3Δ0, vps39Δ::kanMX4*	Open Biosystems
BY4741 *vps39*Δ*psd1*Δ	*MATa, his3Δ1, leu2Δ0, met15Δ0, ura3Δ0, vps39Δ::kanMX4, psd1Δ::hphNT1*	This study

Mitochondria Isolation

Isolation of crude and pure mitochondria was performed as previously described (Iadarola et al., 2020; Meisinger et al., 2006). Briefly, yeast cells were spheroplasted using zymolyase digestion. Spheroplasts were lysed by homogenization using a glass teflon homogenizer. The crude mitochondrial preparation was obtained after centrifugation steps of 1,500xg, 4,000xg, and 12,000xg. We performed sucrose density gradient centrifugation to obtain higher purity mitochondria as described previously (Meisinger et al., 2006). The purity of mitochondrial isolation for these strains has been optimized as per our previous reports (Baker et al., 2016; Iadarola et al., 2020).

SDS-PAGE and Immunoblotting

Mitochondrial proteins (20 µg) were separated on Mini Protean TGX 4-20% stain free gels (BioRad) and transferred onto polyvinylidene fluoride (PVDF) membranes using a Trans-Blot SD semidry transfer cell (Bio-Rad). The membrane was then probed with the following primary antibodies Cox2, 1:50,000 (110271; Abcam) and Por1, 1:50,000 (110326; Abcam). Membranes were incubated with anti-mouse secondary antibodies (1:5,000) for 1 h at room temperature and the blot was developed using Clarity Western ECL reagent (Bio-Rad Laboratories).

Phospholipid extraction, separation, and quantification

Phospholipids were extracted, separated, and quantified as previously described (Baker et al., 2016; Iadarola et al., 2020). Briefly, lipids were extracted from spheroplasts or mitochondria with Folch solution (2:1 chloroform:methanol) (Folch et al., 1957). The

extracted lipids were first washed with water followed by another wash with 1:1 water:methanol, and were then dried under nitrogen gas. Dried phospholipids were resuspended in 100% chloroform and were separated using two-dimensional thin layer chromatography (TLC). Phospholipid spots were scraped from TLC plates and phosphorus from each spot was quantified using the Bartlett method (Bartlett 1959).

Oxygen consumption rate measurement

Oxygen consumption of SC lactate-grown cells was measured using the high resolution O2K Fluorespirometer (Oroboros) at 30ºC. Each measurement was performed on 4 x 10^6 cells in 2.1 mL of SC lactate media. After basal respiration was measured, maximal respiration was determined after injecting 5 µM CCCP to the cells. Non-mitochondrial respiration was measured after addition of 2 µM antimycin A.

[^{3}H] serine radiolabeling

Radiolabeled serine, 10 µCi of [3-^{3}H] serine, (American Radiolabeled Chemicals catalog number 0246) was added to 5 mL SC glucose cultures at a starting OD_{600} of 0.1. After 14 h of growth, cells were harvested by centrifugation at 3000xg for 5 minutes followed by washing with cold water. The washed cells were resuspended in 1 mL of Zymolyase buffer (50 mM Tris-SO4 pH 7.4, 1.2 M glycerol, 100 mM sodium thioglycolate and 1.5 mg zymolyase) and incubated at 30ºC for 15 min with shaking. The spheroplasts were pelleted, resuspended in 250 µL of Folch solution (2:1 chloroform:methanol), and placed on a shaker. After 1 h on shaker, 50 µL of water was added and tubes were vortexed and again placed on shaker for 5 min. The sample was centrifuged at 1,000xg for 2 min for phase separation. The lower organic phase was

transferred to a new 1.5 mL tube and the volume was recorded. The phospholipid containing organic phase was washed with ~20 uL of 1:1 methanol:water solution. The tube was vortexed, centrifuged, and the organic layer was transferred to a new tube. The wash step was repeated one more time. One-dimensional TLC was performed as previously described (Iadarola et al., 2020). Briefly, 5, 10, and 20 µL of lipid extract were loaded onto the boric acid-washed TLC plate for each condition. The plate was run with a solvent system of 25:25:1.5 chloroform:methanol:ammonium hydroxide. Iodine vapors were used to detect the phospholipids. PS, PE, and PC were scraped and put into individual tubes for each condition. 1 mL of Ultima Gold Liquid Scintillation Cocktail (Perkin Elmer catalog number 6013321) was added to each tube for counting using Perkin Elmer Liquid Scintillation Analyzer Tri-Carb 4910 TR. Each sample was counted two times. The average of the counts was used for analysis.

Statistical Analysis

Graphpad prism software was used to determine the mean ± S.D. values from at least three biological replicates, which are defined as independent experiments performed on three different days each starting from a different clone. Statistical analyses were performed by unpaired Student's t-test and the significance is indicated by the p-value in each figure.

Data Availability

All data are presented in the paper.

Results:

Pct1 and Psd2 are essential for Cho-mediated rescue of psd1Δ respiratory growth.

Consistent with the previous study (Birner et al., 2001), we found that Cho supplementation can rescue growth of *psd1Δ* cells in respiratory (SC Lac) medium but can only rescue growth of *psd1Δpsd2Δ* cells in fermentative (SC Glu) medium (Figure 3.2A). These results indicate that PE biosynthesis via Psd2 is essential for Cho-based rescue of *psd1Δ* cells in respiratory growth conditions. Next, we asked if PC biosynthesis via the CDP-Cho Kennedy pathway is essential for Cho-mediated respiratory growth rescue of *psd1Δ* cells by deleting Pct1, an essential enzyme of CDP-Cho pathway (Figure 3.1). Pct1 deleted cells displayed normal growth in fermentable or respiratory media (Figure 3.2B), however, deletion of Pct1 in a *psd1Δ* background abrogated Cho-mediated rescue of respiratory growth (Figure 3.2B). Taken together, these results show that Psd2 and Pct1 are both essential for Cho-mediated rescue of *psd1Δ* cells.

Since Psd2 provides endosomal PE as a substrate for PC biosynthesis via the methylation pathway (Bürgermeister et al., 2004) (Figure 3.1), we wondered whether this PC is essential for *psd1Δ* rescue. To test this idea, we utilized *pem1Δpem2Δpsd1Δ* strain where Pem1 and Pem2, the PE methylation pathway enzymes, are deleted in a *psd1Δ* background. Loss of *pem1Δpem2Δ* did not abrogate Cho-mediated respiratory growth rescue of *psd1Δ* cells (Figure 3.2C). Taken together, these results suggest that Psd2 contributes to Cho-mediated rescue of *psd1Δ* cells by providing PE to cells but not PE as a substrate for PC biosynthesis via the methylation pathway.

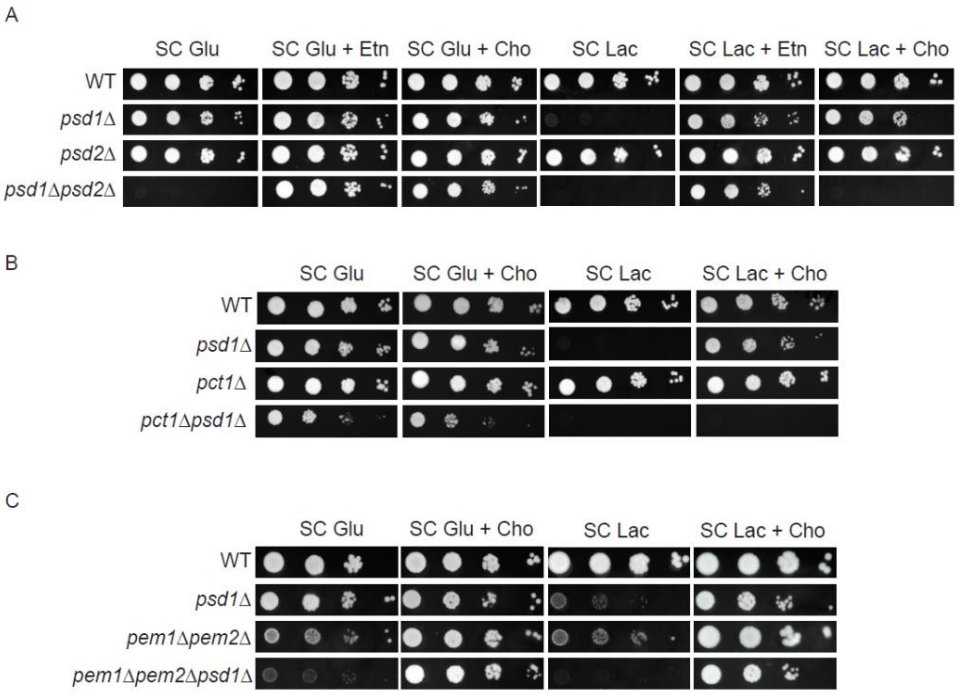

Figure 3.2 Psd2 and Pct1 are essential for Cho-mediated respiratory growth rescue of *psd1Δ* cells.
Ten-fold serial dilution of the indicated yeast mutants (A-C), were seeded onto synthetic complete (SC) glucose and SC lactate plates with and without Etn or Cho supplementation. Images were captured after 2d (SC glucose media) and 5d (SC lactate media) of growth at 30°C. The figures are representative images from three independent biological replicates. Reprinted from Iadarola et al., 2021.

Choline supplementation increases mitochondrial PE in psd1Δ cells.

To understand how supplementing Cho, which feeds into PC biosynthesis, could rescue the respiratory growth of *psd1Δ* cells, we measured the steady state levels of mitochondrial phospholipids. Unexpectedly, we found that Cho supplementation significantly increased mitochondrial PE levels in *psd1Δ* cells (Figure 3.3A). Furthermore, Cho-supplementation also normalized mitochondrial PC levels, which are elevated in *psd1Δ* cells (Figure 3.3B). The increased levels of mitochondrial PE upon Cho

supplementation are similar to what we had previously observed with Etn supplementation (Baker et al., 2016) and can explain the respiratory growth rescue of *psd1Δ* cells. We considered the possibility that Cho supplementation may increase the overall abundance of mitochondrial phospholipids, which may explain the respiratory growth rescue of *psd1Δ* cells. Upon measuring the absolute phospholipid levels per mg of mitochondrial protein, we found that the overall abundance of mitochondrial phospholipids is unaffected in WT and *psd1Δ* cells with or without Cho supplementation (Figure 3.3C). From these results, we infer that the absolute phospholipid levels do not contribute to Cho-mediated rescue, but rather that elevated PE is the most likely reason for the rescue.

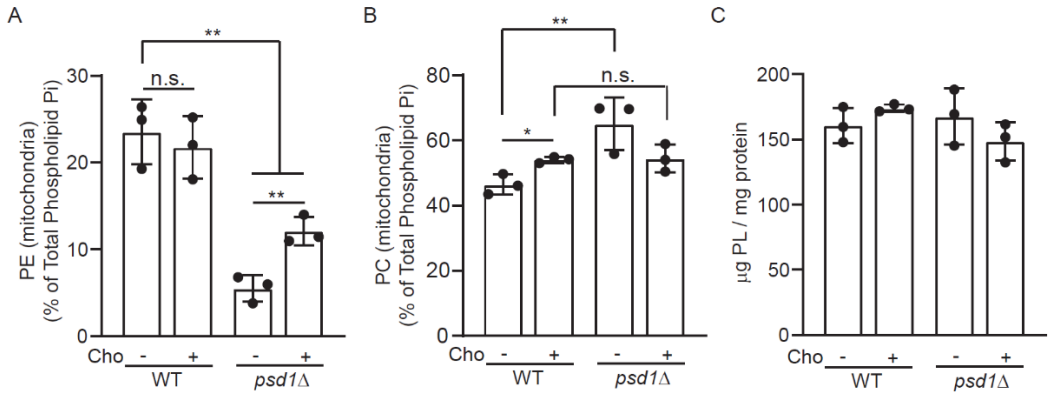

Figure 3.3 Choline supplementation increases mitochondrial PE levels in *psd1Δ* cells. A) PE levels of density gradient purified mitochondria from WT and *psd1Δ* cells cultured in SC lactate ± Cho media. B) PC levels of density gradient purified mitochondria from WT and *psd1Δ* cells cultured in SC lactate ± Cho media. C) Total phospholipid content of density gradient purified mitochondria from SC lactate ± Cho grown cells. PE and PC levels are expressed as the percent of total phospholipid phosphorous. Data are expressed as mean ± SD; n.s. not significant, *p<0.05, **p < 0.01, (n = 3). Each data point represents a biological replicate. Reprinted from Iadarola et al., 2021.

Choline supplementation restores mitochondrial respiration in psd1Δ cells.

The severely compromised respiratory growth of *psd1Δ* cells is attributed to reduced mitochondrial respiration (Baker et al., 2016; Chan and McQuibban, 2012).

Indeed, we have previously shown that partially replenishing mitochondrial PE levels by Etn supplementation can rescue respiratory growth of *psd1Δ* cells by restoring mitochondrial respiration (Baker et al., 2016). Therefore, we asked whether elevating mitochondrial PE levels by Cho supplementation can also restore mitochondrial respiration and found that Cho-supplementation restored both basal and uncoupler-stimulated maximal respiration in *psd1Δ* cells (Figure 3.4A). To investigate the biochemical basis of this rescue, we measured the steady state levels of Cox2, a mitochondrial DNA (mt-DNA) encoded subunit of the MRC complex IV, which is known to be decreased in glucose-grown *psd1Δ* cells (Baker et al., 2016). Consistent with the partial restoration of mitochondrial PE levels, Cho supplementation also partially rescued Cox2 levels in *psd1Δ* cells (Figure 3.4B). The decrease in Cox2 levels has been attributed to the frequent loss of mt-DNA in *psd1Δ* cells, which results in the formation of petite colonies (Baker et al., 2016; Trotter et al., 1993). Therefore, we measured the frequency of petite formation in *psd1Δ* cells and found that Cho supplementation significantly reduced petite formation (Figure 3.4C). These data provide the biochemical basis of Cho-mediated rescue of the respiratory growth of *psd1Δ* cells.

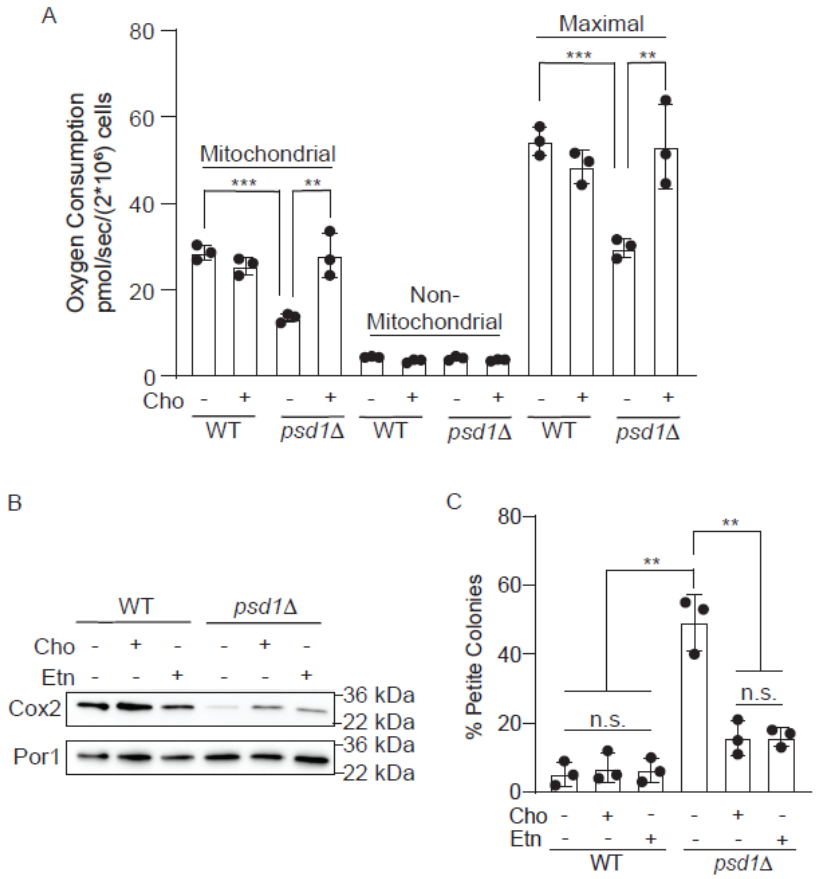

Figure 3.4 Choline supplementation rescues mitochondrial bioenergetics, Cox2 levels, and petite formation in *psd1Δ* cells.
A) Rate of oxygen consumption was measured from WT and *psd1Δ* cells cultured in SC lactate ± Cho media. Maximal respiration refers to respiration after addition of CCCP and non-mitochondrial respiration refers to antimycin-resistant respiration. B) SDS-PAGE/western blot analysis of Cox2 levels from mitochondria isolated from WT and *psd1Δ* cells cultured in SC glucose media with or without Etn or Cho supplementation. Por1, a mitochondrial outer membrane protein, is used as a loading control. C) The percentage of respiratory deficient petite colonies of WT and *psd1Δ* cells cultured in SC glucose media with or without Etn or Cho supplementation. Data are expressed as mean ± SD; n.s. not significant, **p < 0.01, ***p<.001 (n = 3). The western blot image is a representative of three independent experiments and each data point on bar charts represent a biological replicate. Reprinted from Iadarola et al., 2021.

Choline supplementation reduces PE to PC conversion via the methylation pathway.

Next, we focused on understanding the mechanism underlying Cho-based increase in mitochondrial PE levels. Upon steady state phospholipid measurement of purified

mitochondria, we found that unlike in *psd1Δ* cells, Cho supplementation did not increase mitochondrial PE levels in *psd1Δpsd2Δ* cells, implying that Psd2-derived PE is responsible for elevating mitochondrial PE (Figure 3.5A). To understand how Cho-supplementation impacts Psd2-catalyzed PE biosynthesis, we performed a radiolabeling experiment using [^{3}H] serine, which enters the phospholipid biosynthetic pathway by incorporation into phosphatidylserine (PS), the substrate of Psd2 (Figure 3.1). [^{3}H] serine labeling in the presence of Cho supplementation led to an increased accumulation of the radiolabel in PE at the expense of PC (Figure 3.5B), which resulted in a ~10-fold decrease in the radiolabeled PC/PE ratio (Figure 3.5C). These results suggest that the contribution of Psd2-synthesized PE to PC is decreased upon Cho supplementation and this spared PE can be diverted to replenish mitochondrial PE in *psd1Δ* cells.

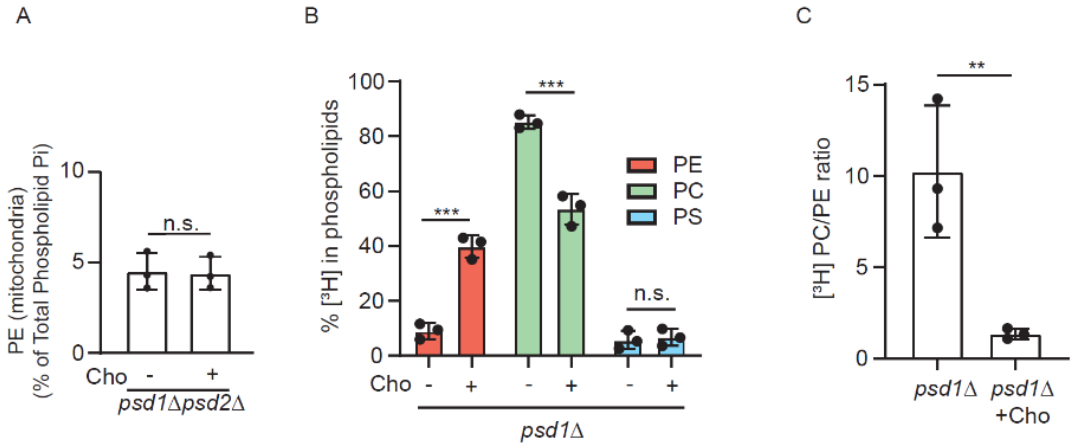

Figure 3.5 PE to PC conversion is reduced upon Cho supplementation.
A) PE levels of density gradient purified mitochondria from *psd1Δpsd2Δ* cells cultured in SC glucose ± Cho media. PE levels are expressed as the percent of total phospholipid phosphorous. B) Percent of [^{3}H] PS, PE, and PC from *psd1Δ* cells grown in SC glucose ± Cho media containing 10 μCi [^{3}H] serine. C) Ratio of [^{3}H] PC/PE from *psd1Δ* cells grown in SC glucose ± Cho media containing 10 μCi [^{3}H] serine. Panels B and C are data from the same experiment. Data are expressed as mean ± SD; n.s. not significant, **p < 0.01, ***p < 0.001 (n = 3). Each data point represents a biological replicate. Reprinted from Iadarola et al., 2021.

Vps39 is essential for Cho-mediated rescue of psd1Δ cells.

We have recently shown that Vps39 is required for Etn-mediated elevation in mitochondrial PE levels (Iadarola et al., 2020). Therefore, we wondered whether Cho-mediated elevation of mitochondrial PE in *psd1Δ* cells also requires Vps39. Consistent with the requirement of Vps39 in Etn-mediated rescue of the respiratory growth of *psd1Δ* cells, we find that Cho-mediated respiratory growth rescue of *psd1Δ* cells also required Vps39 (Figure 3.6A). To determine if Vps39 acts upstream or downstream of Psd2 in Cho-mediated rescue, we employed the [^{3}H] serine radiolabeling strategy to determine if the loss of Vps39 perturbs PS, PE, and PC biosynthesis in *psd1Δ* cells. If Vps39 acts upstream of Psd2, then we expect decreased incorporation of radiolabeled serine in PE and PC. If Vps39 acts downstream of Psd2, then there will be no change in Psd2 activity and the incorporation of radiolabel in PS, PE and PC will be identical to Cho supplemented *psd1Δ* cells. Consistent with this later model, we find that the percent of radiolabeled PS, PE, and PC is the same for *psd1Δ* and *vps39Δpsd1Δ* cells (Figure 3.6B), and the ratio of PC/PE is unchanged between these two strains (Figure 3.6C).

To directly test the requirement of Vps39 in Cho-mediated PE elevation in *psd1Δ* mitochondria (Figure 3.3A), we measured the steady state levels of mitochondrial PE in *vps39Δpsd1Δ* cells with and without Cho supplementation and found that PE levels are not elevated upon Cho-supplementation (Figure 3.6D). Taken together, these results show that loss of Vps39 does not impair PE biosynthesis via Psd2 but specifically abrogates the delivery of Psd2-synthesized PE to *psd1Δ* mitochondria.

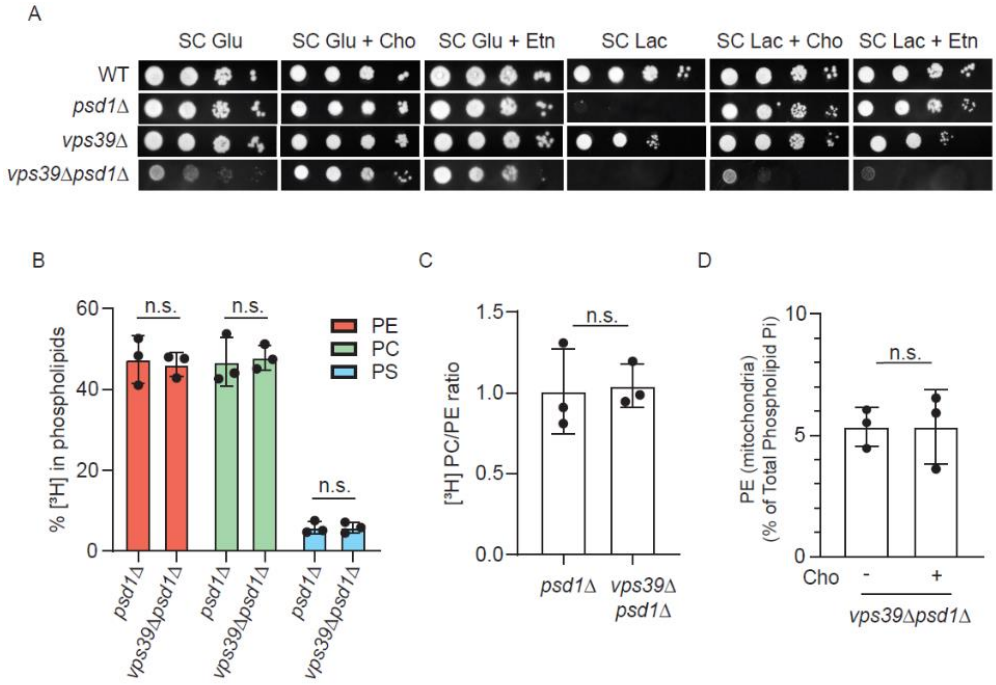

Figure 3.6 Vps39 is essential for Cho-mediated elevation in mitochondrial PE levels in *psd1Δ* cells.

A) Ten-fold serial dilution of the indicated yeast mutants seeded onto indicated agar plates. Images were captured after 2d of growth in SC glucose media and 5d of growth in SC lactate media. The images are representative of three independent biological replicates. B) Percent of [^{3}H] PS, PE, and PC in *psd1Δ* and *vps39Δpsd1Δ* cells grown in SC glucose media supplemented with Cho. C) Ratio of [^{3}H] PC/PE from *psd1Δ* and *vps39Δpsd1Δ* cells grown in SC glucose + Cho. D) PE levels of density gradient purified mitochondria isolated from *vps39Δpsd1Δ* cells cultured in SC lactate ± Cho. Data are expressed as mean ± SD; n.s. not significant (n = 3). Each data point represents a biological replicate. Reprinted from Iadarola et al., 2021.

Discussion:

In this study, we sought to determine the mechanism of Cho-mediated rescue of mitochondrial PE deficiency and found that Cho-supplementation restores mitochondrial bioenergetic functions in PE-deficient *psd1Δ* cells by elevating mitochondrial PE levels through a "lipid sparing" mechanism. Our study has uncovered a novel intracellular phospholipid homeostatic mechanism that maintains the mitochondrial requirements of

bilayer and non-bilayer phospholipids via cross-pathway regulation of the Kennedy and methylation pathways of PC biosynthesis.

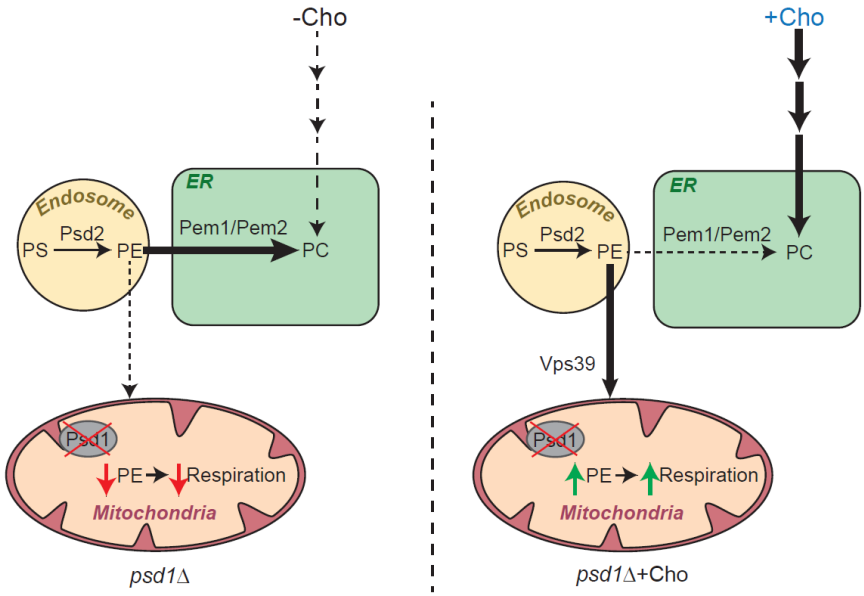

Figure 3.7 A model depicting Cho-mediated restoration of mitochondrial PE levels in Psd1-deficient mitochondria.
The left panel shows that in the absence of exogenous supplementation of Cho, the majority of endosomal PE is utilized for PC biosynthesis via the Pem1/Pem2-methylation pathway and the contribution of endosomal PE to the mitochondria is low. In this scenario, the mitochondrial PE levels remain low, which results in reduced respiration. The panel to the right shows that Cho supplementation stimulates PC biosynthesis via the Kennedy pathway, which diverts endosomal PE to the mitochondria in a Vps39-dependent manner, elevating mitochondrial PE levels and restoring respiration. Reprinted from Iadarola et al., 2021.

Redundant pathways of PE and PC biosynthesis exists in *Saccharomyces cerevisiae,* however, how perturbation in one pathway impacts the flux through the other pathway to maintain homeostatic balance is not fully understood (Carmen and Han, 2011; Henry et al., 2012). By analyzing the incorporation of radiolabeled serine into aminoglycerophospholipids - PS, PE, and PC - in mitochondrial PE-deficient *psd1Δ* cells, we found that Cho-mediated stimulation of PC synthesis via the Kennedy pathway

obviates the need for PC biosynthesis from the PE methylation pathway. The "spared" endosomal PE can instead be diverted to the mitochondria to compensate for the lack of mitochondrial PE biosynthesis in cells lacking Psd1 (Figure 3.7). This observation raises an important question: what is the molecular mechanism that reduces PE to PC conversion via the methylation pathway upon Cho-supplementation? The essential requirement of Pct1 for Cho-mediated rescue of *psd1Δ* cells (Figure 3.2B) suggests that PC synthesis from Cho via the Kennedy pathway is necessary for reducing PE to PC conversion by the methylation pathway. Thus, a possible mechanism by which Cho-derived PC could reduce the flux through the methylation pathway is by inhibiting the methylation pathway enzymes, as has been suggested previously (Janssen et al., 2002).

The requirement of Psd2 for Cho-based elevation of mitochondrial PE (Figure 3.5A), implies that PE biosynthesized in the endosomal compartment by Psd2 is transported to the mitochondria. Therefore, we wanted to identify the molecular player(s) required for this trafficking of PE. Our recent study has implicated Vps39 in PE trafficking from the ER to the mitochondria (Iadarola et al., 2020). So, we asked whether Vps39 also plays a role in trafficking Psd2-synthesized PE to the mitochondria. We found that Vps39 is indeed essential for the Cho-mediated elevation of mitochondrial PE levels in *psd1Δ* cells (Figure 3.6D). Importantly, radiolabeling experiments place Vps39 downstream of Psd2 (Figure 3.6B), thus eliminating its role in PE biosynthesis. Although currently we do not know whether Psd2-synthesized PE is transported directly from the endosomes or through the ER, the results from this study emphasize a broader role of Vps39 in the

trafficking of both the Kennedy pathway-synthesized PE as well as Psd2-synthesized PE to the mitochondria.

One of the important implications of our finding is the possibility of using Cho supplementation as a means to ameliorate mitochondrial dysfunction in human patients with mutations in mitochondrial PISD, a human homolog of yeast Psd1 (Girisha et al., 2019; Zhao et al., 2019; Peter et al., 2019). Since humans do not have the Psd2 equivalent pathway (Vance 2014), the same Psd2-dependent restoration of mitochondrial PE by Cho supplementation is unlikely. However, in mammals, as in yeast, a significant fraction of PE is used up in the biosynthesis of PC via the methylation pathway in hepatocytes (Vance 2014), which can exacerbate PE deficiency in the liver of human patients with partial loss-of-function mutations in PISD (Zhao et al., 2019). Thus, stimulating PC biosynthesis via Cho supplementation in these patients could spare mitochondrial PE for respiratory function and may ameliorate disease symptoms. Thus, the presence of multiple pathways of PE and PC biosynthesis in yeast and humans could allow for a lipid sparing mechanism necessary for Cho-based rescue.

In summary, our study has uncovered a mechanism by which Cho supplementation can restore mitochondrial function in *psd1Δ* cells by directing endosomal PE to the mitochondria. This finding further emphasizes the critical requirements of non-bilayer phospholipids for mitochondrial functions.

CHAPTER IV

A GENOME WIDE ETHANOLAMINE-SENSITIZED SCREEN TO DISCOVER NOVEL GENES REQUIRED FOR PHOSPHATIDYLSERINE TRANSPORT TO THE MITOCHONDRIA

Summary

Mitochondrial membrane biogenesis requires phospholipid transport from the endoplasmic reticulum (ER) to the mitochondria; however, the identity of many of the proteins required for this transport process has remained elusive. Here, we sought to take an unbiased genome-wide approach using a DNA-barcoded yeast deletion mutant library to identify genes required for phosphatidylserine (PS) transport to the mitochondria. PS is a minor component of mitochondrial membranes, but it serves an important function as a substrate for mitochondrial phosphatidylethanolamine (PE) biosynthesis, which is essential for mitochondrial respiratory functions. Our screen comparing growth of yeast mutants is based on the idea that the loss of PS transport to mitochondria will decrease mitochondrial PE resulting in reduced respiratory growth that can be rescued by replenishing PE via ethanolamine (Etn) supplementation. Gene set enrichment analysis of screening results identified a number of mutants involved in PE biosynthetic pathways and mitochondrial respiratory chain (MRC) function, validating our approach. A number of top "hits" from this screen represent potential PS transporter(s) to the mitochondria that can be validated by biochemical approaches. Importantly, data from our screen could serve as a valuable resource to discover novel MRC genes and genes involved in cellular and mitochondrial ethanolamine metabolism.

Introduction

Mitochondrial membranes contain all six major phospholipids and this unique phospholipid composition is important for the proper function and formation of the mitochondrial respiratory chain (MRC) (Horvath and Daum, 2013; Basu Ball et al., 2018b). Most of the phospholipids found in the mitochondria are biosynthesized extra-mitochondrially in the endoplasmic reticulum (ER). Free diffusion of phospholipids through aqueous cytoplasm is not energetically favorable; therefore, there must exist transport machinery to move phospholipids from their site of synthesis to the mitochondria. Traditionally, vesicular transport is considered an important mechanism by which phospholipids are trafficked between organelles within the endomembrane system; however, the mitochondria is not a member of the endomembrane system and cannot receive phospholipids using this mechanism. Thus, phospholipid transport to the mitochondria must be non-vesicular. Lipid transport proteins (LTPs), protein(s) that pickup, carry, and deliver phospholipids from donor to recipient organelles, represent one of the main mechanisms of non-vesicular transport (Wong et al., 2018; Hanada 2018; Balla et al., 2019). More recently, contact sites formed by membrane tethering protein complexes between mitochondria and other organelles including the ER and vacuole have also received attention as means of phospholipid exchange via non-vesicular mechanisms (Wong et al., 2018).

The ER and mitochondria encounter structure (ERMES), a membrane contact site (MCS) protein complex that tethers the ER to the mitochondria, is thought to be machinery required for PS import to the mitochondria (Kornmann et al., 2009). *In vitro* data supports

this claim because ERMES proteins has been shown to bind and transfer PS between liposomes (Kojima et al., 2016). However, *in vivo* data is not as convincing. First, the growth defects associated with ERMES-deleted cells were initially shown to be due to a reduced rate of PS to PE conversion in the mitochondria (Kornmann et al., 2009). However, ERMES deletion growth defects and PS to PE conversion can be rescued with a synthetic tether between the ER and mitochondria, implying that the function of ERMES can be bypassed without lipid binding and transfer (Kornmann et al., 2009). Second, the steady state mitochondrial phospholipid composition is not compromised in ERMES-deficient cells (Nguyen et al., 2012; Baker et al., 2016). The possible explanation for this discrepancy between the *in vitro* and *in vivo* roles or ERMES is the existence of redundant pathways. Indeed, dominant mutations in both Vps13 and Mcp1 have been identified in the ERMES-deleted cells that rescue growth defects (Lang et al., 2015; Tan et al., 2013; John Peter et al., 2017). Vps13 and Mcp1 are members of Vps13-vacuole and mitochondrial patch (Vps13-vCLAMP), or the MCS protein tether between the vacuole and mitochondria (Gonzalez Montoro et al., 2018). Vps13 has also been identified as a lipid transport protein (Kumar et al., 2018); however, its *in vivo* role in maintaining mitochondrial phospholipid homeostasis has not been investigated. The redundant nature of these MCSs and frequent mutation in response to deletion makes dissecting their *in vivo* function very difficult. Although PS transport to mitochondria is also essential for PE biosynthesis in mammalian cells, ERMES homologs are not present in mammalian cells, which further questions the role of ERMES in PS transport. Conversely, in mammalian cells VAT1, a soluble LTP, has been shown to transport PS from the ER to the

mitochondria, however, yeast do not have a VAT1 homolog (Junker and Rapoport, 2015; Watanabe et al., 2020). Clearly, how mitochondria receive PS still remains an open question. Here we sought to discover phospholipid trafficking protein(s) required for the transport of phosphatidylserine (PS) from the ER to the mitochondria.

In the yeast *Saccharomyces cerevisiae,* PS is solely biosynthesized in the ER by Cho1, which catalyzes the addition of a serine head group to phosphatidic acid (PA) (Letts et al., 1983; Bae-Lee and Carmen, 1984) (Figure 4.1A). PS, thus synthesized in the ER, is delivered to different membranes and once it reaches the mitochondria, it is decarboxylated to phosphatidylethanolamine (PE) by Psd1 (Trotter et al., 1993; Clancey et al., 1993; Bürgermeister et al., 2004). PE biosynthesized in the mitochondria is a major source of cellular PE. Importantly, mitochondria specifically require PE for the optimal activity of MRC complexes III and IV (Baker et al., 2016). Accordingly, the *psd1Δ* mutant displays reduced mitochondrial and cellular PE, CIII and CIV activity, respiration, and respiratory growth (Baker et al., 2016). Yeast can also biosynthesize PE through two other pathways. First, Psd1 homolog, Psd2, decarboxylates PS to biosynthesize PE in the endosome, and this PE is mainly used as a substrate for phosphatidylcholine (PC) biosynthesis (Trotter et al., 1995; Gulshan et al., 2010; Bürgermeister et al., 2004). Second, PE can also be biosynthesized from the CDP-Etn Kennedy pathway. The CDP-Etn Kennedy pathway involves three sequential reactions catalyzed by Eki1/Cki1, Ect1, and Ept1/Cpt1 (Kim et al., 1999; Henneberry et al., 2001; McGee et al., 1994) that convert endogenously derived or exogenously supplied Etn to PE. Previously we had shown that addition of Etn to yeast media stimulates PE biosynthesis via CDP-Etn Kennedy pathway

in the ER, and this PE is transported in a to the mitochondria in a Vps39-dependent manner (Baker et al., 2016; Iadarola et al., 2020). Thus, Etn supplementation can replenish mitochondrial PE and rescue respiratory growth of *psd1Δ* cells. This observation provides a basis for our genome-wide screen to discover mitochondrial PS transporter(s). Specifically, we expect that deletion of protein(s) required for PS transport from the ER to the mitochondria would phenocopy *psd1Δ* cells in terms of reduced respiratory growth that can be restored by supplementation of Etn in the media. By culturing a genome-wide collection of yeast deletion mutants in the fermentable and respiratory media with or without Etn supplementation, we have re-discovered genes involved in PE metabolism and identified potential PS transport proteins.

Materials and Methods

Yeast strains, growth media composition, and culture conditions.

Individual yeast *Saccharomyces cerevisiae* cell mutants were maintained and pre-cultured in YPGE media (1% yeast extract, 2% peptone, 3% glycerol, and 1% ethanol). For the final culture, yeast were grown in synthetic complete (SC) medium (0.17% yeast nitrogen base without amino acids, 0.5% ammonium sulfate, 0.2% dropout mix containing amino acids) with either glucose (2%), lactate (2% and pH 5.5), or ethanol (2%) as a carbon sources (Amberg et al., 2005). Etn was added at 2 mM concentrations to SC media, wherever indicated. Cultures were started at an optical density (OD_{600nm}) of 0.1 and were grown to late logarithmic phase at 30^{o}C.

Yeast Deletion Pool and BarSeq Screen Parameters

The yeast deletion collection for the Bar-Seq analysis was derived from the Variomics library constructed previously (Huang et al., 2013). The heterozygous diploid deletion library was sporulated and selected in liquid haploid selection medium (SC-Arg-His-Leu+G418+Canavanine) to obtain haploid cells containing gene deletions, which was obtained from Dr. Craig D. Kaplan. Each mutant within the library was constructed by replacing a gene in the yeast genome with a KanMX antibiotic resistance marker, as well as two 20 base pair DNA barcodes, located upstream and downstream of the KanMX4 cassette (Robinson et al., 2014; Smith et al., 2009). The DNA barcode provides a way to distinguish between each mutant in the pool, of which there are ~6,000 unique single deletion mutants pooled together. Once the deletion pool is cultured, the cells are harvested, genomic DNA is isolated, the nucleotide barcodes are PCR amplified and sequenced. The DNA barcode sequencing results are the "counts," or relative abundance, of each individual strain within the pool of competitively grown strains, directly corresponding to the number of cells of a specific knockout strain present under a given growth condition. Pre-culture of the haploid deletion pool was started at OD_{600} of 0.04 in 50 mL of YPD from the glycerol stock and grown until mid-log phase (14 h) at 30^{o}C with shaking at 225 rpm. The cells were then inoculated into the various conditions of the screen for growth in quadruplicate at a starting $OD600_{nm}$ of 0.1. The cells were grown until late-log stage in each of the growth conditions including SC Glucose (11 h), SC Lactate ± Etn (36 h), and SC Ethanol ± Etn (36 h). Each condition was then further sub-cultured under the same conditions, the cell density was counted, and the cells were

harvested. Genomic DNA (gDNA) was isolated using the YeaStar Genomic DNA Kit (Catalog No. D2002). Quantitative PCR was performed using the SsoAdvanced Universal SYBR Green Supermix kit to determine that 17 cycles should be performed to linearly amplify the barcodes from the gDNA. The 220 bp UPTAG DNA barcode "amplicon" was amplified by PCR using primers UPFwd and UPRev (Table 4.1) in a 50 uL reaction consisting of 100 ng of gDNA, 0.5 uL of each primer, 0.5 uL Phusion polymerase, 10 uL Phusion buffer, and 1 uL dNTPs. The thermocycler was set to 98^{o}C for 3 min, 17 cycles of 98^{o}C for 10 s, 55^{o}C for 30 s, and 72^{o}C for 30 s, and finally 72^{o}C for 10 min for the final extension. After running on a 1% agarose gel in TAE buffer, each amplicon was gel extracted using the QIAquick Gel Extraction Purification Kit. The purified amplicon DNA were then sent to the Texas A&M AgriLife Genomics and Bioinformatics Facility for sequencing on the Illumina HiSeq 4000 for 150 bp paired end sequencing.

Assessing fitness of barcoded yeast strains by DNA sequencing

The sequencing reads were aligned to the barcode sequences using Bowtie2 (version 2.3.1) with the -N flag set to 0. Bowtie2 outputs were processed and counted using Samtools (version 1.3.1). Barcode sequences shorter than 15 nucleotides or mapped to multiple reference barcodes were discarded. The program R was used to combine the reads from the UP tag sequences and calculate the fitness score using T statistics. The sequencing data yielded an average of 10.2 million reads for each sample. After aligning each barcode to its respective gene, the total number of reads for each barcode was counted. Using Bowtie2 and Samtools software, an average of 7.6 million reads per sample were aligned to known yeast genes. The raw counts were linearly

normalized for each sample and a T-score was calculated for each knockout strain. The T-score is a statistical method based on Welch's *t*-test to compare two conditions and are used to determine the statistically significant difference in growth of individual mutant in the Bar-Seq screen. The T-score investigates the difference of weighted deletion mutant counts and significance can be calculated based on a T distribution. $T\ score\ \left(\frac{cond1}{cond2}\right) = \frac{\overline{x}cond1 - \overline{x}cond2}{SDcond1 + SDcond2 + 1}$, $SD = \sqrt{\frac{\sum_{i=1}^{n}(xi - \overline{x})^2}{n-1}}$ where $\overline{x}$ is the mean, n is the number of biological replicates (which was 4 in our case), x_i is the linear normalized counts for each replicate (which refers to raw count for a given gene divided by the total number of counts from that condition multiplied by an arbitrary number to get a positive value), and the condition refers to the media. The sequencing results were validated *in silico* by showing near-perfect correlation between each of the replicates. The master file containing all of the raw counts for each condition and the analyzed data can be seen in Supplementary Table 1.

Gene Ontology analysis

To identify enriched gene ontology (GO) terms, we generated a rank ordered list based on T-Scores (Supplementary Table 2, 3, 4, & 5) and used the reference genome for *Saccharomyces cerevisiae* in GOrilla Gene Ontology enRIchment anaLysis and visuaLizAtion (http://cbl-gorilla.cs.technion.ac.il/), a web-based tool for discovery and visualization of enriched GO terms in ranked gene lists.

Data Availability

The data presented in this chapter is available upon request from Donna M. Iadarola, iadarola@tamu.edu and Dr. Vishal M. Gohil, vgohil@tamu.edu. Supplementary Table 1 is the master fie which includes all of the raw counts in each condition generated from Samtools and the analyzed data. Supplementary Table 2 and 3 are a ranked list of the genes with the smallest to largest T-score in respiratory media (SC Ethanol / SC Lactate) compared to fermentable media (SC Glucose) respectively. Supplementary Table 4 and 5 are a ranked list of the genes with the largest to the smallest T-score for respiratory media supplemented with Etn (SC Ethanol+Etn / SC Lactate+Etn) compared to respiratory media without Etn supplementation (SC Ethanol / SC Lactate), respectively.

Table 4.1 Oligonucleotides used in this study

Oligonucleotide Name	Sequence (5`->3`)
UPFwd	AAATGGTTGGCCTGCAGGGATGTCCACGAGGTCTCT
UPRev	TGACTGGAGTTCAGACGTGTGCTCTTCCGATCTGCACGTCAAGACTGTCAAGG

Results

Etn-sensitized DNA-BarSeq screen to identify PS transporter(s) to the mitochondria

In order to identify gene(s) responsible for a particular phenotype using a DNA-barcoded yeast mutant library, it is first necessary to devise a selection strategy that tests the competitive fitness of each yeast mutant in the library. In order to discover candidate PS transporter(s) to the mitochondria, we devised a growth scheme that would allow a

selective enrichment of respiratory growth deficient mutants as well as mutants whose growth can be improved by Etn supplementation. Loss of the PS transporter to the mitochondria is expected to decrease mitochondrial PE biosynthesis via Psd1, which in turn would decrease mitochondrial respiration and respiratory growth that can be rescued by Vps39-dependent transport of PE formed upon the addition of Etn in the media (Figure 4.1A). Since the PS transporters are expected to phenocopy the growth pattern of *psd1Δ* cells, our growth conditions were based on the growth of the *psd1Δ* mutant in fermentative (SC Glucose), non-fermentative (SC Lactate) and Etn-supplemented non-fermentative (SC Lactate) growth media (Figure 4.1B). In these growth media conditions, we expect *psd1Δ* cells and the putative PS transporter mutant to exhibit normal growth in SC Glucose and SC Lactate + Etn but reduced growth in SC Lactate, which will be reflected in their relative DNA-barcode abundance in our screen (Figure 4.1B). In order to enrich mutants for the expected phenotypes, we employed two rounds of selection by growing the deletion pool in the respective media to late log phase followed by sub-culturing into the same media and expanding the culture to late log phase before harvesting cells.

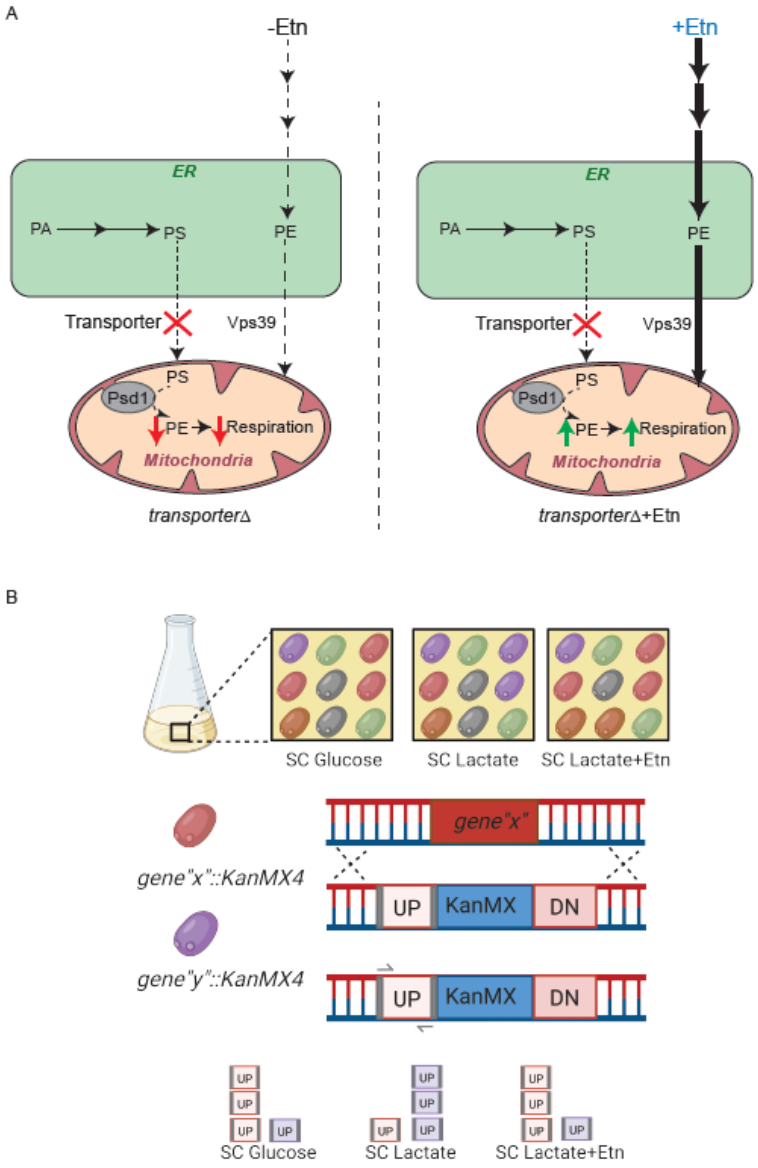

Figure 4.1 A schematic of the Etn-sensitized BarSeq screen designed to identify PS transporter(s) to the mitochondria.

A) Major phosphatidylserine (PS) and phosphatidylethanolamine (PE) biosynthetic pathways in *Saccharomyces cerevisiae.* PS is biosynthesized in the ER and is transported to the mitochondria, where it is converted to PE by Psd1. PE is also biosynthesized in the ER upon ethanolamine (Etn) supplementation and transported to the mitochondria in a Vps39-dependent manner. A deletion in the PS transporter to the mitochondria is expected to have low mitochondrial PE and respiration without Etn supplementation that can be rescued upon Etn supplementation. B) Scheme of the Etn-sensitized BarSeq screen: The yeast deletion library is a collection of ~6,000 single-deletion yeast mutants, where each mutant has a gene replaced with a *kanMX4* cassette flanked by a unique UP tag (UP) and DOWN tag (DN) DNA sequences. Each unique deletion mutant is pooled together

Figure 4.2 Continued A schematic of the Etn-sensitized BarSeq screen designed to identify PS transporter(s) to the mitochondria.
and grown in different media conditions, depicted above as growth in fermentable (SC Glucose) media and non-fermentable (SC Lactate) media with and without 2 mM Etn supplementation. The genomic DNA was isolated from harvested cells and used as a template to amplify the UP tag DNA barcode sequences. Common primers were be used to amplify each barcode amplicon to determine the abundance of each yeast mutant within the pool in the different conditions after sequencing. The mutants with deletion in genes required for respiratory growth were expected to grow poorly in non-fermentable media resulting in reduced barcode counts for those particular gene(s) compared to growth in fermentable media. However, if the same gene(s) function is supported by Etn supplementation, then we expect increased barcode counts for that gene(s) in Etn-supplemented respiratory growth media (depicted by *gene"x"Δ* cells above). PE, phosphatidylethanolamine; PS, phosphatidylserine; Etn, ethanolamine; PA, phosphatidic acid.

Genes required for respiratory growth

We first wanted to identify respiratory deficient mutant strains because the impairment of PS transport to the mitochondria is expected to decrease mitochondrial PE levels, which in turn would compromise respiratory growth. To identify mutants with a respiratory growth phenotype, we compared the relative abundance of each barcode in non-fermentable "respiratory" media (SC Lactate/SC Ethanol) and compared it to fermentable media (SC Glucose) using the T-score. We have included two non-fermentable media conditions - SC Lactate and SC Ethanol - in this screen to exclude carbon source-specific "hits". A negative T-score identifies mutants that grew poorly in respiratory conditions; conversely, a positive T-score identifies mutants with better competitive growth in respiratory conditions. We rank ordered all the mutants from the yeast deletion pool from negative to positive T-scores ($T_{Lactate/Glucose}$ and $T_{Ethanol/Glucose}$). To validate our screening results, we used genes with known roles in mitochondrial respiratory chain (MRC) function that are expected to have a respiratory growth deficiency. As expected, the lower tail of the

distribution for respiratory deficient growth was enriched in MRC genes in both SC Lactate and SC Ethanol media (Figure 4.2A and 4.3A). The top "hits" representing mutants with the most negative T-score included *COX5A, COA6, QCR7, CYC1*, and *SDH2* genes that are involved in cytochrome *c* and respiratory CII, CIII, and CIV function in SC Lactate media (Figure 4.2A). Similarly, top "hits" for SC Ethanol media included *SDH2, CYT1, QCR7, COX14,* and *SDH7* genes that are involved in respiratory CII, CIII, and CIV function (Figure 4.3A).

To systematically identify cellular pathways that were enriched for reduced respiratory growth in our screen, we performed gene ontology analysis using the online tool – *Gene Ontology enrichment analysis and visualization* (GOrilla) (Eden et al., 2009). The gene ontology (GO) analysis identified *mitochondrial respiratory chain complex assembly* [SC Lactate (p value: 4.84E-17); SC Ethanol (p value: 2.78E-18)] and *cytochrome complex assembly* [SC Lactate (p value: 3.12E-12); SC Ethanol (p value: 2.88E-14)] as the most significant biological processes (Figure 4.2B and 4.3B), which further validated our approach.

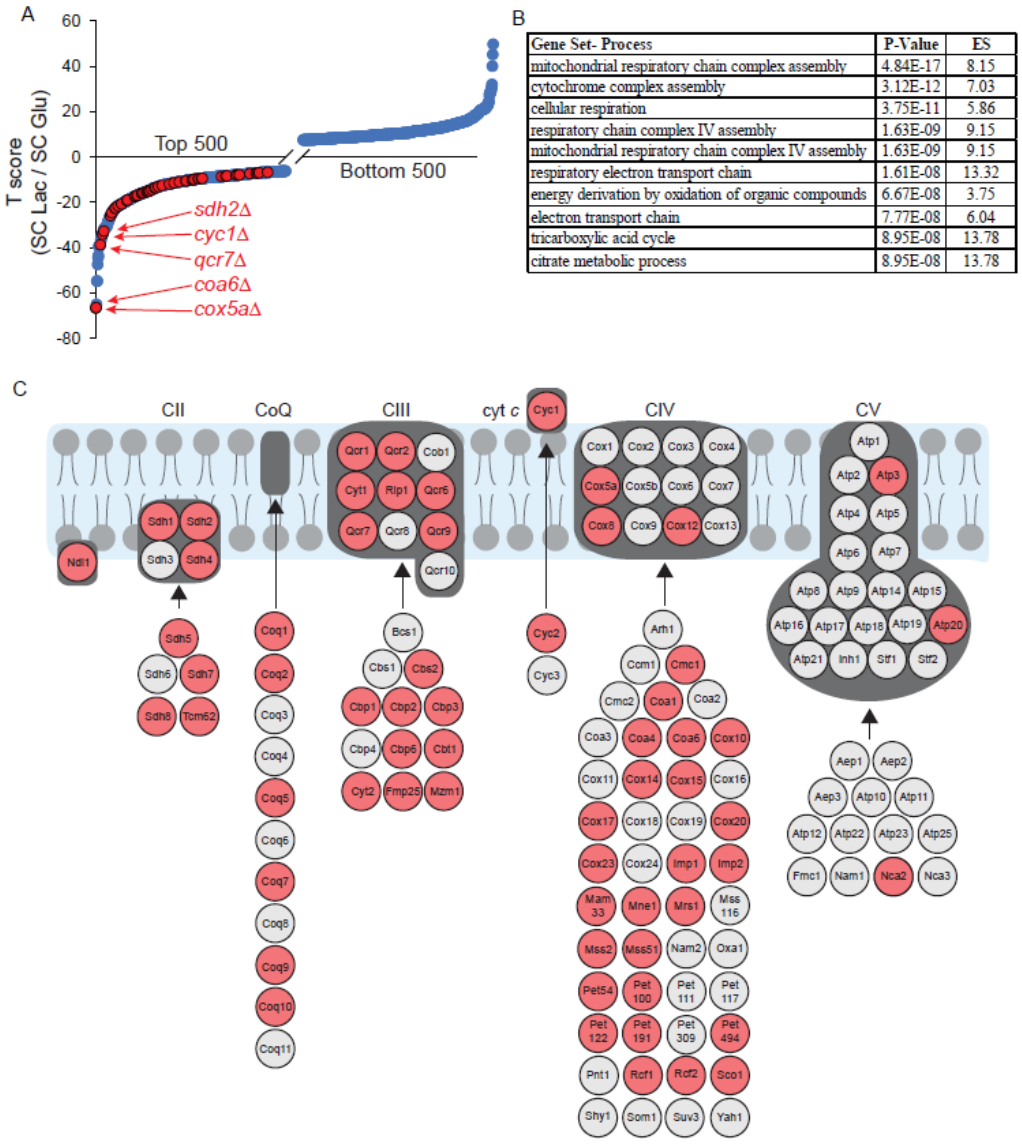

Gene Set- Process	P-Value	ES
mitochondrial respiratory chain complex assembly	4.84E-17	8.15
cytochrome complex assembly	3.12E-12	7.03
cellular respiration	3.75E-11	5.86
respiratory chain complex IV assembly	1.63E-09	9.15
mitochondrial respiratory chain complex IV assembly	1.63E-09	9.15
respiratory electron transport chain	1.61E-08	13.32
energy derivation by oxidation of organic compounds	6.67E-08	3.75
electron transport chain	7.77E-08	6.04
tricarboxylic acid cycle	8.95E-08	13.78
citrate metabolic process	8.95E-08	13.78

Figure 4.3 Genes required for respiratory growth in SC Lactate media.
A) Growth of each mutant in the deletion collection cultured in both SC Lactate media and SC Glucose media was measured and analyzed by the T-score. The T-score of SC Lactate growth compared to SC Glucose growth are plotted for the top and bottom 500 mutants. Known mitochondrial respiratory genes are highlighted in red. B) Gene ontology analysis of the top ten cellular processes that were significantly enriched amongst our top scoring hits from a rank ordered list, where ranking was done from the lowest to the highest T-score. ES indicates the enrichment score. C) A schematic of mitochondrial oxidative phosphorylation subunits and assembly factors, where genes depicted in red were "hits" in the screen with significant T-score values (p value<0.05).

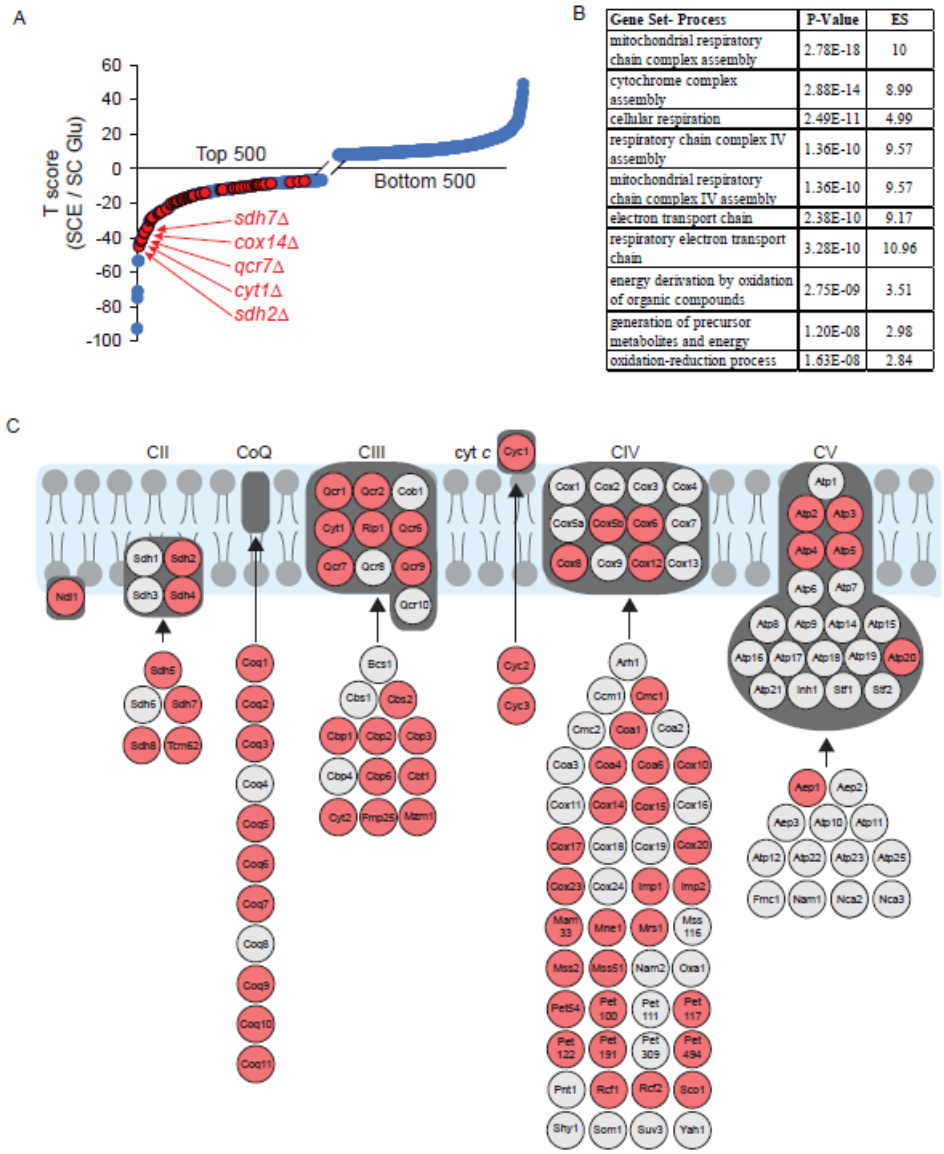

Gene Set- Process	P-Value	ES
mitochondrial respiratory chain complex assembly	2.78E-18	10
cytochrome complex assembly	2.88E-14	8.99
cellular respiration	2.49E-11	4.99
respiratory chain complex IV assembly	1.36E-10	9.57
mitochondrial respiratory chain complex IV assembly	1.36E-10	9.57
electron transport chain	2.38E-10	9.17
respiratory electron transport chain	3.28E-10	10.96
energy derivation by oxidation of organic compounds	2.75E-09	3.51
generation of precursor metabolites and energy	1.20E-08	2.98
oxidation-reduction process	1.63E-08	2.84

Figure 4.4 Genes required for respiratory growth in SC Ethanol media.
A) Growth of each mutant in the deletion collection cultured in both SC Ethanol media and SC Glucose media was measured and analyzed by the T-score. The T-score of SC Ethanol growth compared to SC Glucose growth are plotted for the top and bottom 500 mutants. Known mitochondrial respiratory genes are highlighted in red. B) Gene ontology analysis of the top ten cellular processes that were significantly enriched amongst our top scoring hits from a rank ordered list, where ranking was done from the lowest to the highest T-score. ES indicates the enrichment score. C) A schematic of mitochondrial oxidative phosphorylation subunits and assembly factors, where genes depicted in red were "hits" in the screen with significant T-score values (p value<0.05).

We depict the known respiratory deficient genes that were recovered by our screen on the MRC pathway (Figure 4.2C and 4.3C). Notably, our screen captured genes involved in MRC function associated with every component of the MRC in both conditions (Figure 4.2C and 4.3C). SC Lactate media captured 44% and SC Ethanol media captured 50% of genes involved in the MRC biogenesis and function at p value < 0.05. A majority of the known genes involved in MRC function are common between SC Lactate and SC Ethanol media (Figure 4.4). Similarly, there was a large overlap in the respiratory deficient hits identified via SC Lactate or SC Ethanol growth media (875 genes corresponding to ~75% of hits; Figure 4.4). Interestingly, we noticed a significant number of genes that showed respiratory deficient growth in only one of the two respiratory growth media (~ 300 genes corresponding to ~25% of total hits; Figure 4.4) indicating a carbon-source specific requirement of a subset of genes for respiratory growth.

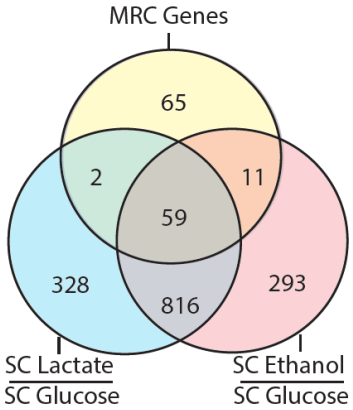

Figure 4.5 Identification of genes required for respiratory growth.
A Venn diagram showing genes from yeast deletion mutants with significant ($p<0.05$) respiratory deficient growth in the two respiratory media (SC Lactate and SC Ethanol) and known genes involved in MRC function.

Pathway Analysis for Etn-based rescue

To identify yeast mutants with increased respiratory growth upon Etn supplementation, we compared the relative frequency of each barcode in Etn-supplemented respiratory media to the media without Etn by using the T-score statistic. A positive T-score identifies mutants that grew better in respiratory conditions with Etn; conversely, a negative T-score identifies mutants that grew poorly with Etn supplementation. We rank ordered all the mutants from positive to negative T-scores. The distribution of the growth of deletion mutants with Etn supplementation shows two tails, indicating that Etn can positively and negatively affect the growth of various mutants (Figure 4.5A and 4.6A). Notably, several genes known to be involved in PE metabolism were recovered as high scoring "hits" in our screen and were present in the upper tail of distribution as expected (Figure 4.5A and 4.6A). For example, we recovered *PSD1* and *PSD2,* which encode PE biosynthetic enzymes (Clancey et al., 1993; Trotter and Voelker, 1995), *PDR17,* which is a phosphatidylinositol transfer protein required for Psd2-mediated PE biosynthesis (Wu et al., 2000), *CKI1,* which encodes a Kennedy pathway enzyme required for PE biosynthesis and *UPS2,* which is required for PS transport from the outer mitochondrial membrane to the inner mitochondrial membrane (Aaltonen et al., 2016; Miyata et al., 2016) (Figure 4.5A & B and Figure 4.6A & B). Recovery of these genes as top hits validates our screening approach and suggests that other top ranked genes in this screen could have a role in PS/PE biosynthesis or intracellular trafficking processes.

Consistently, the unbiased GO analysis of the rank-ordered gene sets from both SC Lactate and SC Ethanol ± Etn conditions identified *phosphatidylethanolamine metabolic process* and *phosphatidylethanolamine biosynthetic process* as cellular processes with high enrichment scores (Figure 4.5C and 4.6C). Identification of PE biosynthetic pathway as a top ranking cellular process provides a strong validation for our screen and suggests that PE/Etn metabolism plays a critical role in other cellular processes identified as top ranking pathways, including vacuolar protein processing, regulation of vacuolar fusion, cellular hyperosmotic response, mitophagy, and mitochondrial electron transport chain (Figure 4.5C and 4.6C). Notably, the GO analysis for "cellular components" identified *mitochondria* with the highest enrichment score suggesting that Etn and/or PE synthesized from Etn compensates for defects in various aspects of mitochondrial functions. This was a surprising find that we followed up on by determining which genes involved in MRC function show improved growth upon Etn supplementation (Figure 4.5D and 4.6D). The analysis of hits in SC Ethanol with Etn supplementation identified over 45% of genes involved in MRC function (Figure 4.6D) and over 30% of MRC genes in SC Lactate + Etn condition, whose loss can be at least partially rescued with Etn supplementation (Figure 4.5D). Taken together, our results suggest a broader role of Etn metabolism in mitochondrial function.

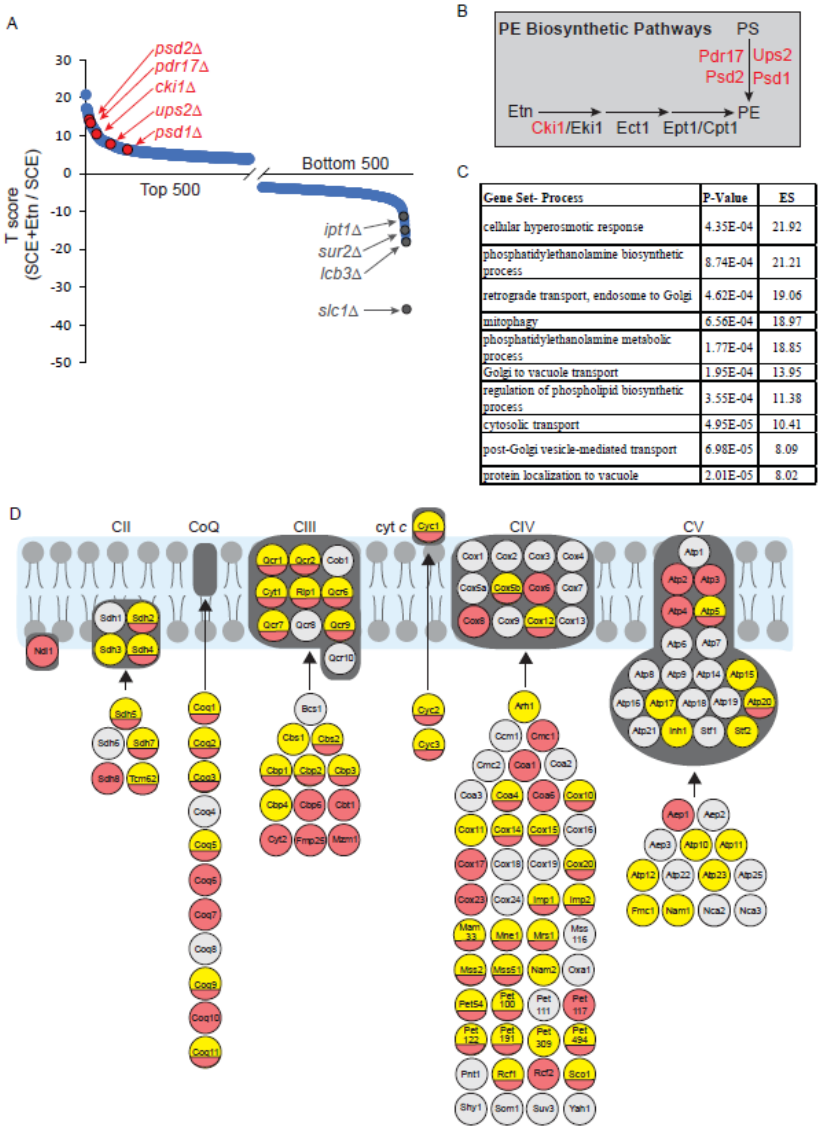

Gene Set- Process	P-Value	ES
cellular hyperosmotic response	4.35E-04	21.92
phosphatidylethanolamine biosynthetic process	8.74E-04	21.21
retrograde transport, endosome to Golgi	4.62E-04	19.06
mitophagy	6.56E-04	18.97
phosphatidylethanolamine metabolic process	1.77E-04	18.85
Golgi to vacuole transport	1.95E-04	13.95
regulation of phospholipid biosynthetic process	3.55E-04	11.38
cytosolic transport	4.95E-05	10.41
post-Golgi vesicle-mediated transport	6.98E-05	8.09
protein localization to vacuole	2.01E-05	8.02

Figure 4.6 Yeast mutants showing improved growth upon Etn supplementation in SC Lactate media.

A) The T-score (SC Lactate + Etn/SC Lactate) is plotted for the top and bottom 500 mutants. Known genes involved in PE biosynthesis are highlighted in red. Known genes involved in sphingolipid biosynthesis are highlighted in gray. B) A schematic of known genes involved in PE biosynthesis. Genes identified as top hits in the screen are highlighted in red. C) Gene ontology analysis of the top ten cellular processes that were significantly enriched amongst our top scoring hits from a rank ordered list, where ranking was done from the highest to the lowest T-score. ES indicates the enrichment score. D) A schematic of mitochondrial oxidative phosphorylation subunits and assembly factors, where genes depicted in red were "hits" in the screen with significant T-score values (p value<0.05) for respiratory deficient growth and genes depicted in yellow were "hits" in the screen with

Figure 4.7 Continued Yeast mutants showing improved growth upon Etn supplementation in SC Lactate media.

significant T-score values (p value<0.05) for strains with improved growth upon Etn supplementation. Genes shown in half red and half yellow circles represents respiratory deficient mutants that are rescued by Etn supplementation.

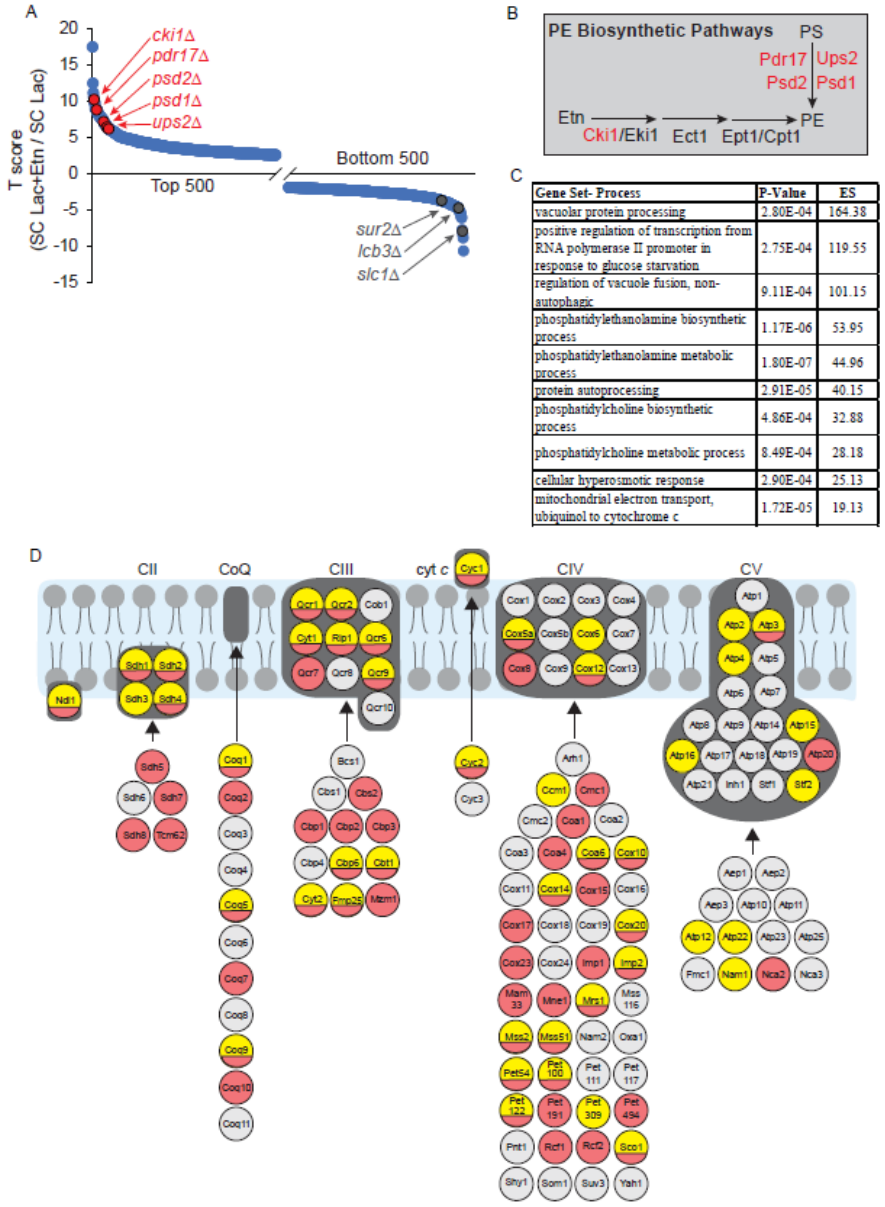

Gene Set- Process	P-Value	ES
vacuolar protein processing	2.80E-04	164.38
positive regulation of transcription from RNA polymerase II promoter in response to glucose starvation	2.75E-04	119.55
regulation of vacuole fusion, non-autophagic	9.11E-04	101.15
phosphatidylethanolamine biosynthetic process	1.17E-06	53.95
phosphatidylethanolamine metabolic process	1.80E-07	44.96
protein autoprocessing	2.91E-05	40.15
phosphatidylcholine biosynthetic process	4.86E-04	32.88
phosphatidylcholine metabolic process	8.49E-04	28.18
cellular hyperosmotic response	2.90E-04	25.13
mitochondrial electron transport, ubiquinol to cytochrome c	1.72E-05	19.13

Figure 4.8 Yeast mutants showing improved growth upon Etn supplementation in SC Ethanol media.

A) The T-score of (SC Ethanol + Etn/SC Ethanol) is plotted for the top and bottom 500 mutants. Known genes involved in PE biosynthesis are highlighted in red. Known genes

Figure 4.9 Continued Yeast mutants showing improved growth upon Etn supplementation in SC Ethanol media.
involved in sphingolipid biosynthesis are highlighted in gray. B) A schematic of known genes involved in PE biosynthesis. Genes identified as top hits in the screen are highlighted red. C) Gene ontology analysis of the top ten cellular processes that were significantly enriched amongst our top scoring hits from a rank ordered list, where ranking was done from the highest to the lowest T-score. ES indicates the enrichment score. D) A schematic of mitochondrial oxidative phosphorylation subunits and assembly factors, where genes depicted in red were "hits" in the screen with significant T-score values (p value<0.05) for respiratory deficient growth. Genes depicted in yellow were "hits" in the screen with significant T-score values (p value<0.05) for strains with improved growth upon Etn supplementation. Genes shown in half red and half yellow circles represents respiratory deficient mutants that are rescued by Etn supplementation.

A link between sphingolipid and Etn metabolism

Although the original goal of our screen was to identify yeast mutants whose growth was rescued by Etn, we were also curious to know yeast mutants whose growth was negatively affected by Etn supplementation. Therefore, we focused on genes present in the lower tail of rank-ordered distribution for Etn-sensitized growth in respiratory media (Figure 4.5A and 4.6A). GO analysis identified *sphingolipid biosynthetic pathway* as the top cellular process that is negatively affected by Etn supplementation (Table 4.2).

Table 4.2 Biological processes negatively affected by Etn in SC Ethanol media

GO annotations	P-value
sphingolipid biosynthetic process	9.23E-05
cellular lipid metabolic process	9.27E-05
phospholipid dephosphorylation	1.39E-04
lipid metabolic process	1.47E-04
galactose metabolic process	1.91E-04
small molecule catabolic process	2.92E-04
sphingolipid metabolic process	3.07E-04
cellular component assembly involved in morphogenesis	4.62E-04
lipid biosynthetic process	5.92E-04
negative regulation of supramolecular fiber organization	6.00E-04
aldehyde catabolic process	6.62E-04
cellular aldehyde metabolic process	6.96E-04
membrane lipid biosynthetic process	7.61E-04
aromatic amino acid transport	9.70E-04

The sphingolipid biosynthetic pathway is connected to Etn metabolism via the Dpl1 enzyme that catalyzes the last step in the catabolism of sphingolipids and generates phospho-Etn (Saba et al., 1997). It is conceivable that in the presence of excess Etn, Dpl1 is inhibited, which would result in a buildup of toxic phosphorylated sphingolipid intermediates (Kim et al., 2000). Interestingly, the lower tails of the distributions (Figure 4.5A and 4.6A) includes many uncharacterized open reading frames (ORF's) (Table 4.3). Since these ORF's are enriched along with genes involved in sphingolipid metabolism, results from the screen could be used to identify novel proteins in sphingolipid metabolism in yeast.

Table 4.3 Yeast mutants whose growth is negatively affected by Etn (p-value<0.01)

Putative uncharacterized genes involved in sphingolipid biosynthesis
YKL066W
YLR407W
YMR244W
YJL135W
YOL046C
YIL059C
YDR467C
YJL119C
YDR290W
YMR209C

Discussion

Here, we designed a genome-wide screen of a yeast deletion mutant library to identify genes required for PS transport to the mitochondria. Our screen was able to identify many genes required for the biosynthesis of PE and the intra-mitochondrial PS transporter, Ups2, as top hits. Recovery of these genes as top hits validates our screening approach and provides a strong confidence that follow-up microbiological, genetics, and biochemical investigations on the top hits from this screen can identify protein(s) involved in PS transport from its site of synthesis in the ER to the mitochondria. Additionally, hits from the screen have the potential to provide information on cellular processes that depend on PE and or Etn metabolism, such as genes involved in sphingolipid metabolism. Moreover, the screen also revealed an unexpected role of Etn in rescuing multiple defects in mitochondrial function, though the mechanism of this rescue remains to be determined. Finally, fitness comparison between mutants grown in fermentable and non-fermentable media identified a number of known MRC genes and analysis of other hits could lead to

the discovery of novel MRC proteins or regulators of mitochondrial bioenergetics. Thus, our screening data offers a valuable resource to connect gene function to PE and mitochondrial energy metabolism.

To identify gene(s) required for PS transport to the mitochondria, a follow-up growth-based secondary screen should be performed on candidates with high positive T-scores for growth in respiratory media with and without Etn supplementation (Figures 4.5A and 4.6A and Supplementary Tables 4 and 5). The following criteria could be useful in further prioritizing genes from these lists to identify PS transporter(s) to the mitochondria: 1) Presence of lipid-binding domains such as the synaptotagmin-like mitochondrial lipid binding (SMP) domain and the pleckstrin homology (PH) domain should be checked as PS transporter(s) are expected to bind PS. 2) Known localization to the mitochondria or ER, as the candidate PS transporter is likely to be present at the donor or the recipient membranes. 3) Presence of ubiquitination sites, as a previous study from the Voelker group has shown that PS transport to the mitochondria is regulated by ubiquitination via Met30 (Schumacher et al., 2002). 4) Known localization to mitochondrial contact sites because many lipid transport proteins (LTPs) are being shown to localize at the Membrane Contact Sites (MCS) as that allows shorter distance for the LTP to travel. 5) Conservation across eukaryotes, because PS is known to be transported from the ER to the mitochondria from yeast to mammals. 6) Presence of multiple “hits” in the same complex because the probability of enrichment of different proteins belonging to the same complex is very low. 7) A “hit” in both respiratory media conditions because loss of PS transport would decrease mitochondrial

PE biosynthesis, which in turn would impair mitochondrial respiration and respiratory growth. After prioritizing the PS transporter candidates using the above criteria, their role in PS transport can be determined by a battery of biochemical and genetic experiments. For example, measurement of steady state levels of PS and PE in purified ER and mitochondria by thin layer chromatography could provide direct *in vivo* evidence because the knockout of the PS transporter to the mitochondria should display low steady state mitochondrial PS and PE levels without a change in their levels in the ER. Additionally, the rate of PS to PE conversion in mitochondria is expected to be reduced.

Notably, components of the ER-mitochondria membrane tethering complex, ERMES, or subunits of the vacuole-mitochondria contact site complex, vCLAMP, were not identified as high-scoring hits in the screen. In fact, none of the core components of these MCSs showed a significant respiratory growth improvement upon Etn supplementation. Our data thus questions the role of ERMES and vCLAMP in PS transport and is more consistent with the previous studies, which demonstrated that ERMES and vCLAMP are not essential for PS transport to the mitochondria (Nguyen et al., 2012; Baker et al., 2016; Iadarola et al., 2020).

In addition to obtaining information pertaining to the main objective of the screen - identifying the mitochondrial PS transporter(s) - we also obtained important information on biological processes and pathways that are likely influenced by Etn or Etn-derived PE. For example, first, we noticed that the fitness of the deletion mutants in the sphingolipid biosynthesis pathway is negatively affected upon Etn supplementation (Figure 4.5A and

4.6A). Second, we identified a number of uncharacterized ORF's that likely code for regulators or "missing enzymes" of sphingolipid pathway (Table 4.3). Third, we unexpectedly found that Etn can rescue respiratory deficient growth of a number of MRC mutants (Figure 4.5 and 4.6).

This later finding raises an important question – what is the mechanism by which Etn rescues respiratory defects of disparate MRC mutants? The role of Etn in respiratory growth rescue of genes involved in MRC function could be PE-dependent or PE-independent. The evidence for a PE-independent role of Etn comes from our previous study where we had shown that the respiratory growth defect of cardiolipin-deficient yeast cells can be ameliorated by Etn without it being incorporated in PE (Basu Ball et al., 2018a). Etn was shown to improve MRC complex assembly and activity while reducing oxidative stress in multiple yeast models of cardiolipin deficiency (Basu Ball et al., 2018a). However, the mechanism by which Etn-mediated this "mito-protective" effect has remained elusive so far. The results from our screen suggest that the mito-protective of Etn is not limited to cardiolipin deficiency but applies to a large number of MRC genes. Recent studies have shown that stimulation of anaplerotic pathways rescues cardiolipin-deficient cells (Li et al., 2019; Raja et al., 2019), suggesting a possible mechanism of Etn-mediated rescue, where Etn acts as an anaplerotic substrate of the TCA cycle. Interestingly, Etn has been suggested to act as an anaplerotic substrate in higher eukaryotes (Weissbach and Sprinson, 1953), however, it has not yet been determined in the yeast. Notably, stimulating anaplerotic pathways in mitochondrial diseases affecting MRC genes has been shown to reduce disease pathologies (Bottani et al., 2020; Chen 2018). Activating

anaplerotic pathways has been proposed to compensate for the loss of components of the MRC by increasing the substrate (reducing equivalents NADH/$FADH_2$) of the MRC and decreasing reductive stress (Titov et al., 2016). We looked for this possibility by examining our screening data to see if mutants of the TCA cycle with respiratory deficiencies are rescued by Etn supplementation. Our screen identified ~50% of TCA cycle mutants with significant respiratory growth deficiency in SC Ethanol media, including *mdh1Δ, mae1Δ, idh2Δ, kgd1Δ, kgd2Δ, sdh1Δ, sdh2Δ, sdh4Δ, yjl045wΔ,* and *fum1*. Of the genes with respiratory growth deficiencies, 50% have a significant respiratory growth improvement upon Etn supplementation, including *mdh1Δ, idh2Δ, kgd2Δ, sdh2Δ,* and *sdh4Δ*. This demonstrates that respiratory growth deficiency of both TCA cycle and oxidative phosphorylation mutants can be rescued upon Etn supplementation. This data suggests that Etn can also rescue respiratory deficiencies upstream of the MRC, perhaps by acting as an anaplerotic substrate. In further support of this idea, none of the genes in the glyoxylate shunt required for anaplerosis have their respiratory growth defects rescued by Etn.

It is important to understand the mechanism by which Etn rescues these deletion mutants as it could inspire development of novel therapeutics for diseases characterized by impaired mitochondrial bioenergetics. We propose the following possible mechanisms by which Etn can rescue respiratory growth deficiency: 1) Etn feeds into anaplerotic pathways that supplement TCA intermediates, as described earlier. 2) Etn import into the mitochondria is mediated by a proton antiporter, as has been shown for mammalian cells (Taylor et al., 2020). A proton antiporter-mediated transport of Etn would help maintain

the mitochondrial membrane potential in the face of an MRC defect, allowing other membrane potential-dependent mitochondrial functions to continue. 3) Etn can exert a mito-protective effect by inducing a stress response.

In summary, our genome-wide BarSeq screen is an important resource that could help identify PS transport proteins, aid in discovering PE-dependent and -independent roles of Etn in mitochondrial functions, uncover novel regulators of sphingolipid metabolism, and disclose novel components and regulators of the MRC. Importantly, our nutrient-sensitized screening strategy to discover novel genes and metabolic pathways relevant to a given nutrient should inspire similar screens for other nutrients.

CHAPTER V

CONCLUSIONS

The work described in this thesis is focused on understanding how phospholipids are transported to the mitochondria, a longstanding problem in cell biology that has remained intractable for many decades. Mitochondrial membranes consist of all major phospholipids of which phosphatidylethanolamine (PE) has been shown to be critically required for mitochondrial respiratory chain function. PE is the second most abundant phospholipid of the mitochondrial membranes, which can be biosynthesized *in situ* from phosphatidylserine (PS) imported from the endoplasmic reticulum (ER), and it can also be imported from other organelles. In my thesis work, I focused on discovering transport machinery of both PE and PS to the mitochondria.

First, I examined the role of mitochondrial membrane contacts sites (MCSs) in phosphatidylethanolamine (PE) transport from the endoplasmic reticulum (ER) to the mitochondria. I discovered that the mitochondrial MCS and vesicular fusion protein, Vps39, is essential for the transport of PE from the ER to the mitochondria. I showed that the loss of Vps39 specifically abrogates PE transport to the mitochondria, without compromising its biosynthesis in the ER, its transport to other subcellular organelles, or the transport of other phospholipids to the mitochondria. I found that the PE levels in both the ER and the mitochondria affect the abundance and recruitment of Vps39 to these organelles. This finding suggests that Vps39 is recruited to these organelles in a PE-dependent manner. Furthermore, I identified essential domains of Vps39 that are required for PE transport to the mitochondria. Surprisingly, I found that the role of Vps39 in

phospholipid trafficking is independent of both its contact site formation and vesicular fusion function. Importantly, the role of Vps39 is conserved in PE trafficking as I found that the human homolog of Vps39 could substitute for the yeast protein *in vivo*.

To study the role of Vps39 in mitochondrial PE transport, I manipulated PE levels in yeast using genetics and nutritional supplementation, which required a detailed understanding of phospholipid biosynthetic pathways. During the literature survey of phospholipid metabolism, I came across a study which reported that choline (Cho), a biosynthetic precursor of phosphatidylcholine (PC), could rescue the respiratory growth of mitochondrial PE-deficient yeast lacking PE biosynthetic enzyme Psd1 (Birner et al., 2001). This finding warranted further investigation because a study from our lab showed that PE is essential for mitochondrial respiration, whereas PC is largely dispensable (Baker et al., 2016), implying that an elevation in mitochondrial PC levels should not rescue the respiratory deficiency of PE-deficient mitochondria. I determined that the mechanism of Cho-mediated respiratory growth rescue of mitochondrial PE-deficient yeast is from partial replenishing of mitochondrial PE levels, not PC levels. I demonstrated that this rescue mechanism is dependent on Cho conversion to PC as well as synthesis of PE via Psd2 in the endosome. I showed through metabolic labeling experiments that in the absence of Cho, Psd2-synthesized PE is mostly used for PC biosynthesis and is unavailable for replenishing mitochondrial PE in Psd1-deficient cells. However, stimulating PC biosynthesis by Cho supplementation spares Psd2-synthesized PE from PC biosynthesis and instead redirects it to the mitochondria. I tested if Vps39 was also required for endosomal PE transport to the mitochondria. Indeed, I found that Vps39 is

required for the transport of endosomal PE to the mitochondria specifically placing it downstream of Psd2 in Cho-mediated rescue.

After elucidating PE transport mechanisms to mitochondria, I focused on identifying molecular machinery required for phosphatidylserine (PS) transport to the mitochondria. PS is a minor constituent of the mitochondrial membrane phospholipids but serves as a substrate for mitochondrial PE biosynthesis, and thus abrogating PS transport would eliminate mitochondrial PE, which is the second most abundant mitochondrial phospholipid and is essential for mitochondrial respiration. In the last three decades, a number of research groups have attempted to identify proteins required for PS transport to the mitochondria, but the mechanism and molecular players involved in this process still remains controversial. To identify genes required for PS transport to the mitochondria in an unbiased manner, I designed a genome-wide screen that utilized a DNA-barcoded yeast deletion mutant library. Our screening approach was based on the idea that loss of PS transport will decrease mitochondrial PE resulting in reduced respiratory growth that can be rescued by the addition of Etn, which partially replenishes mitochondrial PE. This screen recovered a number of mutants involved in PE biosynthetic pathways while revealing novel mutants that could be involved in mitochondrial PS import. A follow-up biochemical study is required to validate gene(s) identified in the screen as bona fide PS transport proteins.

Future Directions

One major outcome of my work was the finding that Vps39 is essential for PE transport from the ER to the mitochondria. I provide strong genetic and *in vivo* biochemical evidence that directly implicates Vps39 in PE transport to the mitochondria; however, the precise biochemical function of Vps39 in the transport process remains to be elucidated. Based on the recent discoveries about lipid transport proteins (LTPs), I predict that Vps39 is a soluble-carrier LTP that binds PE in the ER, transports it through the cytosol, and releases it on the outer membrane of the mitochondria. To directly demonstrate that Vps39 is an LTP, an *in vitro* lipid transport system needs to be established. This will involve purifying the soluble Vps39 protein and using liposome-based assays to show that Vps39 can both bind and transfer PE *in vitro*. The mechanism by which LTPs pick up specific phospholipids from a donor membrane is still not understood; but structural studies of newly identified LTPs can contribute to understanding this mechanism.

Our Etn-sensitized has yielded a rich catalog of genes required for PS transport, mitochondrial respiratory chain function, and other biochemical processes that are linked to Etn including sphingolipid metabolism. The top "hits" of the screen need to be tested biochemically to determine which genes are required for PS transport to the mitochondria. Based on the requirement of PS transport to the mitochondria for mitochondrial function, I predict that there will be redundant pathways for mitochondrial PS transport. To determine which genes are essential for PS transport to the mitochondria: 1) steady state mitochondrial phospholipid levels of the single deletion mutant would show reduced

mitochondrial PS and PE levels and 2) metabolic labeling using [^{3}H] serine in a *psd2Δ* background would show reduced PS to PE to PC conversion.

Another major finding of my work is the cross-pathway regulation of Ect1 and Pct1, two proteins that encode the rate-limiting step in the Kennedy pathway of PE and PC biosynthesis, respectively. I predict that Ect1 and Pct1 form a complex that is required for recruitment to the membrane and subsequent activity in a *psd1Δ* background. First, the activity of Ect1 and Pct1 can be determined using metabolic labeling of [^{3}H] Etn and [^{3}H] Cho, and subsequent assaying for labeled PE and PC in *pct1Δ* and *ect11Δ* cells, respectively. The activity of Ect1 and Pct1 should also be determined with metabolic labeling in a *psd1Δ* background because low cellular PE levels could affect the recruitment of Ect1 and Pct1 to the membrane. Co-immunoprecipitation could be used to examine if Ect1 and Pct1 physically interact and form a complex.

An additional finding from my study is that Vps39 genetically interacts with both mitochondrial and extra-mitochondrial PE biosynthetic machinery in respiratory media conditions. The genetic interaction study raises an important question: why is there a respiratory growth defect in Dpl1 and Psd2 deleted cells in a *vps39Δ* background? *vps39Δdpl1Δ* and *vps39Δpsd2Δ* cells are not rescued upon Etn supplementation, indicating that the cause of the respiratory deficiency is not a reduction in cellular PE levels. Additional experiments are needed to unravel the role of Vps39 in intracellular PE trafficking. In summary, my thesis work has uncovered novel factors in PS and PE transport to the mitochondria.

REFERENCES

Aaltonen MJ, Friedman JR, Osman C, Salin B, di Rago JP, Nunnari J, Langer T, Tatsuta T. (2016). MICOS and phospholipid transfer by Ups2-Mdm35 organize membrane lipid synthesis in mitochondria. J Cell Biol. 213, 525-534.

Acín-Pérez R, Fernández-Silva P, Peleato ML, Pérez-Martos A, Enriquez JA. (2008). Respiratory active mitochondrial supercomplexes. Mol Cell. 32, 529-539.

AhYoung AP, Jiang J, Zhang J, Khoi Dang X, Loo JA, Zhou ZH, Egea PF. (2015). Conserved SMP domains of the ERMES complex bind phospholipids and mediate tether assembly. Proc Natl Acad Sci U S A. 112, E3179-188.

Amberg DC, Burke DJ, Strathern JN, (2005). Methods in Yeast Genetics. A Cold Spring Harbor Laboratory Course Manual, Cold Spring Harbor, NY: Cold Spring Harbor Laboratory Press.

Bae-Lee MS, Carman GM. (1984). Phosphatidylserine synthesis in Saccharomyces cerevisiae. Purification and characterization of membrane-associated phosphatidylserine synthase. J Biol Chem. 259, 10857-10862.

Baker CD, Basu Ball W, Pryce EN, Gohil VM. (2016). Specific requirements of nonbilayer phospholipids in mitochondrial respiratory chain function and formation. Mol Biol Cell. 27, 2161-2171.

Balderhaar HJ, Ungermann C. (2013). CORVET and HOPS tethering complexes - coordinators of endosome and lysosome fusion. J Cell Sci. 126, 1307-1316.

Balla T. (2013). Phosphoinositides: tiny lipids with giant impact on cell regulation. Physiol Rev. 93, 1019-1137

Bartlett GR. (1959). Phosphorus assay in column chromatography. J Biol Chem. 234, 466-468.

Basu Ball W[a], Baker CD, Neff JK, Apfel GL, Lagerborg KA, Žun G, Petrovič U, Jain M, Gohil VM. (2018). Ethanolamine ameliorates mitochondrial dysfunction in cardiolipin-deficient yeast cells. J Biol Chem. 293, 10870-10883.

Basu Ball W[b], Neff JK, Gohil VM. (2018). The role of nonbilayer phospholipids in mitochondrial structure and function. FEBS Lett. 592, 1273-1290.

Bean BDM, Dziurdzik SK, Kolehmainen KL, Fowler CMS, Kwong WK, Grad LI, Davey M, Schluter C, Conibear E. (2018). Competitive organelle-specific adaptors recruit Vps13 to membrane contact sites. J Cell Biol. 217, 3593-3607.

Becker T, Horvath SE, Böttinger L, Gebert N, Daum G, Pfanner N. (2013). Role of phosphatidylethanolamine in the biogenesis of mitochondrial outer membrane proteins. J Biol Chem. 288, 16451-16459.

Birner R, Bürgermeister M, Schneiter R, Daum G. (2001). Roles of phosphatidylethanolamine and of its several biosynthetic pathways in Saccharomyces cerevisiae. Mol Biol Cell. 12, 997-1007.

Bleijerveld OB, Brouwers JF, Vaandrager AB, Helms JB, Houweling M. (2007). The CDP-ethanolamine pathway and phosphatidylserine decarboxylation generate different phosphatidylethanolamine molecular species. J Biol Chem. 282, 28362-28372.

Boldogh I, Vojtov N, Karmon S, Pon LA. (1998). Interaction between mitochondria and the actin cytoskeleton in budding yeast requires two integral mitochondrial outer membrane proteins, Mmm1p and Mdm10p. J Cell Biol. 141, 1371-1381.

Bottani E, Lamperti C, Prigione A, Tiranti V, Persico N, Brunetti D. (2020). Therapeutic Approaches to Treat Mitochondrial Diseases: "One-Size-Fits-All" and "Precision Medicine" Strategies. Pharmaceutics. 12, 1083.

Böttinger L, Horvath SE, Kleinschroth T, Hunte C, Daum G, Pfanner N, Becker T. (2012). Phosphatidylethanolamine and cardiolipin differentially affect the stability of mitochondrial respiratory chain supercomplexes. J Mol Biol. 423, 677-686.

Bürgermeister M, Birner-Grünberger R, Nebauer R, Daum G. (2004). Contribution of different pathways to the supply of phosphatidylethanolamine and phosphatidylcholine to mitochondrial membranes of the yeast Saccharomyces cerevisiae. Biochim Biophys Acta. 1686, 161-168.

Bustillo-Zabalbeitia I, Montessuit S, Raemy E, Basañez G, Terrones O, Martinou JC. (2014). Specific interaction with cardiolipin triggers functional activation of Dynamin-Related Protein 1. PLoS One. 9, e102738

Calzada E, Avery E, Sam PN, Modak A, Wang C, McCaffery JM, Han X, Alder NN, Claypool SM. (2019). Phosphatidylethanolamine made in the inner mitochondrial membrane is essential for yeast cytochrome bc_1 complex function. Nat Commun. 10, 1432.

Carman GM, Han GS. (2011). Regulation of phospholipid synthesis in the yeast Saccharomyces cerevisiae. Annu Rev Biochem. 80, 859-883.

Casares D, Escribá PV, Rosselló CA. (2019). Membrane Lipid Composition: Effect on Membrane and Organelle Structure, Function and Compartmentalization and Therapeutic Avenues. Int J Mol Sci. 20, 2167.

Chan EY, McQuibban GA. (2012). Phosphatidylserine decarboxylase 1 (Psd1) promotes mitochondrial fusion by regulating the biophysical properties of the mitochondrial membrane and alternative topogenesis of mitochondrial genome maintenance protein 1 (Mgm1). J Biol Chem. 287, 40131-40139

Chen Q, Kirk K, Shurubor YI, Zhao D, Arreguin AJ, Shahi I, Valsecchi F, Primiano G, Calder EL, Carelli V, Denton TT, Beal MF, Gross SS, Manfredi G, D'Aurelio M. (2018). Rewiring of Glutamine Metabolism Is a Bioenergetic Adaptation of Human Cells with Mitochondrial DNA Mutations. Cell Metab. 27, 1007-1025.e5.

Clancey CJ, Chang SC, Dowhan W. (1993). Cloning of a gene (PSD1) encoding phosphatidylserine decarboxylase from Saccharomyces cerevisiae by complementation of an Escherichia coli mutant. J Biol Chem. 268, 24580-24590.

Connerth M, Tatsuta T, Haag M, Klecker T, Westermann B, Langer T. (2012). Intramitochondrial transport of phosphatidic acid in yeast by a lipid transfer protein. Science. 338, 815-818.

Cowart LA, Obeid LM. (2007). Yeast sphingolipids: recent developments in understanding biosynthesis, regulation, and function. Biochim Biophys Acta. 1771, 421-431.

Daum G. (1985). Lipids of mitochondria. Biochim Biophys Acta. 822, 1-42.

de Kroon AI, Rijken PJ, De Smet CH. (2013). Checks and balances in membrane phospholipid class and acyl chain homeostasis, the yeast perspective. Prog Lipid Res. 52, 374-394

DeVay RM, Dominguez-Ramirez L, Lackner LL, Hoppins S, Stahlberg H, Nunnari J. (2009). Coassembly of Mgm1 isoforms requires cardiolipin and mediates mitochondrial inner membrane fusion. J Cell Biol. 186, 793-803.

Dunn KW, Kamocka MM, McDonald JH. (2011). A practical guide to evaluating colocalization in biological microscopy. Am J Physiol Cell Physiol. 300, C723-C742.

Eden E, Navon R, Steinfeld I, Lipson D, Yakhini Z. (2009). GOrilla: a tool for discovery and visualization of enriched GO terms in ranked gene lists. BMC Bioinformatics. 10, 48.

Elbaz-Alon Y, Rosenfeld-Gur E, Shinder V, Futerman AH, Geiger T, Schuldiner M. (2014). A dynamic interface between vacuoles and mitochondria in yeast. Dev Cell. 30, 95-102.

Fischl AS, Carman GM. (1983). Phosphatidylinositol biosynthesis in Saccharomyces cerevisiae: purification and properties of microsome-associated phosphatidylinositol synthase. J Bacteriol. 154, 304-311.

Flis VV, Daum G. (2013). Lipid transport between the endoplasmic reticulum and mitochondria. Cold Spring Harb Perspect Biol. 5, a013235.

Folch J, Lees M, Sloane Stanley GH. (1957). A simple method for the isolation and purification of total lipides from animal tissues. J Biol Chem. 226, 497-509.

Gabriel K, Milenkovic D, Chacinska A, Müller J, Guiard B, Pfanner N, Meisinger C. (2007). Novel mitochondrial intermembrane space proteins as substrates of the MIA import pathway. J Mol Biol. 365, 612-620.

Gatta AT, Levine TP. (2017). Piecing Together the Patchwork of Contact Sites. Trends Cell Biol. 27, 214-229.

Gaynor PM, Carman GM. (1990). Phosphatidylethanolamine methyltransferase and phospholipid methyltransferase activities from Saccharomyces cerevisiae. Enzymological and kinetic properties. Biochim Biophys Acta. 1045, 156-163.

Ghosh S, Basu Ball W, Madaris TR, Srikantan S, Madesh M, Mootha VK, Gohil VM. (2020). An essential role for cardiolipin in the stability and function of the mitochondrial calcium uniporter. Proc Natl Acad Sci U S A. 117, 16383-16390.

Girisha KM, von Elsner L, Neethukrishna K, Muranjan M, Shukla A, Bhavani GS, Nishimura G, Kutsche K, Mortier G. (2019). The homozygous variant c.797G>A/p.(Cys266Tyr) in PISD is associated with a Spondyloepimetaphyseal dysplasia with large epiphyses and disturbed mitochondrial function. Hum Mutat. 40, 299-309.

Gohil VM, Greenberg ML. (2009). Mitochondrial membrane biogenesis: phospholipids and proteins go hand in hand. J Cell Biol 184, 469-472.

Gohil VM, Thompson MN, Greenberg ML. (2005). Synthetic lethal interaction of the mitochondrial phosphatidylethanolamine and cardiolipin biosynthetic pathways in Saccharomyces cerevisiae. J Biol Chem. 280, 35410-35416.

González Montoro A, Auffarth K, Hönscher C, Bohnert M, Becker T, Warscheid B, Reggiori F, van der Laan M, Fröhlich F, Ungermann C. (2018). Vps39 Interacts with Tom40 to Establish One of Two Functionally Distinct Vacuole-Mitochondria Contact Sites. Dev Cell. 45, 621-636.e7.

Gulshan K, Shahi P, Moye-Rowley WS. (2010). Compartment-specific synthesis of phosphatidylethanolamine is required for normal heavy metal resistance. Mol Biol Cell. 21, 443-455.

Haas A, Scheglmann D, Lazar T, Gallwitz D, Wickner W. (1995). The GTPase Ypt7p of Saccharomyces cerevisiae is required on both partner vacuoles for the homotypic fusion step of vacuole inheritance. EMBO J. 14, 5258-5270.

Hanada K. (2018). Lipid transfer proteins rectify inter-organelle flux and accurately deliver lipids at membrane contact sites. J Lipid Res. 59, 1341-1366.

Henneberry AL, Lagace TA, Ridgway ND, McMaster CR. (2001). Phosphatidylcholine synthesis influences the diacylglycerol homeostasis required for SEC14p-dependent Golgi function and cell growth. Mol Biol Cell. 12, 511-520.

Henry SA, Kohlwein SD, Carman GM. (2012). Metabolism and regulation of glycerolipids in the yeast Saccharomyces cerevisiae. Genetics. 190, 317-349.

Holthuis JC, Menon AK. (2014). Lipid landscapes and pipelines in membrane homeostasis. Nature. 510, 48-57.

Hönscher C, Mari M, Auffarth K, Bohnert M, Griffith J, Geerts W, van der Laan M, Cabrera M, Reggiori F, Ungermann C. (2014). Cellular metabolism regulates contact sites between vacuoles and mitochondria. Dev Cell. 30, 86-94.

Horvath SE, Daum G. (2013). Lipids of mitochondria. Prog Lipid Res. 52, 590-614.

Huang Z, Chen K, Zhang J, Li Y, Wang H, Cui D, Tang J, Liu Y, Shi X, Li W, Liu D, Chen R, Sucgang RS, Pan X. (2013). A functional variomics tool for discovering drug-resistance genes and drug targets. Cell Rep. 3, 577-585.

Iadarola DM, Basu Ball W, Trivedi PP, Fu G, Nan B, Gohil VM. (2020). Vps39 is required for ethanolamine-stimulated elevation in mitochondrial phosphatidylethanolamine. Biochim Biophys Acta Mol Cell Biol Lipids. 1865, 158655.

Iadarola DM, Joshi A, Caldwell CB, Gohil VM. (2021). Choline restores respiration in Psd1-deficient yeast by replenishing mitochondrial phosphatidylethanolamine. J Biol Chem. 100539.

Janke C, Magiera MM, Rathfelder N, Taxis C, Reber S, Maekawa H, Moreno-Borchart A, Doenges G, Schwob E, Schiebel E, Knop M. (2004). A versatile toolbox for PCR-based tagging of yeast genes: new fluorescent proteins, more markers and promoter substitution cassettes. Yeast. 21, 947-962.

Janssen MJ, de Jong HM, de Kruijff B, de Kroon AI. (2002). Cooperative activity of phospholipid-N-methyltransferases localized in different membranes. FEBS Lett. 513, 197-202.

Jeong H, Park J, Jun Y, Lee C. (2017). Crystal structures of Mmm1 and Mdm12-Mmm1 reveal mechanistic insight into phospholipid trafficking at ER-mitochondria contact sites. Proc Natl Acad Sci U S A. 114, E9502-E9511.

Jeong H, Park J, Lee C. (2016). Crystal structure of Mdm12 reveals the architecture and dynamic organization of the ERMES complex. EMBO Rep. 17, 1857-1871.

Jiang F, Ryan MT, Schlame M, Zhao M, Gu Z, Klingenberg M, Pfanner N, Greenberg ML. (2000). Absence of cardiolipin in the crd1 null mutant results in decreased mitochondrial membrane potential and reduced mitochondrial function. J Biol Chem. 275, 22387-22394.

John Peter AT, Herrmann B, Antunes D, Rapaport D, Dimmer KS, Kornmann B. (2017). Vps13-Mcp1 interact at vacuole-mitochondria interfaces and bypass ER-mitochondria contact sites. J Cell Biol. 216, 3219-3229.

Joseph-Horne T, Hollomon DW, Wood PM. (2001). Fungal respiration: a fusion of standard and alternative components. Biochim Biophys Acta. 1504, 179-195.

Joshi AS, Thompson MN, Fei N, Hüttemann M, Greenberg ML. (2012). Cardiolipin and mitochondrial phosphatidylethanolamine have overlapping functions in mitochondrial fusion in Saccharomyces cerevisiae. J Biol Chem. 287, 17589-17597.

Kaplan MR, Simoni RD. (1985). Intracellular transport of phosphatidylcholine to the plasma membrane. J Cell Biol. 101, 441-445.

Kawano S, Tamura Y, Kojima R, Bala S, Asai E, Michel AH, Kornmann B, Riezman I,

Riezman H, Sakae Y, Okamoto Y, Endo T. (2018). Structure-function insights into direct lipid transfer between membranes by Mmm1-Mdm12 of ERMES. J Cell Biol. 217, 959-974.

Kim KH, Carman GM. (1999). Phosphorylation and regulation of choline kinase from Saccharomyces cerevisiae by protein kinase A. J Biol Chem. 274, 9531-9538.

Kim S, Fyrst H, Saba J. (2000). Accumulation of phosphorylated sphingoid long chain bases results in cell growth inhibition in Saccharomyces cerevisiae. Genetics. 156, 1519-1529.

Kodaki T, Yamashita S. (1987). Yeast phosphatidylethanolamine methylation pathway. Cloning and characterization of two distinct methyltransferase genes. J Biol Chem. 262, 15428-15435.

Kojima R, Endo T, Tamura Y. (2016). A phospholipid transfer function of ER-mitochondria encounter structure revealed in vitro. Sci Rep. 6, 30777.

Kornmann B, Currie E, Collins SR, Schuldiner M, Nunnari J, Weissman JS, Walter P. (2009). An ER-mitochondria tethering complex revealed by a synthetic biology screen. Science. 325, 477-481.

Kumar N, Leonzino M, Hancock-Cerutti W, Horenkamp FA, Li P, Lees JA, Wheeler H, Reinisch KM, De Camilli P. (2018). VPS13A and VPS13C are lipid transport proteins differentially localized at ER contact sites. J Cell Biol. 217, 3625-3639

Lahiri S, Toulmay A, Prinz WA. (2015). Membrane contact sites, gateways for lipid homeostasis. Curr Opin Cell Biol. 33, 82-87.

Lang A, John Peter AT, Kornmann B. (2015). ER-mitochondria contact sites in yeast: beyond the myths of ERMES. Curr Opin Cell Biol. 35, 7-12.

Lasserre JP, Dautant A, Aiyar RS, Kucharczyk R, Glatigny A, Tribouillard-Tanvier D, Rytka J, Blondel M, Skoczen N, Reynier P, Pitayu L, Rötig A, Delahodde A, Steinmetz LM, Dujardin G, Procaccio V, di Rago JP. (2015). Yeast as a system for modeling mitochondrial disease mechanisms and discovering therapies. Dis Model Mech. 8, 509-526.

Letts VA, Klig LS, Bae-Lee M, Carman GM, Henry SA. (1983). Isolation of the yeast structural gene for the membrane-associated enzyme phosphatidylserine synthase. Proc Natl Acad Sci U S A. 80, 7279-7283.

Lev S. (2012). Nonvesicular lipid transfer from the endoplasmic reticulum. Cold Spring Harb Perspect Biol. 4, a013300.

Li Y, Lou W, Raja V, Denis S, Yu W, Schmidtke MW, Reynolds CA, Schlame M, Houtkooper RH, Greenberg ML. (2019). Cardiolipin-induced activation of pyruvate dehydrogenase links mitochondrial lipid biosynthesis to TCA cycle function. J Biol Chem. 294, 11568-11578.

Lürick A, Gao J, Kuhlee A, Yavavli E, Langemeyer L, Perz A, Raunser S, Ungermann C. (2017). Multivalent Rab interactions determine tether-mediated membrane fusion. Mol Biol Cell. 28, 322-332.

McGee TP, Skinner HB, Bankaitis VA. (1994). Functional redundancy of CDP-ethanolamine and CDP-choline pathway enzymes in phospholipid biosynthesis: ethanolamine-dependent effects on steady-state membrane phospholipid composition in Saccharomyces cerevisiae. J Bacteriol. 176, 6861-6868

McMaster CR. (2018). From yeast to humans - roles of the Kennedy pathway for phosphatidylcholine synthesis. FEBS Lett. 592, 1256-1272.

Meisinger C, Pfanner N, Truscott KN. (2006). Isolation of yeast mitochondria. Methods Mol Biol. 313, 33-39.

Mejia EM, Hatch GM. (2016). Mitochondrial phospholipids: role in mitochondrial function. J Bioenerg Biomembr. 8, 99-112

Menon AK, Stevens VL. (1992). Phosphatidylethanolamine is the donor of the ethanolamine residue linking a glycosylphosphatidylinositol anchor to protein. J Biol Chem. 267, 15277-15280.

Min-Seok R, Kawamata Y, Nakamura H, Ohta A, Takagi M. (1996). Isolation and characterization of ECT1 gene encoding CTP: phosphoethanolamine cytidylyltransferase of Saccharomyces cerevisiae. J Biochem. 120, 1040-1047.

Miyata N, Watanabe Y, Tamura Y, Endo T, Kuge O. (2016). Phosphatidylserine transport by Ups2-Mdm35 in respiration-active mitochondria. J Cell Biol. 214, 77-88.

Nebauer R, Schuiki I, Kulterer B, Trajanoski Z, Daum G. (2007). The phosphatidylethanolamine level of yeast mitochondria is affected by the mitochondrial components Oxa1p and Yme1p. FEBS J. 274, 6180-6190.

Nguyen TT, Lewandowska A, Choi JY, Markgraf DF, Junker M, Bilgin M, Ejsing CS, Voelker DR, Rapoport TA, Shaw JM. (2012). Gem1 and ERMES do not directly affect phosphatidylserine transport from ER to mitochondria or mitochondrial inheritance. Traffic. 13, 880-890.

Nishimura T, Stefan CJ. (2020). Specialized ER membrane domains for lipid metabolism and transport. Biochim Biophys Acta Mol Cell Biol Lipids. 1865, 158492.

Novick P, Schekman R. (1979). Secretion and cell-surface growth are blocked in a temperature-sensitive mutant of Saccharomyces cerevisiae. Proc Natl Acad Sci U S A. 76, 1858-1862.

Osman C, Merkwirth C, Langer T. (2009). Prohibitins and the functional compartmentalization of mitochondrial membranes. J Cell Sci. 122, 3823-2830.

Park JS, Thorsness MK, Policastro R, McGoldrick LL, Hollingsworth NM, Thorsness PE, Neiman AM. (2016). Yeast Vps13 promotes mitochondrial function and is localized at membrane contact sites. Mol Biol Cell. 27, 2435-2449.

Paulus H, Kennedy EP. (1960). The enzymatic synthesis of inositol monophosphatide. J Biol Chem. 235, 1303-1311.

Peter VG, Quinodoz M, Pinto-Basto J, Sousa SB, Di Gioia SA, Soares G, Ferraz Leal G, Silva ED, Pescini Gobert R, Miyake N, Matsumoto N, Engle EC, Unger S, Shapiro F, Superti-Furga A, Rivolta C, Campos-Xavier B. (2019). The Liberfarb syndrome, a multisystem disorder affecting eye, ear, bone, and brain development, is caused by a founder pathogenic variant in thePISD gene. Genet Med. 21, 2734-2743.

Plemel RL, Lobingier BT, Brett CL, Angers CG, Nickerson DP, Paulsel A, Sprague D, Merz AJ. (2011). Subunit organization and Rab interactions of Vps-C protein complexes that control endolysosomal membrane traffic. Mol Biol Cell. 22, 1353-1363.

Prinz WA, (2010). Lipid trafficking sans vesicles: where, why, how? Cell. 143, 870-874.

Prinz WA. (2014). Bridging the gap: membrane contact sites in signaling, metabolism, and organelle dynamics. J Cell Biol. 205, 759-769.

Raja V, Salsaa M, Joshi AS, Li Y, van Roermund CWT, Saadat N, Lazcano P, Schmidtke M, Hüttemann M, Gupta SV, Wanders RJA, Greenberg ML. (2019). Cardiolipin-deficient cells depend on anaplerotic pathways to ameliorate defective TCA cycle function. Biochim Biophys Acta Mol Cell Biol Lipids. 1864, 654-661.

Robinson DG, Chen W, Storey JD, Gresham D. (2014). Design and analysis of Bar-seq experiments. G3 (Bethesda). 4, 11-18.

Saba JD, Nara F, Bielawska A, Garrett S, Hannun YA. (1997). The BST1 gene of Saccharomyces cerevisiae is the sphingosine-1-phosphate lyase. J Biol Chem. 272, 26087-26090.

Saita S, Tatsuta T, Lampe PA, König T, Ohba Y, Langer T. (2018). PARL partitions the lipid transfer protein STARD7 between the cytosol and mitochondria. EMBO J. 37, e97909.

Santos AX, Riezman H. (2012). Yeast as a model system for studying lipid homeostasis and function. FEBS Lett. 586, 2858-2867.

Schägger H, Pfeiffer K. (2000). Supercomplexes in the respiratory chains of yeast and mammalian mitochondria. EMBO J. 19, 1777-1783.

Schmidt O, Pfanner N, Meisinger C. (2010). Mitochondrial protein import: from proteomics to functional mechanisms. Nat Rev Mol Cell Biol. 11, 655-667.

Schuler MH, Di Bartolomeo F, Mårtensson CU, Daum G, Becker T. (2016). Phosphatidylcholine Affects Inner Membrane Protein Translocases of Mitochondria. J Biol Chem. 291, 18718-18729.

Schumacher MM, Choi JY, Voelker DR. (2002). Phosphatidylserine transport to the mitochondria is regulated by ubiquitination. J Biol Chem. 277, 51033-51042.

Smith AM, Heisler LE, Mellor J, Kaper F, Thompson MJ, Chee M, Roth FP, Giaever G, Nislow C. (2009). Quantitative phenotyping via deep barcode sequencing. Genome Res. 19, 1836-1842.

Tamura Y, Harada Y, Nishikawa S, Yamano K, Kamiya M, Shiota T, Kuroda T, Kuge O, Sesaki H, Imai K, Tomii K, Endo T. (2013). Tam41 is a CDP-diacylglycerol synthase required for cardiolipin biosynthesis in mitochondria. Cell Metab. 17, 709-718.

Tamura Y, Kawano S, Endo T. (2020). Lipid homeostasis in mitochondria. Biol Chem. 401, 821-833.

Tamura Y, Sesaki H, Endo T. (2014). Phospholipid transport via mitochondria. Traffic. 15, 933-945.

Tan T, Ozbalci C, Brügger B, Rapaport D, Dimmer KS, (2013). Mcp1 and Mcp2, two novel proteins involved in mitochondrial lipid homeostasis, J. Cell Sci. 126, 3563-3574.

Tasseva G, Bai HD, Davidescu M, Haromy A, Michelakis E, Vance JE. (2013). Phosphatidylethanolamine deficiency in Mammalian mitochondria impairs oxidative phosphorylation and alters mitochondrial morphology. J Biol Chem. 288, 4158-4173.

Tatsuta T, Scharwey M, Langer T. (2014). Mitochondrial lipid trafficking. Trends Cell Biol. 24, 44-52.

Taylor A, Grapentine S, Ichlpuniani J, Bakovic M. (2020). The novel roles of choline transporter-like 1 and 2 in ethanolamine transport. bioRxiv. 08.27.270223

Titov DV, Cracan V, Goodman RP, Peng J, Grabarek Z, Mootha VK. (2016). Complementation of mitochondrial electron transport chain by manipulation of the NAD+/NADH ratio. Science. 352, 231-235.

Trotter PJ, Pedretti J, Voelker DR. (1993). Phosphatidylserine decarboxylase from Saccharomyces cerevisiae. Isolation of mutants, cloning of the gene, and creation of a null allele. J Biol Chem. 268, 21416-21424.

Trotter PJ, Voelker DR. (1995). Identification of a non-mitochondrial phosphatidylserine decarboxylase activity (PSD2) in the yeast Saccharomyces cerevisiae. J Biol Chem. 270, 6062-6070.

Trotter PJ, Voelker DR. (1995). Identification of a non-mitochondrial phosphatidylserine decarboxylase activity (PSD2) in the yeast Saccharomyces cerevisiae. J Biol Chem. 270, 6062-6070.

Tsukagoshi Y, Nikawa J, Yamashita S. (1987). Molecular cloning and characterization of the gene encoding cholinephosphate cytidylyltransferase in Saccharomyces cerevisiae. Eur J Biochem. 169, 477-486.

Flis VV, Daum G. (2013) Lipid transport between the endoplasmic reticulum and mitochondria, Cold Spring Harb. Perspect. Biol. pii:a013235.

van Meer G, Voelker DR, Feigenson GW. (2008). Membrane lipids: where they are and how they behave. Nat Rev Mol Cell Biol. 9, 112-124.

Vance DE. (2014). Phospholipid methylation in mammals: from biochemistry to physiological function. Biochim Biophys Acta. 1838, 1477-1487.

Vance JE, Aasman EJ, Szarka R. (1990). Brefeldin A does not inhibit the movement of phosphatidylethanolamine from its sites for synthesis to the cell surface. J Biol Chem. 266, 8241-8247.

Vance JE. (2015). Phospholipid synthesis and transport in mammalian cells. Traffic. 16, 1-18.

Voelker DR. (2009). Genetic and biochemical analysis of non-vesicular lipid traffic. Annu Rev Biochem. 78, 827-856.

Watanabe Y, Tamura Y, Kakuta C, Watanabe S, Endo T. (2020). Structural basis for interorganelle phospholipid transport mediated by VAT-1. J Biol Chem. 295, 3257-3268.

Watanabe Y, Tamura Y, Kawano S, Endo T. (2015). Structural and mechanistic insights into phospholipid transfer by Ups1-Mdm35 in mitochondria. Nat Commun. 6, 7922.

Weissbach A, Sprinson DB. (1953). The metabolism of 2-carbon compounds related to glycine. II. Ethanolamine. J Biol Chem. 203, 1031-1037.

Wong LH, Gatta AT, Levine TP. (2018). Lipid transfer proteins: the lipid commute via shuttles, bridges and tubes. Nat Rev Mol Cell Biol. 20, 85-101.

Wu WI, Routt S, Bankaitis VA, Voelker DR. (2000). A new gene involved in the transport-dependent metabolism of phosphatidylserine, PSTB2/PDR17, shares sequence similarity with the gene encoding the phosphatidylinositol/phosphatidylcholine transfer protein, SEC14. J Biol Chem. 275, 14446-14456.

Wuestehube LJ, Schekman RW. (1992). Reconstitution of transport from endoplasmic reticulum to Golgi complex using endoplasmic reticulum-enriched membrane fraction from yeast. Methods Enzymol. 219, 124-136.

Yang Y, Lee M, Fairn GD. (2018). Phospholipid subcellular localization and dynamics. J Biol Chem. 293, 6230-6240.

Zhao T, Goedhart CM, Sam PN, Sabouny R, Lingrell S, Cornish AJ, Lamont RE, Bernier FP, Sinasac D, Parboosingh JS; Care4Rare Canada Consortium, Vance JE, Claypool SM, Innes AM, Shutt TE. (2019). *PISD* is a mitochondrial disease gene causing skeletal dysplasia, cataracts, and white matter changes. Life Sci Alliance 2, e201900353

Zinser E, Sperka-Gottlieb CD, Fasch EV, Kohlwein SD, Paltauf F, Daum G. (1991). Phospholipid synthesis and lipid composition of subcellular membranes in the unicellular eukaryote Saccharomyces cerevisiae. J Bacteriol. 1991 173, 2026-2034.

APPENDIX A

ROLE OF VPS39 IN INTRACELLULAR PE TRAFFICKING

As described in Chapter 2, I have shown that Vps39 is essential for transporting PE synthesized in the ER via the CDP-Etn Kennedy pathway to the mitochondria (Iadarola et al., 2020). I also provide genetic and biochemical evidence that Vps39 is also essential for the transport of PE synthesized in the endosome by Psd2 to the mitochondria. Together, these studies suggest a broader role of Vps39 in intracellular PE trafficking. Since in wild type cells mitochondrial Psd1 is the major source of PE in cells, I wondered if Vps39 is also involved in PE export from the mitochondria. I decided to test this idea using a genetic approach, which was based on the following two assumptions: First, a defect in PE export is expected to increase mitochondrial PE, which would negatively impact respiratory growth as mitochondrial PE levels are tightly regulated. Second, a defect in mitochondrial PE export when combined with the loss of non-mitochondrial PE biosynthesis pathways would inhibit growth because extra-mitochondrial PE is required for cell division. I utilized known PE metabolic and trafficking pathways to construct mutants that would test the above two assumptions (Figure A.1A).

To determine if Vps39 is required for PE export from the mitochondria, I overexpressed Psd1 in *vps39Δ* cells, which is expected to increase mitochondrial PE levels, and found a modest decrease in respiratory growth (Figure A.1B). In an alternate approach, I deleted Yme1, a negative regulator of Psd1 to test its effect on cell growth.

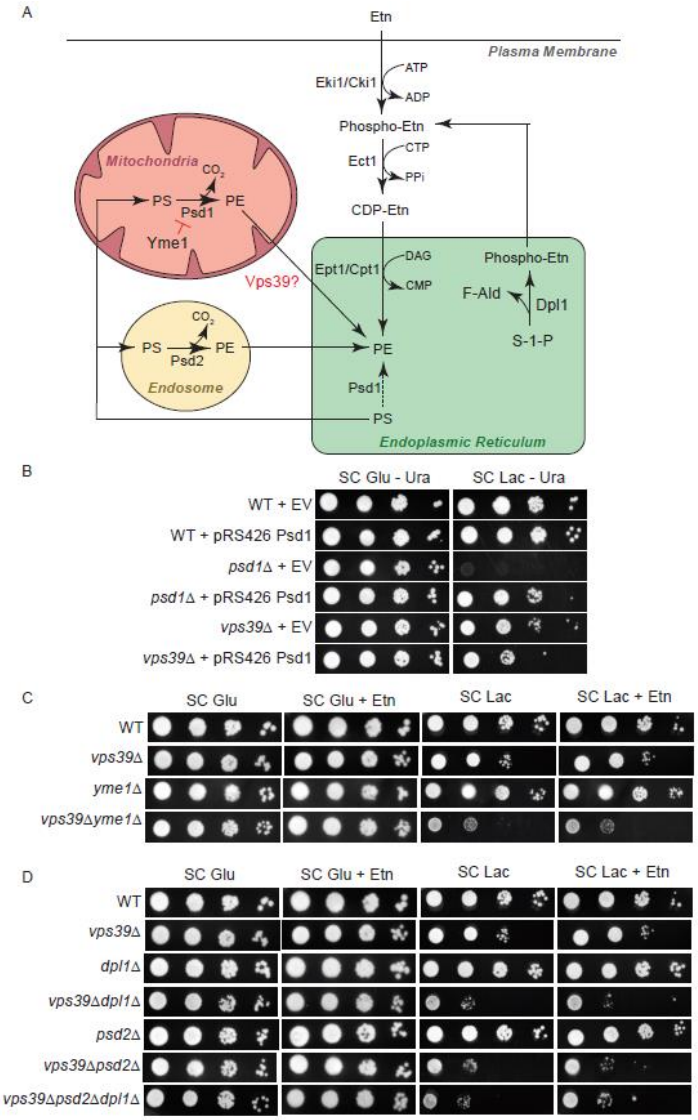

Figure A.1 Vps39 exhibit negative genetic interactions with PE biosynthetic genes in respiratory growth conditions.

A) Schematic of the major PE biosynthetic pathways in *Saccharomyces cerevisiae.* Psd1 is predominantly localized to the mitochondria and is the primary source of PE to the entire cell, however the molecular machinery required for PE export from the mitochondria has not been identified. Yme1 is a AAA-protease that regulate Psd1 abundance in the mitochondria. Endosomal Psd2 is a minor contributor of cellular PE. The Kennedy pathway can synthesize PE from the exogenous supplementation of Etn or from sphingolipids catabolized by Dpl1. B) Ten-fold serial dilution of the indicated yeast mutants were seeded onto synthetic complete (SC) Glucose - Ura and SC Lactate - Ura plates. Images were captured after 2d (SC Glucose media) and 5d (SC Lactate media) of growth at 30 °C. C-D) Ten-fold serial dilution of the indicated yeast mutants were seeded onto SC Glucose ± Etn ± Cho and SC Lactate ± Etn ± Cho plates. Images were captured after 2d (SC Glucose media) and 5d (SC Lactate media) of growth at 30°C. The images are representative

Figure A.2 Continued Vps39 exhibit negative genetic interactions with PE biosynthetic genes in respiratory growth conditions.
of three independent biological experiments. EV, empty vector; S-1-P, sphinganine-1-phosphate; F-Ald, fatty aldehyde; PE, phosphatidylethanolamine; PS, phosphatidylserine; Etn, ethanolamine; ATP, adenosine triphosphate, ADP, adenosine diphosphate; CTP, cytidine triphosphate; CDP, cytidine diphosphate; CMP, cytidine monophosphate; DAG, diacylglycerol; PPi, pyrophosphate.

A previous study has shown that *yme1Δ* cells have an increased abundance of Psd1 and mitochondrial PE levels because Psd1 is no longer degraded (Nebauer et al., 2007). Consistent with the hypothesis that excess mitochondrial PE is detrimental to growth, the *vps39Δyme1Δ* cells exhibit a pronounced growth defect in respiratory media that is not rescued by Etn (Figure A.1C). To test the second assumption that the loss of extra-mitochondrial PE would impair the growth of a *vps39Δ* mutant, I deleted *DPL1* and *PSD2*, genes required for extra-mitochondrial PE biosynthesis (Figure A.1A). Contrary to my hypothesis, the deletion mutants of Vps39 in combination with perturbation of extra-mitochondrial PE biosynthesis did not cause a growth deficiency in fermentable media (Figure A.1D). This was surprising because PE and PC, which is formed from PE, is required for cell growth independent of growth media. Similarly, Etn supplementation did not improve the respiratory growth deficiency observed in *vps39Δpsd2Δ* and *vps39Δdpl1Δ* mutants (Figure A.1D), implying that the respiratory growth defect of these mutants is not due to a depletion of cellular PE or PC. Importantly, I found that the triple mutant, *vps39Δpsd2Δdpl1Δ,* is not synthetic lethal. Again, this was unexpected because disruption of all the extra-mitochondrial PE biosynthetic pathways in combination with the blocked export of mitochondrial PE should completely abrogate the biosynthesis of PC. A possible explanation for our findings is the claim that a small fraction of Psd1 is localized to the

ER (Friedman et al., 2018). If Psd1 also localizes to the ER, then PC biosynthesis can occur even when PE transport from the mitochondria is non-functional.

To investigate if the localization of Psd1 is contributing to the extra-mitochondrial PE pool, I transformed *psd1Δ* cells with three different Psd1 constructs with varying localization signals (Friedman et al., 2018). The first Psd1 construct is the unaltered endogenous yeast Psd1, which is expected to localize to both the ER and mitochondria. The second Psd1 construct, $Psd1_{mito}$, solely localizes to the mitochondria because the endogenous signal sequence is replaced with the signal sequence of mitochondrial resident protein Mic60. The third Psd1 construct, $Psd1_{ER}$, solely localizes to the ER because the endogenous signal sequence is replaced with the signal sequence of resident ER protein Sec66. All constructs of Psd1 are able to rescue the respiratory growth of *psd1Δ* cells, indicating that they are functional constructs (Figure A.2A). In line with the role of Vps39 in PE import to the mitochondria, $Psd1_{ER}$ is unable to rescue the respiratory growth of *vps39Δpsd1Δ* cells in respiratory media, further supporting our previous results (Iadarola et al., 2020; Iadarola et al., 2021).

To test if the dual localization of Psd1 is masking the function of Vps39 in PE export from the mitochondria, I constructed the triple knockout *vps39Δpsd1Δpsd2Δ* cells. The *vps39Δpsd1Δpsd2Δ* cells are auxotrophic for Etn in fermentable media similar to *psd1Δpsd2Δ* cells; but in contrast, the triple mutant is not rescued by Etn supplementation in respiratory media (Figure A.2B), suggesting that we have abrogated PE transport to the mitochondria. If the fermentable growth deficiency of *vps39Δpsd1Δpsd2Δ* cells is rescued by Psd1 and $Psd1_{ER}$ constructs but not the $Psd1_{mito}$ construct, then we can conclude that in

the absence of extra-mitochondrial PE biosynthesis, the transport of PE from the mitochondria via Vps39 is required to support cellular growth.

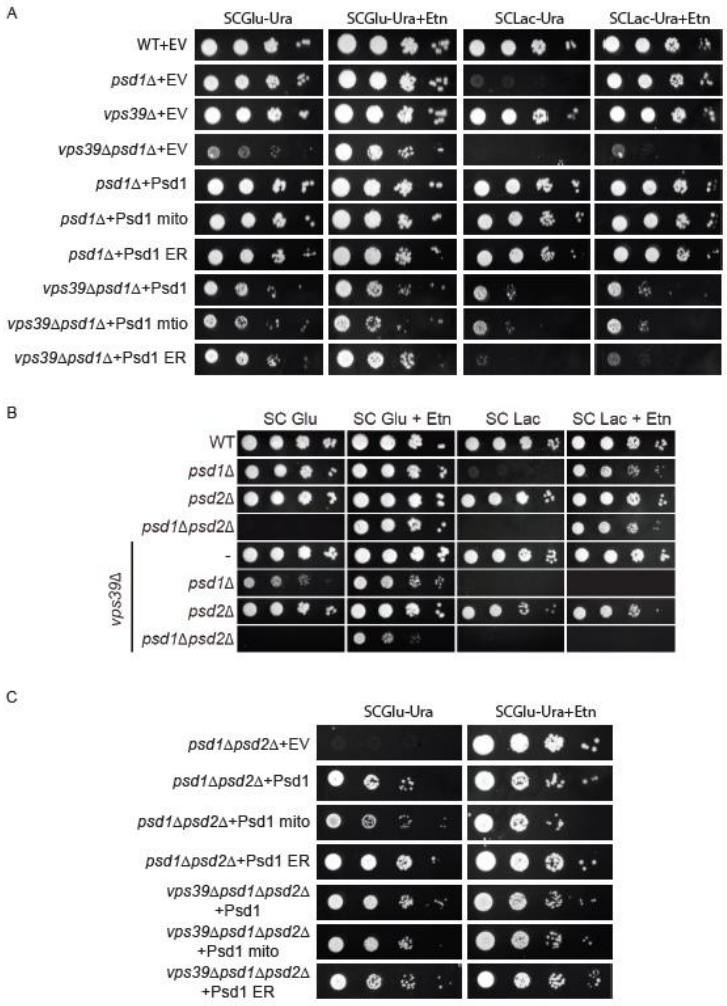

Figure A.3 Mitochondrial PE export is not impaired by the absence of Vps39.
A) Ten-fold serial dilution of the indicated yeast mutants were seeded onto SC Glucose -Ura ± Etn and SC Lactate -Ura ± Etn plates. Images were captured after 2d (SC Glucose media) and 5d (SC Lactate media) of growth at 30°C. B) Ten-fold serial dilution of the indicated yeast mutants were seeded onto SC Glucose ± Etn and SC Lactate ± Etn plates. Images were captured after 2d (SC Glucose media) and 5d (SC Lactate media) of growth at 30°C. C) Ten-fold serial dilution of the indicated yeast mutants were seeded onto SC Glucose -Ura ± plates. Images were captured after 2d (SC Glucose media) and 5d (SC Lactate media) of growth at 30°C. The image in panel B is representative of three independent biological experiments (n=3) and the images in panels A and C are representative of one biological replicate (n=1). EV, empty vector.

However, contrary to our hypothesis, all three Psd1 constructs rescued the fermentable growth deficiency of *vps39Δpsd1Δpsd2Δ* cells (Figure A.2C). Based on these results, we have developed three possible models for why our genetic data does not align with our hypothesis: 1) in addition to Vps39, there exists another mitochondrial PE transporter that can sustain fermentable growth in the absence of Vps39, 2) Vps39 is only involved in PE transport from the mitochondria in respiratory media, and 3) Vps39 is not involved in PE transport from the mitochondria.

To complement the genetic approach, I utilized a steady state radiolabeling approach using [^{3}H] serine, which gets incorporated into PS and subsequently into PE and PC, allowing us to track the inter-organelle trafficking of PE. In a *psd2Δ* background, PS synthesized in the ER from serine will be transported to the mitochondria for decarboxylation by Psd1 and will be transported back to the ER for methylation by Pem1/Pem2 to form PC. Therefore, if PE transport from the mitochondria is disrupted by the deletion of Vps39, then *vps39Δpsd2Δ* cells should exhibit an accumulation of labeled PE levels and a decrease in labeled PC levels. In my initial trial of steady state radiolabeling of aminoglycerophospholipids in *vps39Δpsd2Δ* cells grown in SC Glucose media, I observed a slight accumulation of PE levels and a slight decrease in PC levels (Figure A.3A&B). Although this trend is consistent with the role of Vps39 in PE export from mitochondria, the effect size is too small to suggest that Vps39 is the sole PE transporter from the mitochondria because PC levels are only mildly decreased. Complete abrogation of PE transport from the mitochondria is expected to abolish PC biosynthesis entirely. This experiment should be repeated a minimum of two times to ensure the validity

of this result. Additionally, this experiment should be repeated in respiratory media to determine if the role of Vps39 is specific to respiratory conditions.

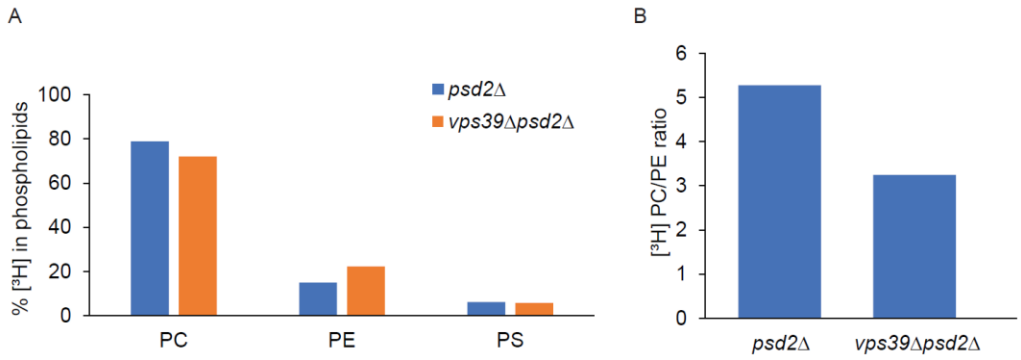

Figure A.4 PE to PC conversion is slightly reduced in the absence of Vps39.
A) Percent of [^{3}H] PS, PE, and PC from the indicated cells grown in SC Glucose media containing 10 µCi [^{3}H] serine. B) Ratio of [^{3}H] PC/PE from the indicated cells grown in SC Glucose media containing 10 µCi [^{3}H] serine. Panels B and C are from the same experiment. This experiment has been performed one time (n=1).

My previous work identified the essential role of Vps39 in trafficking extra-mitochondrial Etn- and Psd2-synthesized PE to the mitochondria (Iadarola 2020; Iadarola et al., 2021). To further examine the role of Vps39 in PE transport to the mitochondria, I sought to determine if Vps39 is required for all routes of PE transport to the mitochondria. It has been previously reported that in addition to Etn and Cho supplementation, lyso-PE supplementation can restore mitochondrial PE in *psd1Δ* cells. Lyso-PE is converted to PE by ER-localized acyltransferase, Ale1, and is then transported to the mitochondria. To determine if Vps39 is required for the transport of Ale1-synthesized PE to the mitochondria, I supplemented *vps39Δpsd1Δ* cells with lyso-PE. The respiratory growth deficiency of *psd1Δ* cells is rescued upon supplementation of lyso-PE; however, the respiratory growth deficiency of *vps39Δpsd1Δ* cells is not rescued implying that Vps39 is

indeed required for lyso-PE derived PE transport to the mitochondria (Figure A.4). This result in combination with my previously published results (Iadarola et al., 2020; Iadarola et al., 2021) suggests that Vps39 is essential for respiratory growth rescue of *psd1Δ* via all the three extra-mitochondrial PE biosynthetic pathways.

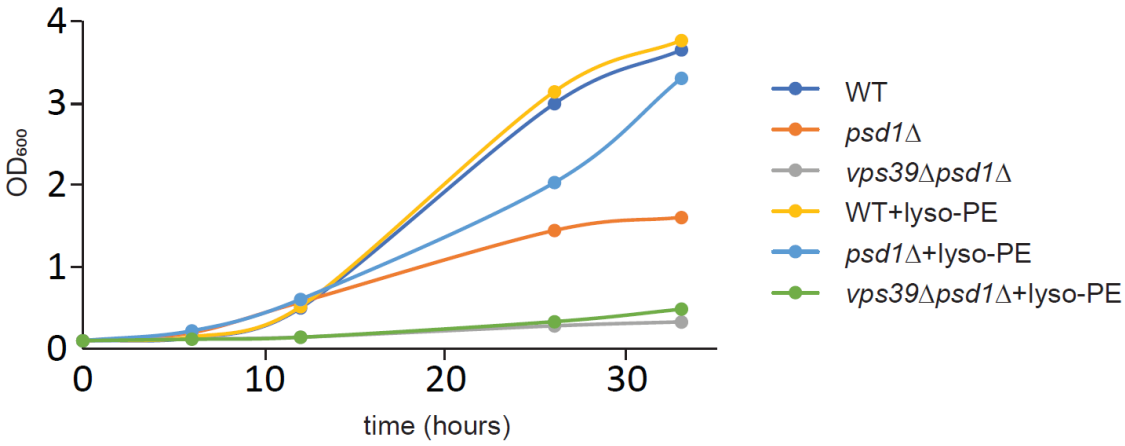

Figure A.5 Vps39 is essential for the transport of Ale1-synthesized PE to the mitochondria.
The growth of the indicated yeast strains cultured in SC Lactate + 1% Tergitol ± lyso-PE at 30°C were monitored by measuring absorbance at 600 nm. The growth curves are a representative of three biological replicates (n=3). OD, optical density.

To determine if human Vps39 (hVps39) also functions in PE transport to the mitochondria, as does its yeast homolog, I expressed hVps39 in *Saccharomyces cerevisiae* downstream of the yeast promoter for Vps39. I show that hVps39 partially rescues the respiratory defect of *vps39Δpsd1Δ* cells (Figure A.5), indicating that hVps39 may also function in the mitochondrial PE transport pathway, like yeast Vps39. Both Etn and Cho supplementation can restore the respiratory growth of *vps39Δpsd1Δ* cells expressing hVps39 suggesting that hVps39 mediates PE transport to the mitochondria independent of the source of PE biosynthesis. Taken together, this study strongly suggests that the role of

Vps39 in the transport of non-mitochondrial PE to the mitochondria is essential and conserved.

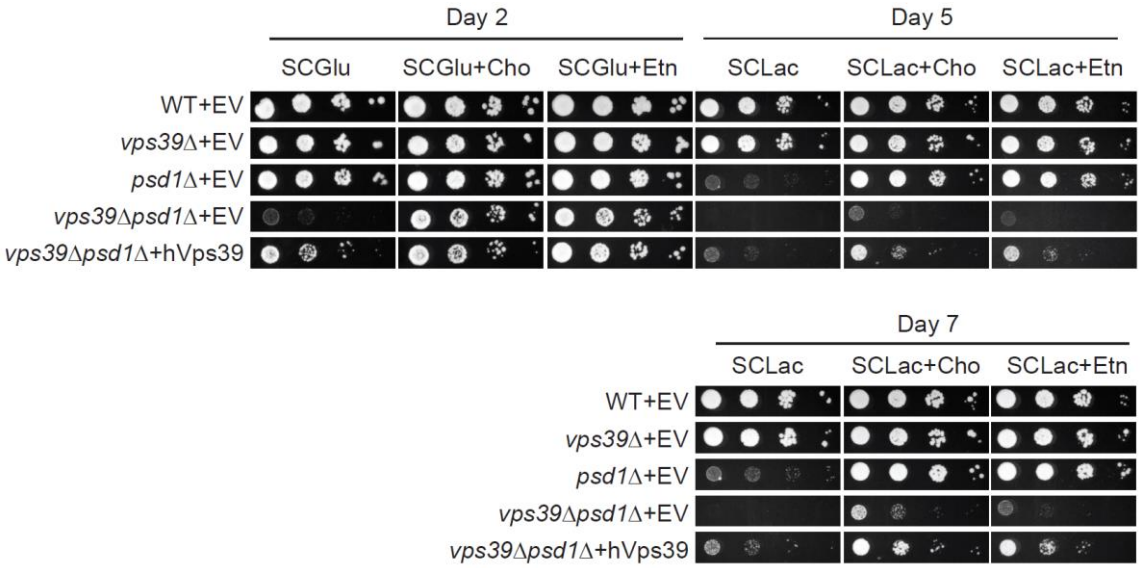

Figure A.6 Yeast and human Vps39 are essential for PE transport to the mitochondria in yeast.
Ten-fold serial dilution of the indicated yeast mutants were seeded onto SC Glucose -Ura ± Etn ± Cho and SC Lactate - Ura ± Etn ± Cho plates. Images were captured after 2d (SC Glucose media) and 5d/7d (SC Lactate media) of growth at 30°C. The images are representative of three independent biological experiments. EV, empty vector.

APPENDIX B

CROSS REGULATION AND REDUNDANCIES OF THE CDP-ETN AND CDP-CHO KENNEDY PATHWAYS

Previously, I identified that Cho-mediated respiratory growth rescue of *psd1Δ* cells is dependent on Pct1 function, and therefore dependent on the CDP-Cho Kennedy pathway (Iadarola et al., 2021). It was also shown that Etn-mediated respiratory growth rescue of *psd1Δ* cells is dependent on Ect1, the rate limiting enzyme of the CDP-Etn Kennedy pathway (Baker et al., 2016). These data are consistent with the proposed roles of Pct1 and Ect1 in their respective Kennedy pathways. Interestingly, I found that the Etn-mediated respiratory growth rescue of *psd1Δ* cells is also dependent on Pct1 (Figure B.1A). This is an unexpected result because Etn supplementation stimulates CDP-Etn Kennedy pathway of PE biosynthesis, which relies on Ect1 but not Pct1 and therefore, should have restored the respiratory growth defect of *pct1Δpsd1Δ* cells. The CDP-Cho and CDP-Etn Kennedy pathways both utilize phospholipid precursors, Cho and Etn, in three sequential enzymatic reactions to biosynthesis PC and PE, respectively (Figure 1.2, Chapter 1). Previous studies have already shown that Cki1 and Eki1, the first phosphorylation reactions of the Kennedy pathways are redundant (Kim et al., 1999). Only the second cytidylylation reaction via Pct1 and Ect1 was considered to be unique for Cho and Etn utilization, respectively. Upon investigation of the respiratory growth of *ect1Δpsd1Δ* cells, I observed a similar abrogation of both Cho- and Etn- mediated respiratory growth rescue (Figure B.1A). This was also a surprise because *ect1Δpsd1Δ*

cells contain functional Pct1. Together these data suggest that Ect1 is required for Pct1 function and vice versa.

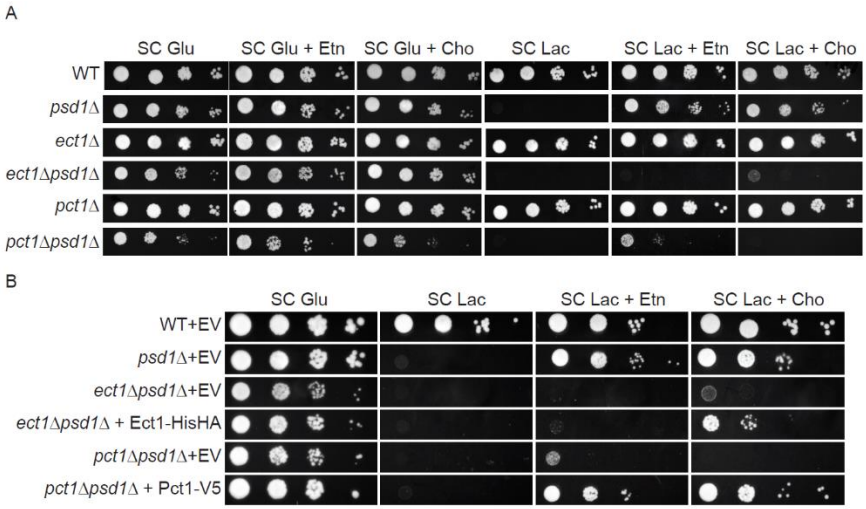

Figure B.1 Ect1 and Pct1 function is dependent on each other.
A) Ten-fold serial dilution of the indicated phospholipid yeast mutants were seeded onto SC Glucose ± Etn ± Cho and SC Lactate ± Etn ± Cho plates. Images were captured after 2d (SC Glucose media) and 5d (SC Lactate media) of growth at 30°C. B) Ten-fold serial dilution of the indicated phospholipid yeast mutants were seeded onto SC Glucose -Ura and SC Lactate -Ura ± Etn ± Cho plates. The images are representative of three independent biological experiments. EV, empty vector; Etn, ethanolamine; Cho, choline.

We hypothesized that Pct1 and Ect1 were functionally reliant on each other due to these proteins forming a complex. To probe for an Ect1/Pct1 complex, we cloned the tagged versions of each enzyme, Pct1-V5 and Ect1-HisHA, and expressed them in *pct1Δ* and *ect1Δ* cells, respectively. As expected, Pct1-V5 complemented the *pct1Δpsd1Δ* mutant upon Cho and Etn supplementation, but to our surprise, Ect1-HisHA only complemented *ect1Δpsd1Δ* cells upon Cho supplementation but not Etn supplementation (Figure B.1B). This implies that the enzymatic function of Ect1 is disrupted by the tag. However, the HisHA tag on Ect1 did not perturb the Cho-mediated rescue of *ect1Δpsd1Δ* cells,

suggesting that the Cho-mediated rescue is dependent on the presence but not the enzymatic function of Ect1. Because the presence of nonfunctional Ect1 was sufficient to restore Pct1 function, we hypothesize that Ect1 and Pct1 are in a complex in which Ect1 regulates the abundance, activity, or localization of Pct1. To test if Ect1 is required to maintain Pct1 stability, I quantified Pct1-V5 protein abundance in WT and *ect1Δ* cells. Interestingly, the stability of Pct1-V5 is unchanged in the presence or absence of Ect1 (data not shown). Future studies will need to be performed to determine if Pct1 activity and localization is dependent on Ect1.

Finally, we wanted to determine if the terminal Kennedy pathway enzymes Ept1 and Cpt1 are regulated in a similar manner to Ect1 and Pct1. Therefore, we asked if Ept1 function is dependent on Cpt1 and vice versa. This would be unlikely because previous reports identified that Ept1 and Cpt1 are redundant for Etn and Cho utilization *in vivo* by radiolabeling experiments (Henneberry et al., 2001; McGee et al., 1994; Menon and Stevens, 1992). Here, we validate these findings by observing the respiratory growth of Cpt1 and Ept1 deletion strains in a *psd1Δ* background. *cpt1Δpsd1Δ* and *ept1Δpsd1Δ* cells are rescued by both Cho and Etn supplementation, whereas the triple mutant *cpt1Δept1Δpsd1Δ* is not rescued by either (Figure B.2A). Complementation with both Ept1 and Cpt1 in *cpt1Δept1Δpsd1Δ* cells confirms that each enzyme can utilize Etn to rescue the respiratory growth deficiency of *psd1Δ* cells (Figure B.2B). This shows that *in vivo*, Cpt1 and Ept1 are redundant in function and can equally support the needs of a cell with a mitochondrial PE deficiency upon Etn or Cho supplementation. Additionally,

unlike Ect1 and Pct1, we find that Ept1 and Cpt1 do not require each other for their functions in a *psd1Δ* background.

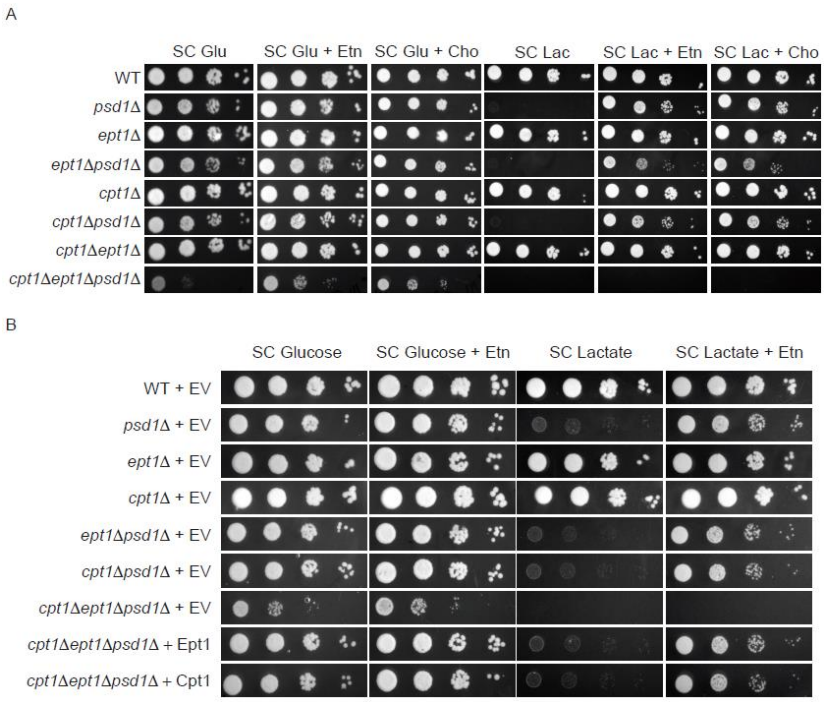

Figure B.2 Ept1 and Cpt1 do not require each other for PE/PC biosynthesis.
A) Ten-fold serial dilution of the indicated phospholipid yeast mutants were seeded onto SC Glucose ± Etn ± Cho and SC Lactate ± Etn ± Cho plates. Images were captured after 2d (SC Glucose media) and 5d (SC Lactate media) of growth at 30°C. B) Ten-fold serial dilution of the indicated phospholipid yeast mutants were seeded onto SC Glucose -Ura ± Etn and SC Lactate -Ura ± Etn plates. The images are representative of three independent biological experiments. EV, empty vector; Etn, ethanolamine; Cho, choline.